

**BACKBONE MODEL FOR CONFINED
MASONRY WALLS FOR PERFORMANCE-
BASED SEISMIC DESIGN**

by

Zahra Riahi

A THESIS SUBMITTED IN PARTIAL FULFILLMENT OF
THE REQUIREMENTS FOR THE DEGREE OF
MASTER OF APPLIED SCIENCE

in

The Faculty of Graduate Studies

(Civil Engineering)

THE UNIVERSITY OF BRITISH COLUMBIA

August 2007

© Zahra Riahi, 2007

Abstract

Nonlinear models are of paramount importance in the emerging field of performance-based earthquake engineering. In this study, an analytical model is developed capable of simulating the measured backbone of typical confined masonry (CM) walls whose response under lateral loads is mainly governed by shear deformations. Equations are developed for the cracking and maximum shear strength, and the cracking and ultimate deformation capacities. This model is based on the results of both monotonic and reversed cyclic experiments assembled in an extensive database, and developed through an iterative linear regression analysis.

Owing to their anomalies, specimens with compression diagonal loading, height-to-length aspect ratio greater than 1.2, axial stress to masonry compressive strength ratio larger than 0.12, and those with column longitudinal reinforcement ratio below 1%, are not considered for the purpose of creating the empirical equations.

Several statistical and graphical tools are utilized to identify the most significant panel and tie column design variables; to set the functional forms that best relate them to model parameters; and to diagnose influential points that may exert undue impact on the analysis results.

The effect of openings and panel aspect ratio on the strength characteristics of CM walls, the capability of existing equations to predict the observed backbone response, and the limitations of the proposed equations are discussed in detail. Model variability is also presented in lognormal fragility curves for different model parameters and at all limit states.

The proposed backbone model is found to simulate reasonably well the seismic behaviour of CM walls whose properties conform to the assumptions of the model. However, it fails to track the observed backbone response of anomalous or atypical CM walls.

Table of Contents

Abstract.....	ii
Table of Contents	iii
List of Tables.....	vii
List of Figures	ix
Acknowledgements	xii
Dedication.....	xiii
Chapter 1: Introduction	1
1.1 Motivation and background	1
1.2 Objectives	2
1.3 Scope.....	2
1.4 Organization and outline.....	3
Chapter 2: Literature review	5
2.1 Introduction.....	5
2.2 Damage pattern and overall seismic behaviour	6
2.3 Masonry unit and mortar characteristics.....	10
2.4 Wall density	11
2.5 Confining elements	12
2.6 Openings	16
2.7 Axial stress.....	17
2.8 Panel aspect ratio	18
2.9 Masonry-concrete interface.....	18
2.10 Panel reinforcement	19
2.11 Existing models.....	22
2.12 Closing remarks	25
2.13 References.....	27

Chapter 3: Performance-based seismic models for confined masonry walls	33
3.1	Introduction..... 33
3.2	Backbone model and limit states 36
3.3	Proposed empirical equations 38
3.3.1	Data interpretation and model specification 38
3.3.2	Experimental database and criteria for the removal of data..... 40
3.3.3	Prediction of masonry shear cracking strength using f_m 46
3.3.4	Equations for shear cracking strength..... 47
3.3.4.1	Equation development 47
3.3.4.2	Comparison with existing models..... 48
3.3.4.3	The effect of openings..... 50
3.3.5	Equations for maximum shear strength 51
3.3.5.1	Equation development 51
3.3.5.2	Comparison with existing equations 53
3.3.6	The effect of panel aspect ratio on strength characteristics 54
3.3.7	Equation development for drift capacity at cracking limit state 56
3.3.8	Equation development for ultimate drift capacity of CM walls..... 57
3.3.9	Prediction of drift capacity at maximum limit state..... 59
3.3.10	Comparison of drift models with existing empirical limits 60
3.4	Discussion 61
3.4.1	Summary of the proposed equations..... 61
3.4.2	Limitations of the backbone model..... 64
3.4.3	Evaluation of the proposed equations 66
3.4.4	Recommendations and future directions..... 69
3.5	References..... 72
Chapter 4: Summary and future research	77
4.1	Summary 77
4.2	Future research directions 78
Appendix A: Confined masonry database	80
A.1	Introduction..... 80
A.2	General information 81

A.2.1	Reinforcement characteristics	81
A.2.2	ID	82
A.2.3	Test category	82
A.2.4	Scaling.....	82
A.3	Panel Characteristics	83
A.4	Tie column properties	88
A.5	Bond beam characteristics	92
A.6	Openings	95
A.7	Floors	96
A.8	Loading configuration.....	96
A.9	Results.....	98
A.9.1	Damage pattern and failure modes	98
A.9.1.1	Shear failure	99
A.9.1.2	Flexural failure mode.....	100
A.9.1.3	Sliding shear.....	101
A.9.1.4	The effect of each reinforcement method on damage pattern.....	101
A.9.2	Determination of result parameters.....	101
A.10	Simplified database	104
A.11	References	106
Appendix B: Multiple regression analysis using the least square method..		112
B.1	Getting started	112
B.2	Assumptions of Linear regression analysis.....	116
B.2.1	Linearity	116
B.2.2	Normality	117
B.2.3	Homoscedasticity	118
B.2.4	Independence	118
B.2.5	Model specification.....	119
B.2.6	Multicollinearity	119
B.2.7	Influential observations.....	120
B.3	Iterative regression process.....	121
B.4	Data removal in the present study	122

Appendix C: Derivation of equations and results	128
C.1 Derivation of the fundamental equations	128
C.1.1 Cracking drift capacity	128
C.1.2 Ultimate drift ratio	129
C.2 Presentation of the results	130

List of Tables

Table 2-1: Existing models for cracking and maximum shear strength of CM walls.....	23
Table 2-2: Deformation capacity of CM walls at 50% probability of failure	24
Table 3-1: Existing models for cracking and maximum shear strength of CM walls.....	34
Table 3-2: The characteristics of Data considered for model development.....	44
Table 3-3: Important CM design variables considered in model development.....	46
Table 3-4: Comparison between existing models and actual response of CM walls	50
Table 3-5 : Mean ductility factor for different unit materials	59
Table 3-6: Comparison between the proposed drift models and existing limits	60
Table 3-7: Statistical characteristics of the proposed equations for panels with $H/L \leq 1.2$	62
Table 3-8: Practical ranges of important design variables for predicting the seismic response of CM walls using the proposed model.....	66
Table A-1: Reinforcement detailing of CM panels.....	81
Table A-2 (a): Panel Geometry and reinforcement details, (b): material properties.....	84
Table A-3: Panel property statistics.....	85
Table A-4: Tie column characteristics.....	90
Table A-5: Statistics of Tie column design variables.....	90
Table A-6: Bond beam characteristics.....	93
Table A-7: Statistics of bond beam design variables.....	94
Table A-8: Opening characteristics.....	95
Table A-9: Floor characteristics.....	96
Table A-10: Loading characteristics.....	97
Table A-11: Statistics of loading parameters.....	97
Table A-12: Result parameters.....	103
Table A-13: Basic assumptions and procedure to determine result parameters.....	104
Table B-1: Diagnostic tools to identify the influential points.....	121
Table B-2: Preliminary data removal (prior to the formation of simplified database).....	122
Table B-3: Criteria for data removal during the analysis.....	123
Table B-4: List of the data points that were entirely removed from the analysis.....	123

Table B-5: Data points excluded from the final equation of v_m	123
Table B-6: Data removal for the prediction of v_{cr}	124
Table B-7: Data removal for the prediction of v_{max}	125
Table B-8: Data removal for the prediction of δ_{cr}	125
Table B-9: Data removal for prediction of δ_{ult}	126
Table C-1: Masonry shear strength (v_m).....	130
Table C-2: Shear cracking strength (v_{cr}).....	132
Table C-3: Maximum shear strength (v_{max}).....	134
Table C-4: Cracking drift capacity (δ_{cr}).....	135
Table C-5: Ultimate drift capacity (δ_{ult}).....	136

List of Figures

Figure 2-1: (a) A completely demolished URM dwelling, (b) An intact CM building, 2003 Bam earthquake, Iran (Eshghi and Naserasadi, 2005).....	6
Figure 2-2: Illustration of the seismic behavior beyond cracking limit state.....	7
Figure 2-3: Post-peak behaviour of a typical CM wall (Zabala et al, 2004).....	8
Figure 2-4: CM house with damage concentration in the first story(a) Alcocer et al, 2004 (b) 1997 Punitaqui earthquake, Chile (Gomez et al, 2002).....	9
Figure 2-5: Flexural failure and penetration of cracks into tie columns ends (Zabala et al, 2004).9	
Figure 2-6: Collapse of CM building due to inadequate wall density, 2001 Atico earthquake, Peru (San Bartolome et al, 2004).....	12
Figure 2-7: The beneficial effects of confinement on the seismic response of masonry panels (Tomazevic and Klemenc, 1997(a)).....	13
Figure 2-8: Extensive damage to the column-beam joint due to improper reinforcement detailing, 1985 Lloleto Earthquake, Chile (Gomez et al, 2002).....	15
Figure 2-9: Constructive effect of opening confinement on post-cracking seismic performance of CM walls (Leonardo et al, 2004).....	17
Figure 2-10: Extensive damage to masonry piers due to the lack of proper opening confinement, 1985 Lloleto Earthquake, Chile (Gomez et al, 2002).....	17
Figure 2-11: Separation of masonry walls and tie column due to the lack of proper bond (Yushimura et al, 2004).....	19
Figure 2-12: The effect of panel reinforcement on damage distribution (Aguilar et al, 1996).....	20
Figure 2-13: The effect of panel horizontal reinforcement on the seismic performance of CM walls (Aguilar et al, 1996).....	20
Figure 2-14: Comparison between existing models for a typical CM wall (a) Cracking shear strength, (b) Maximum shear strength.....	24
Figure 2-15: Deformation capacity of CM walls made of solid units (Alcocer et al, 2003).....	25
Figure 3-1: The methodology employed to develop the analytical model.....	36
Figure 3-2: (a) Determination of model parameters based on the recorded response, (b) The analytical backbone of the current study.....	36

Figure 3-3: (a) Obscure trend between model parameter and design variable, (b) The effectiveness of separating the data into groups with almost the same characteristics to reveal the trends.....	39
Figure 3-4: Local strength loss and multiple values for δ_{ult} as examples of anomalies that led to the removal of SP-117 for ultimate limit state (Flores et al, 2004).....	41
Figure 3-5 : Diagonal compression loading.....	42
Figure 3-6: The ability of the proposed equation to predict v_m	47
Figure 3-7 : Fitness of the proposed model to the experimental data.....	48
Figure 3-8: Ability of the proposed equation and existing models to predict v_{cr}	49
Figure 3-9: The effect of openings on cracking shear strength of CM walls.....	51
Figure 3-10: Fitness of the proposed model to the experimental data.....	53
Figure 3-11: Comparison between the proposed and existing models to predict v_{max}	54
Figure 3-12: Lack of distinct relationship between μ and $\rho_{hc}f_{yh}$	58
Figure 3-13: The capability of the proposed equation to predict the ductility factor.....	58
Figure 3-14: Lognormal distribution of $\delta_{max}/\delta_{ult}$	60
Figure 3-15: Fragility curves for model parameters at different limit states.....	63
Figure 3-16: Fragility curves for Specimen 254 (Flores, 2004).....	64
Figure 3-17: Comparison of measured and proposed backbone curves for conforming specimens (a) SP-62: Marrinilli and Castilla, 2006, (b) SP-254: Flores, 2004.....	67
Figure 3-18: Inability of the model to predict the deformation capacity of a CM wall with excessively large axial stress (Aguilar et al, 1996).....	67
Figure 3-19: Inability of the model in predicting the seismic response of a highly deficient CM wall (Meli and Salgado, 1969).....	68
Figure 3-20: The effect of bed joint reinforcement on the seismic behaviour of CM walls, and the inability of the model to predict the maximum and ultimate response parameters (Aguilar et al, 1996).....	68
Figure 3-21: Inability of the model to predict the recorded response due to the predominance of flexural deformations (Meli and Salgado, 1969).....	69
Figure A-1: Different testing methods.....	82
Figure A-2: Distribution of different unit types in the database.....	83
Figure A-3: Distribution of some of the most important panel design variables.....	87
Figure A-4: Distribution of the number of tie columns.....	88
Figure A-5: Distribution of different types of tie columns.....	89
Figure A-6: Distribution of tie columns with different reinforcement detailing.....	89

Figure A-7: Statistical distribution of tie column design variables.....	92
Figure A-8: Statistical distribution of bond beam design variables.....	95
Figure A-9: Distribution of different loading configurations.....	96
Figure A-10: Statistical distribution of loading variables.....	98
Figure A-11: Distribution of possible failure modes for CM walls.....	99
Figure A-12: Limit states and the smooth backbone.....	102
Figure B-1: Statistical distribution of CM wall design variables.....	115
Figure B-2: Clear trend in the plot of residuals vs. the predictor variable as a measure of the model misspecification.....	117
Figure B-3: Normality of the residuals.....	117
Figure B-4: Homogeneity of the residuals.....	118
Figure C-1: The concept of ductility.....	129

Acknowledgements

Foremost, I would like to express my sincere gratitude to my advisor, Dr. Kenneth Elwood, for his insight, guidance, and wise supervision throughout this research project. Without his assistance and patience its completion would not have been possible.

My sincere thanks are also due to Dr. Abrams, Dr. Alcocer, and Dr. Astroza for their constructive suggestions during development of the database and empirical seismic model. Their critical comments significantly contributed in overcoming a number of difficult research problems.

I am also deeply indebted to Hugon Juarez and Jose Centeno for their assistance with Spanish papers. They each spent much time teaching me fundamentally important Spanish terms, and translating critical references into English. I also extend my thanks to Mohsen Javedani for his help with the STATA software.

I am genuinely grateful to Earthquake Engineering Research Institute (EERI) for their support for this project, and the most helpful faculty in structural engineering at the University of British Columbia for providing coherent answers to my endless questions.

Many thanks to my dear friends and talented colleagues, Arezoo, Farzad, Houman, Isobella, Layla, Mona, Mohammad, Nasim, Soheil and Tim. Your support undoubtedly contributed to the quality of this work. The flaws that remain result from my own shortcomings.

Most important I would like to thank my family for the unending love and wisdom you have given throughout my education. You are a boundless source of strength and inspiration.

April, 2007

Vancouver, B.C.

To my parents,

For their endless love and support

Notations

H_w / L_w	=	panel aspect ratio
N	=	the number of observations
N_{tc}	=	the number of tie columns
f_c	=	concrete compressive strength
f_m	=	masonry compressive strength
f_{yh}	=	yield strength of column transverse reinforcement
f_{yv}	=	yield strength of column longitudinal reinforcement
f_{yhv}	=	yielding strength of panel horizontal reinforcement
v_m	=	masonry shear strength
v_{cr}	=	cracking shear strength
v_{max}	=	maximum shear strength
α	=	the effect of panel aspect ratio on panel resistance
β	=	the ratio of the opening area to the wall gross area
γ	=	the effect of unit material on the panel rigidity
δ_{cr}	=	cracking drift capacity
δ_{max}	=	drift capacity at max limit state
δ_{ult}	=	ultimate drift capacity
δ_y	=	drift capacity of the equivalent linear system
μ	=	ductility factor
ρ_{hc}	=	tie column transverse reinforcement ratio
ρ_{vc}	=	tie column longitudinal reinforcement ratio
σ_v	=	axial stress

Introduction

1.1 Motivation and background

The use of masonry as a composite material has been favored in the construction of buildings and civil infrastructures, simple and sophisticated, because of its durability, aesthetic appeal, and economic advantages. However, the inherent weakness of masonry in tension has been repeatedly demonstrated in seismic events. The need to overcome seismic deficiency of unreinforced masonry (URM) panels has led to the development of structural walls with different reinforcement patterns.

Confined masonry (CM), which consists of an URM masonry panel bordered with slender columns and beams, is one such alternative. Confining elements, tie columns and bond beams, are cast after the construction of the wall. These elements are usually constructed of reinforced concrete, although timber, reinforced masonry, and other materials have been used occasionally.

Extensive study over the past few decades has aimed at identification of the structural and seismic performance aspects of CM walls. CM has mainly evolved empirically, however, and current codes rely only upon conventional force-based equations originally developed for URM/RM panels, in order to predict the behaviour of such load bearing elements. The effects of confinement, despite its important potential for improving the seismic behaviour of CM walls, have been largely overlooked in the few existing models. The emerging field of performance-based seismic design relies on nonlinear models for the force-deformation response of structural systems in order to control the sustained earthquake damage.

Therefore, while CM walls have been extensively studied in experimental tests worldwide, it is of high priority to develop a model capable of capturing both deformation and strength characteristics. Provided these characteristics are consistently quantified and assembled in a comprehensive database, the results of such experiments may be used effectively to develop a model for the nonlinear seismic performance of

CM walls up to large deformation levels. It is the goal of the current study to develop a model to predict the nonlinear backbone response of CM walls subjected to lateral loads.

1.2 Objectives

The primary objectives of this research are:

1. to review the past CM studies conducted up-to-date;
2. to assemble the results of all available CM experiments into comprehensive databases that elaborate both specimen characteristics and test results;
3. to link specific characteristics of CM walls with the observed seismic behaviour, associated failure modes, and damage patterns, and to select the appropriate limit states and model parameters;
4. to utilize the results of experimental tests for developing a performance-based model capable of capturing the nonlinear response of CM walls up to large deformation levels; and
5. to compare and contrast the proposed equations with both experimental data and existing models, in order to investigate the accuracy and applicability of the developed model.

To collect the experimental data, define the limit states, and develop the analytical backbone model, this research builds upon previous analytical and experimental studies conducted up-to-date. The database being developed by Universidad Nacional Autonoma de Mexico (UNAM, 2004), which outlines the results of experimental tests on all types of masonry walls, was a significant contributor to the construction of the databases developed and used in the present study.

1.3 Scope

The methodology and tools employed in construction of the databases, extraction of results, and development of an analytical model may, in general, be applied to any structural system. However, to propose the empirical equations, this thesis focuses on the experimental results of typical CM walls whose behaviour is mainly governed by shear deformations.

Chapter 1: Introduction

These walls are provided only with two tie columns along their boundaries, both reinforced with multiple longitudinal rebar, and the panels are left unreinforced in both vertical and horizontal directions. Other constraints are: tie column longitudinal reinforcement ratio between 1% and 3%, panel aspect ratio equal or less than two, and axial stress to masonry compressive strength ratio less than 0.12. The results of dynamic and pseudo-dynamic tests, although documented in an explicit database, were not considered for the purpose of model development. Only cyclic and monotonic quasi-static tests have been taken into account. The backbone model was developed on a deterministic basis and model uncertainties were accounted for using coefficients of variation.

1.4 Organization and outline

This manuscript-based thesis is organized in four main chapters and three appendices. The appendices report the process of data selection, developing both dynamic and static databases as the basis of the analytical work, and contain the results of the proposed equations for each model parameter.

Chapter 1: provides an introduction to the thesis.

Chapter 2: serves as a state-of-the-art review of research on CM construction.

Chapter 3: reports on data selection and inspection, elaborates the methodology employed to establish the final empirical equations, and presents these predictive formulae for cracking, maximum load, and ultimate limit states. This chapter will be submitted to the Journal of Structural Engineering of the American Society of Civil Engineers for peer-review and publication.

Chapter 4: provides a summary and conclusions of the present study, together with recommendations for future research directions.

Appendix A: contains a comprehensive account of the methodology employed to develop the databases, and describes material properties, geometry, reinforcement details, damage patterns, and failure modes of the specimens included in the datasets.

Chapter 1: Introduction

Appendix B: provides an introduction to linear regression analysis, and the method used to identify influential points believed to exert undue impact on analysis results.

Appendix C: reports on the derivation of equations as the basis of the proposed model, and the results of the analysis.

Literature Review

2.1 Introduction

Confined masonry (CM), as an effective structural system for low- and medium-rise dwellings and apartment buildings up to five stories, is widely used in central and south America, central and south Asia, and eastern and south Europe.

The use of masonry walls confined with slender vertical (tie column) and horizontal (bond beam) elements along their borders can be traced back to the beginning of the last century. CM walls, in fact, have been first utilized for the reconstruction of some Italian cities flattened in such seismic events as the 1908 Messina earthquake (Murty et al., 2006), and the earthquake of July 23, 1930 (Freeman, 1932). Holding the walls together and in joint with other structural components, providing some out-of-plane seismic resistance, and introducing some level of ductility to unrienced masonry (URM) walls were among the main objectives of panel confinement.

As an alternative to URM and adobe buildings, CM has overcome many seismic deficiencies to which the two latter systems were highly vulnerable. However, material properties, workmanship and construction sequence together with maintenance quality are among the key construction factors that can significantly affect the seismic performance of this class of structural walls; and therefore, aside from structural considerations, should receive their due attention.

Demonstration of its superior seismic performance in successive moderate and severe earthquakes, as is evident from Figure 2-1, has led to a steady increase in the application of CM walls. This improvement has been achieved at only marginally higher cost, thereby giving this structural system an economic feasibility. Furthermore, taking advantage of the available materials and previous construction practice, to which the local developers are familiar, also have accommodated considerably the dissemination of this structural system.

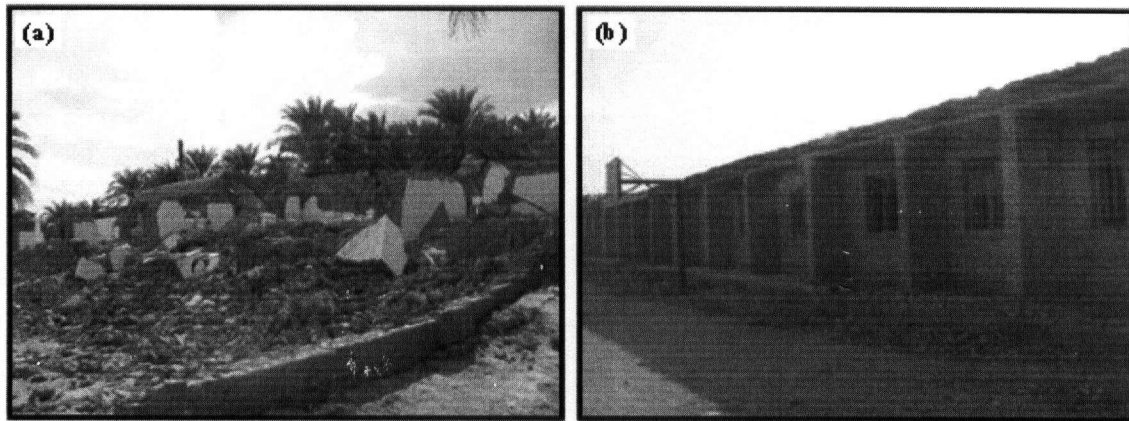


Figure 2-1: (a) A completely demolished URM dwelling, (b) An intact CM building, 2003 Bam earthquake, Iran (Eshghi and Naserasadi, 2005)

Although the details of CM walls have tended to be developed over time based on local customary construction practices, with design and construction therefore to some extent empirical, experimental and analytical studies together with damage observations have effectively contributed to a comprehensive understanding of their seismic behaviour in terms of dominant failure modes and damage patterns, and have shown how some of the seismic deficiencies to which these load bearing walls are vulnerable can be overcome.

Damage pattern and overall seismic behaviour, masonry unit and mortar properties, openings, panel reinforcement, and the effects of such factors as axial stress and panel aspect ratio are amongst the most frequent topics investigated in analytical studies, laboratory tests, and field observations. These topics, together with existing models for prediction of seismic performance of CM walls, are described in detail throughout this chapter.

2.2 Damage pattern and overall seismic behaviour

Despite the presence of stiffness decay due to the formation of flexural cracks along the height of tie columns and micro cracks that exist in masonry units, in elastic range and at the early stages of loading, CM walls may still be approximated as elastic shear beams whose stiffness is provided by both panel and confining elements (Yañez et al, 2004; Alcocer et al, 2004; Irimies, 2000; Gibu and Zavala, 2002). At this stage, as experimental results indicate, strain in tie-column longitudinal reinforcement changes alternately from

positive to negative, implying the monolithic behaviour of CM walls (Tomazovic and Klemenc, 1997(a), Zavala et al, 1998).

Onset of inclined shear cracks in the middle of solid panels and their extension towards tie columns result in further decrease in the stiffness of the panel. The time at which the first major crack forms usually coincides with a substantial detectable decline in effective stiffness. These cracks usually pass through mortar joints in a zig-zag pattern (Marinilli and Castilla, 2004; Yañez et al, 2004; Irimies, 2002).

Post-cracking behaviour of typical CM walls, whose response is mainly governed by shear deformations, is directly influenced by friction, brick interlock, and shear resistance of tie column ends (Flores and Alcocer, 1996). As is shown in Figure 2-2, at this stage, the cracked wall pushes tie columns sideways, and produces permanent tension in them (Tomazovic and Klemenc, 1997(a); Zavala et al, 1998). The masonry panel, in turn, would be under the effect of more compressive stresses, provided that an adequate bond allows sufficient load transfer between wall and confining elements.

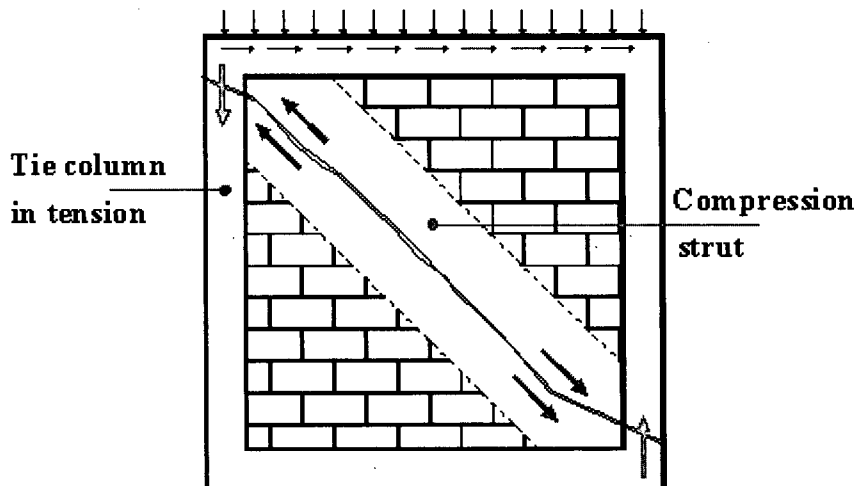


Figure 2-2: Illustration of the seismic behavior beyond cracking limit state

Confinement, in fact, alters the failure mode of URM walls and slows down the rate at which stiffness would decay, therefore improving the post-cracking seismic performance of CM walls. Peak point of the recorded response which defines the maximum load state is usually sustained at the extension of cracks into tie column ends. To prevent these cracks from opening up considerably, it is recommended to restrain the drift capacity of CM walls to some reasonable degree (Alcocer, 1996). This limit, however, is under the

direct influence of panel and confining elements characteristics, and therefore should be determined for each wall appropriately.

As shown in Figure 2-3, post-peak behaviour of CM walls is significantly influenced by reinforcement detailing of tie columns ends. Formation of vertical cracks at wall-column interface, and partial separation of these elements (Zabala et al, 2004; Ishibashi et al, 1992), and penetration of cracks into masonry units (Tomazevic and Klemenc, 1997(a)) at large deformation levels is usually followed by masonry crushing in the middle of the panel, extensive concrete cracking and crushing, and longitudinal rebar rupture/buckling at tie column critical end zones (Alcocer et al, 2004; Tomazevic and Klemenc, 1997(a)). Stiffness of the panel at large deformation levels is mainly provided by confining elements which act to slow the rate of stiffness degradation (Ishibashi et al, 1992). The residual stiffness of a CM wall is about 20% of its initial stiffness at 20% strength loss from the maximum measured shear (Alcocer et al, 2004).

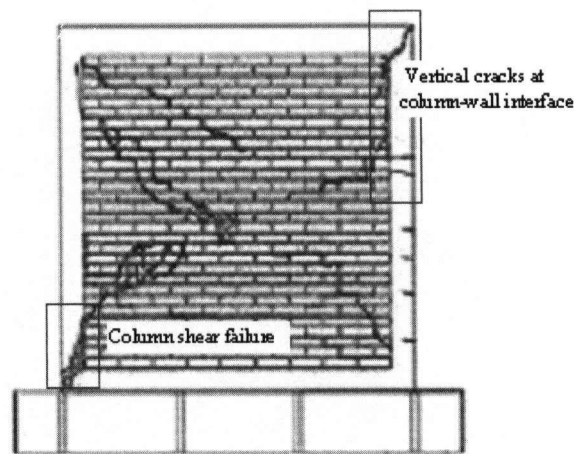


Figure 2-3: Post-peak behaviour of a typical CM wall (Zabala et al, 2004)

For multi-story CM walls, experimental results and aftermath of earthquakes (Figure 2-4) suggest, damage mainly concentrates in the first story, and in the direction of motion. This damage concentration leads to the softening action of first story panels which may be ascribed to the larger-than-unity shear span ratios that these walls usually have, and is confirmed by close match of the first story response curves of such multi-story walls with the seismic response of an isolated CM wall. Dissipation of almost all energy in the critical first story further stresses the leading role of proper confinement of these CM walls (Irimies, 2002; Alcocer et al, 2004; Tomazevic and Klemenc, 1997(b)).

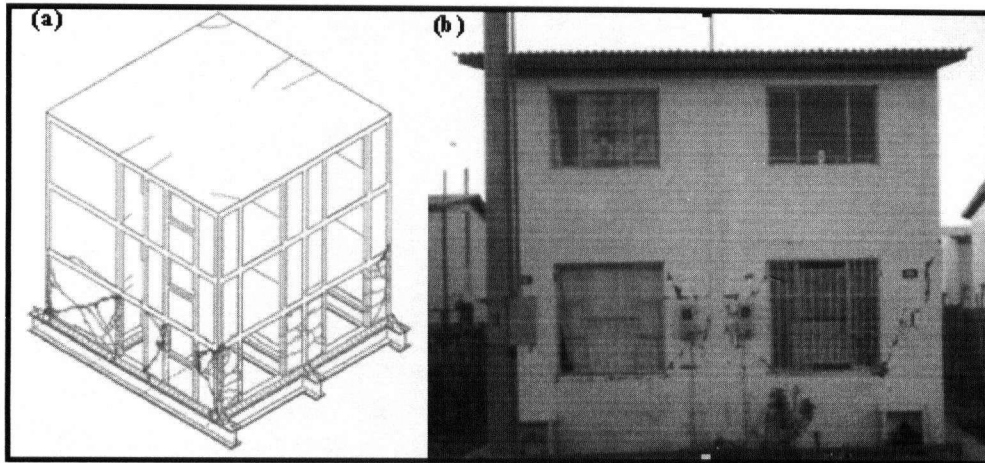


Figure 2-4: CM house with damage concentration in the first story(a) Alcocer et al, 2004 (b) 1997 Punitaqui earthquake, Chile (Gomez et al, 2002)

Such characteristics as low tie column longitudinal reinforcement and high panel aspect ratio, however, may lead to the predominance of flexural deformations. When seismic behavior of CM walls is governed by flexural deformations, as is shown in Figure 2-5 horizontal bending cracks at lower courses of the panel may extend into tie columns ends and shear them off at large deformation levels (Zabala et al 2004). This further emphasizes the vital role of tie column ends shear resistance in the overall seismic behaviour of CM walls.

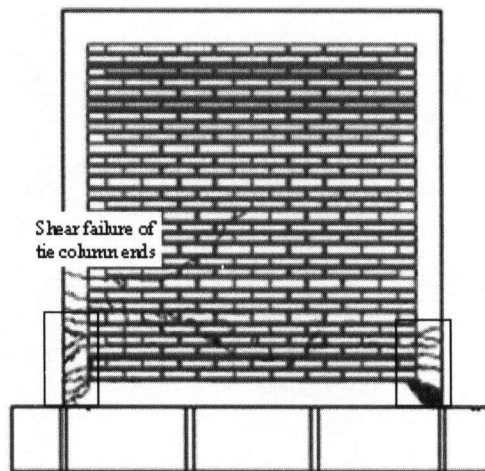


Figure 2-5: Flexural failure and penetration of cracks into tie columns ends (Zabala et al, 2004)

2.3 Masonry unit and mortar characteristics

As one of the constituent components of the panel, masonry units should possess satisfactory properties to ensure acceptable seismic performance of the resultant CM wall. Experimental tests indicate that solid clay bricks, which are among the most frequent unit types used for the construction of CM walls, possess superior seismic characteristics compared to their hollow counterparts (Yamin and Garcia, 1997; Alcocer et al, 2003; Meli, 1991). To be considered solid, however, and to have sufficient deformation capacity, the net area of these units should be at least 75% (Gibu and Zavala, 2002).

Hollow masonry units, commonly used for reinforced masonry (RM) systems, are in practice also relied on for construction of CM walls. To avoid premature masonry crushing in the presence of relatively high axial loads, however, these units should be provided only with vertical holes (Alcocer et al, 2003). Furthermore, the use of this type of masonry unit is not favourable in high seismic zones, due to inherent brittle behaviour that could be ascribed to their high rigidity (Castilla and Marinilli, 2000). Among different types of hollow units, clay bricks possess superior seismic characteristics compared to concrete blocks and calcium silicate units. As a result, hollow calcium silicate bricks are the least favourable unit type for construction of CM walls, especially when high deformation capacities are desired (Yañez et al, 2004; Tomazevic et al, 2004). CM walls made of hand-made solid bricks undergo more severe stiffness degradation compared to those made of industry-manufactured units with high quality control. The use of industry-manufactured bricks would in general help improve the seismic performance of the system in the event of severe earthquake at only marginally higher cost, and is therefore favoured (Gibu and Zavala, 2002; Zabala et al, 2004; Astroza and Schmidt, 2004). However, if designed and constructed properly, CM walls made of hand-made units, as the results of full-scale tests by Zabala et al (2004) confirm, would still perform satisfactorily in earthquakes.

The use of multi-perforated bricks for CM walls, is also increasing, due to their economic advantages. However, the results of experimental tests by Alcocer and Zepeda (1999) indicate that the seismic resistance of CM walls made of these brick units may be only accounted for if provided with minimum panel reinforcement and external tie columns

(RC tie columns cast against the masonry panel) with proper reinforcement detailing. Furthermore, mortar penetration into the holes of these bricks also substantially affects the shear capacity of the panel, and mortar should therefore be provided with sufficient fluidity to fill the holes uniformly (Alcocer and Zepeda, 1999).

To ensure sufficient bond, high-quality mortar with sufficient fluidity and bricks without smooth surfaces should be utilized (Mercado, 2004). In addition, masonry units and mortar should be compatible in their mechanical and absorption properties to compensate somewhat for the high heterogeneity that masonry, as a composite material, suffers from. Similar elastic modulus is one of the essential aspects of compatibility which leads to the propagation of cracks through both constituent materials of the panel (cracks usually initiate in mortar joints and at larger deformation levels pass through the units as well) (Bourzam, 2002). If brick shear strength is very low compared to mortar, inclined cracks, however, will mainly pass through masonry units, thus increasing the potential for masonry crushing at high seismic demands (Ishibashi et.al, 1992).

2.4 Wall density

Depending on the number of stories, seismicity, soil conditions, and the code used as the basis of design and construction of CM structures, wall density (total shear wall area in each principal direction divided by the floor area) can vary considerably. However, as damage observations and the results of analytical studies by Astroza et al, 1993 indicate, a minimum wall density of 1.15% or 0.85% should be used in each principal direction to ensure light or moderate wall damage, respectively.

Wall density per unit weight (wall density in the first story divided by total weight of the structure), as research results of Moroni et al, 2000 indicate, may be employed as a better measure of seismic vulnerability compared to the wall density itself. To confine damage to light or moderate, wall density per unit weight should exceed 0.018 or 0.012 m²/ton (Moroni et al, 2000). As the results of an extensive survey suggest, many CM buildings that satisfy minimum wall density fail to comply with the suggested minimum wall density per unit weight (Moroni et al, 2000).

Sufficient wall density in both principal directions, as is shown in Figure 2-6, is required to prevent extensive damage to the structure at the event of sever earthquakes.



Figure 2-6: Collapse of CM building due to inadequate wall density, 2001 Atico earthquake, Peru (San Bartolome et al, 2004)

However, acceptable seismic performance of CM structures is guaranteed only if adequate wall density is supplemented with proper material quality and reinforcement of tie columns. Furthermore, large wall densities, although beneficial to the load-carrying capacity of CM structures, would limit deformation demands. In consequence, providing the building with as many walls as possible is not always the best solution for improving seismic performance and there is always a trade-off between resistance and ductility.

2.5 Confining elements

Confinement, as the results of experimental tests and aftermath of earthquakes indicate, improves post-cracking seismic performance of masonry walls, in that tie columns and bond beams work to hold structural elements together. Their presence, therefore, will prevent premature wall disintegration at the occurrence of cracking (Tomazevic and Klemenc, 1997(a); Yoshimura, et al, 2004). As is evident from Figure 2-7 the rates at which strength and stiffness degrade are far less for CM walls compared with URM panels. As a result, improvement in deformation and energy dissipation characteristics greatly surpass that of shear resistance for CM walls (Tomazevic and Klemenc, 1997(c)).

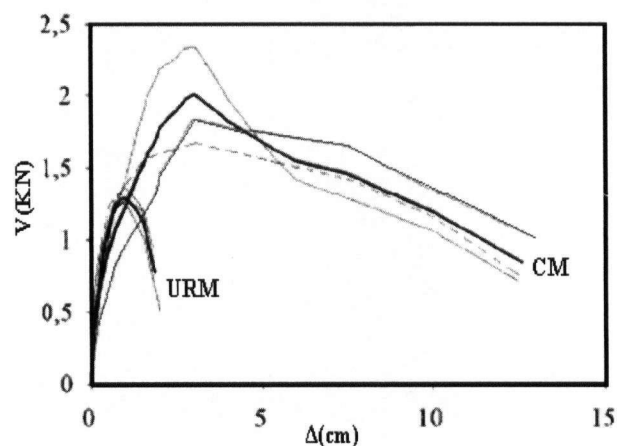


Figure 2-7: The beneficial effects of confinement on the seismic response of masonry panels (Tomazevic and Klemenc, 1997(a))

The effectiveness of confining elements, however, is directly influenced by such parameters as their location, type, size, shape, reinforcement detailing, and the number of tie columns and bond beams. These parameters, although having been adjusted over time based on the results of damage observations and experimental tests, are greatly influenced by the state-of-practice in each region.

The location of tie columns, whose dimensions usually correspond to panel thickness, vary highly from one region of the world to another. To ensure acceptable seismic performance, codes usually call for tie columns at wall corners, intersections, and also at opening ends. Bond beams, on the other hand are recommended to be provided at each floor, and at both sill and lintel levels (Viridi and Raskkoff, 2005; UNIDO/UNDP, 1984; San Bartolome et al, 2004). The dimensions of these confining elements are, however, influenced by both wall thickness and floor type.

The maximum distance between tie columns is usually kept at twice that of bond beams to mitigate the risk of out-of-plane failures which are among the common causes of URM instability in severe earthquakes (San Bartolome et al, 2004).

Experimental tests by Alcocer and Zepeda, 1999 indicate that RC tie columns are superior to their interior counterparts (hollow masonry units, reinforced and grouted), and therefore, their use is preferred, especially in highly seismic regions. Tie columns should be provided with sufficient longitudinal reinforcement to avoid the predominance of flexural deformations and wall uplift as a result of rebar yielding at the base of columns

(Zabala et al, 2004; Iiba et al, 1996). The minimum tie column longitudinal reinforcement is recommended to be higher than 1% in Eurocode 8 (2002). However, Mexican code (NTC-M, 2004) calls for the minimum steel area of $0.2f_c/f_{yc}t_c^2$, provided that the rebar diameter is greater than 6 mm. In fact, increase in the amount of column longitudinal reinforcement substantially improves load-carrying capacity of CM walls. Therefore, critical first story columns located at wall corners are recommended to be provided with larger longitudinal reinforcement ratios, especially when these CM buildings are located on firm soils or in epicentral regions of active faults (Meli, 1991; San Bartolome et al, 1992; Aguilar et al, 1996). However, the strikingly higher flexural capacity of heavily reinforced tie columns would trigger a brittle shear failure mode, and therefore, providing tie columns with as much reinforcement as possible is not always the best solution (Yoshimura et al, 2004).

Transverse reinforcement, on the other hand, augments the dowel action of longitudinal rebar and introduces some level of confinement to the core concrete. As a result, its presence is highly beneficial to the deformation and energy dissipation characteristics of CM walls when provided in appropriate amounts (Yamin and Garcia, 1997; Flores and Alcocer, 1996). Although the stipulated code values vary slightly depending on the region they are developed for, almost all codes (Eurocode 8, 2002; INN, 1997; NTC-M, 2004; NSR, 1998) call for the minimum transverse reinforcement of 6 mm hoops at 150 to 200 mm respectively.

Since post-peak behaviour of CM walls is governed by the reinforcement detailing of tie columns ends, these critical zones should be provided with tightly spaced stirrups (Zabala et al, 2004). Columns with denser stirrups at their ends, as experimental tests suggest, suffer far less damage, which in turn delays the final collapse of the wall (Aguilar et al, 1996). End zones of bond beams, likewise, should be provided with tightly spaced stirrups, because shear cracks, as is shown in Figure 2-8 penetrate into beam-column joints at large deformations and shear these zones off (Astroza and Schmidt, 2004). As a result, the minimum stipulated transverse reinforcement is recommended to get increased at these critical end zones by reducing the distance between successive stirrups to almost half the rest of the span (about 100 mm).



Figure 2-8: Extensive damage to the column-beam joint due to improper reinforcement detailing, 1985 Lolleo Earthquake, Chile (Gomez et al, 2002)

In general, tie columns are recommended to be provided with multiple rebar to avoid their premature rupture, and to enhance the energy dissipation characteristics of CM walls (San Bartolome et al, 1992). Simplification of tie column reinforcement detailing by replacing multiple rebar and stirrups with single equivalent rebar and spiral hoops, as the results of Yoshimura (1995) indicate, would lead to the occurrence of sliding at panel-foundation interface. However, in the presence of both vertical and horizontal panel reinforcement, post-cracking behaviour is almost independent of tie column reinforcement detailing, and therefore columns of such panels, and those with small cross-sections, could be provided with simpler reinforcing details (Yoshimura and Kikuchi, 1995).

Post-cracking seismic performance of CM walls is further improved by the inclusion of intermediate confining elements, simply because they restrain the extent of damage (Blong et al, 1998; Marinilli and Castilla, 2006). However, these intermediate confining elements cannot completely stop the cracks, and as experimental tests indicate, cracks usually pass through them.

Intermediate tie columns and bond beams are recommended for use in the critical first stories of CM buildings in highly active seismic regions, and when panel shear resistance is insufficient on its own (as is the case for poor-quality hand-made units, and at opening borders). These secondary elements, that play their role best when distributed evenly throughout the panels, could be provided with smaller cross sections and simplified

reinforcement details (Lui and Wang, 2000). Placing intermediate tie columns too close together, however, would simulate RM systems and also is not economically viable (Sarma et al, 2003).

2.6 Openings

Experimental tests and damage observations indicate that shear cracks usually initiate at opening corners and extend towards the middle of piers. Size, shape, location and confinement detailing of openings have a great impact on the seismic performance of CM walls. This behaviour is in fact highly correlated to the inclination of the diagonal struts forming either side of the openings, and the shear capacity of tie columns that are utilized to border them (Yañez, et al, 2004).

Opening size and the degree of coupling affect both initial stiffness and cracking pattern. The rate at which stiffness degrades, however, is almost independent of these factors (Ishibashi et al, 1992). While excessively large openings could reduce shear capacity of CM walls by almost 50% (Gostic and Zarnic, 1999), their effect on seismic performance is almost negligible when size is restrained to approximately 10% of the wall gross area (Yañez, et al, 2004). Furthermore, symmetrical distribution of openings and utilizing a spandrel below them are among key factors that can alleviate the harmful effects of openings (UNIDO/ UNDP, 1984; Alcocer et al, 2003; Yañez, et al, 2004).

Opening confinement is also substantially beneficial in preventing the instability of heavily damaged triangular portions besides the openings that can fall out under relatively high axial stresses (Flores et al, 2004). Opening confinement, as is illustrated in Figure 2-9, improves post-cracking deformation and shear capacities of CM walls, and introduces more stability to the response curves. Tie columns at opening extremes help the integral action of the panel and are recommended to be provided with tightly spaced stirrups at the corners of the openings. This will arrest extensive concrete cracking and crushing at opening corners until large deformation levels, thus improving the seismic response of the panel (Flores et al, 2004; Ishibashi et al, 1992; Alcocer et al, 2003).

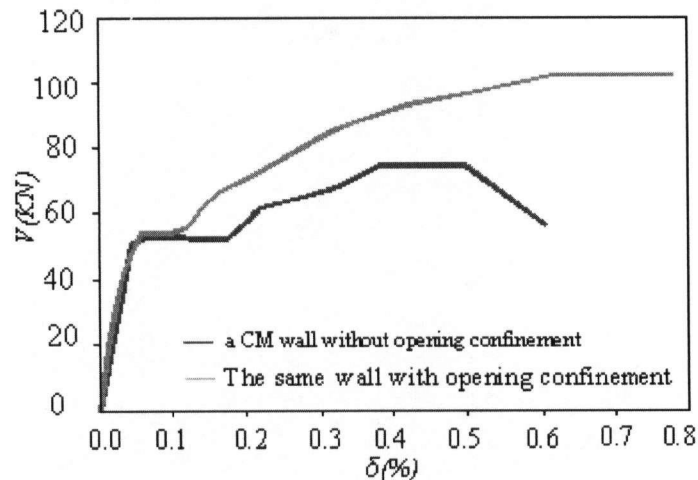


Figure 2-9: Constructive effect of opening confinement on post-cracking seismic performance of CM walls (Leonardo et al, 2004)

Despite the fact that many codes call for horizontal and vertical confining elements at opening borders, it is sometimes not clear what size of openings should be provided with these tie columns and bond beams. Furthermore, failing to comply with these requirements in practice, as is evident from Figure 2-10 usually results in the occurrence of the extensive damage in masonry piers that are left unconfined at one end.



Figure 2-10: Extensive damage to masonry piers due to the lack of proper opening confinement, 1985 Lloleto Earthquake, Chile (Gomez et al, 2002)

2.7 Axial stress

As the results of both experimental and analytical studies suggest, axial stress is highly beneficial to shear capacity and energy dissipation characteristics of CM walls. These effects are more pronounced when panels are left unreinforced in both vertical and

horizontal directions, as is the case for typical CM walls (Yoshimura et al, 2004; Ishibashi et al, 1992).

However, axial stress adversely affects the ultimate deformation capacity of CM walls, especially when its value is excessively high compared to masonry compressive strength. The use of two-way slabs which distribute vertical loads more evenly is therefore highly favoured, especially when the wall is made of hollow masonry units that are more susceptible to premature crushing (San Bartolome et al, 2004; Bariola and Delgado, 1996; Astroza and Schmidt, 2004).

2.8 Panel aspect ratio

Panel aspect ratio is among key factors which alter both damage pattern and failure mode of CM walls. Relatively squat CM walls with aspect ratios close to one are frequently used in practice. Seismic behavior of such walls, as has been repeatedly demonstrated in previous earthquakes, is usually governed by shear deformations. However, as H/L increases, flexural deformations become more dominant, cracks are likely to occur sooner, stiffness degrades at higher rates, and therefore, strength characteristics of the panel are affected (San Bartolome, 2004; Yoshimura et al, 2004; Grumazescu and Gavillescu, 1999).

Although of paramount importance, the effect of panel aspect ratio has been overlooked in many codes and regulations that address seismic behaviour of CM walls. For particularly slender CM walls, flexural deformations greatly surpass those of shear, and therefore these walls are likely to fail in flexural mode. As a result, walls with higher aspect ratios always possess greater deformation capacities compared to their squat counterparts (Astroza and Schimdt, 2004; Alvarez, 1996).

2.9 Masonry-concrete interface

Effectiveness of tie columns to confine masonry panels and to improve their seismic performance is under the direct influence of the existing bond at the masonry-concrete interface. Experimental tests (Figure 2-11) and aftermath of earthquakes indicate that when concrete-masonry adherence is relied upon merely to provide the required bond, the occurrence of vertical cracks and partial disintegration of the panel and confining

elements at large deformations adversely affect the seismic performance of CM walls (Alcocer and Meli, 1993).

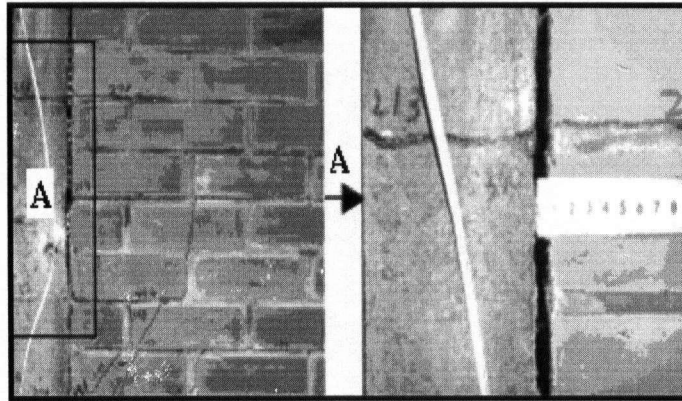


Figure 2-11: Separation of masonry walls and tie column due to the lack of proper bond (Yushimura et al, 2004)

However, casting concrete against toothed end walls which act as shear keys, or providing the CM wall with connection rebar (U-shape or L-shape rebar that are anchored adequately into walls) help improve the bond and load transfer, and therefore, partial separation of masonry panel and tie columns is effectively controlled (Arya, 2000; UNIDO/ UNDP, 1984; Irimies, 2000). When extensively damaged masonry panels are replaced, these connection rebar can be effectively utilized to interconnect the newly-constructed panel with its confining elements (Yoshmiura and Kikuchi, 1995). Connection rebar would introduce more stability to the response curve if it is continuous throughout the panel, and therefore further improvement in deformation capacity of CM walls will be achieved (Kumazava and Ohkubo, 2000).

2.10 Panel reinforcement

Panel horizontal reinforcement improves shear resistance, deformation capacity, and energy dissipation characteristics of CM walls because, in its presence, cracks are distributed more evenly throughout the panel as is shown in Figure 2-12.

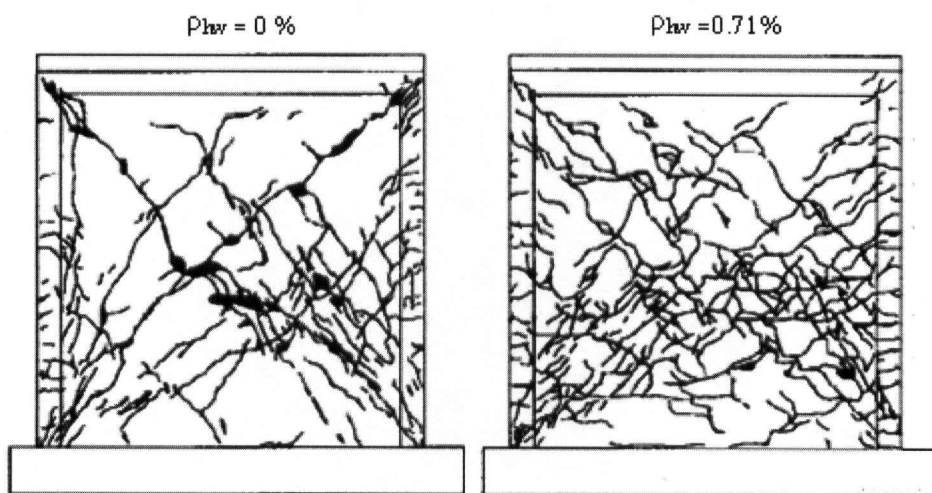


Figure 2-12: The effect of panel reinforcement on damage distribution (Aguilar et al, 1996)

Moreover, the rate at which stiffness and strength degrade will substantially decline, and therefore, more stable response curves are achieved, even at large deformation levels. However, based on the results of experimental tests, the effect of panel horizontal reinforcement on the elastic characteristics of CM walls is almost negligible (Yoshimura et al, 2004; Hernandez and Meli, 1976; Aguilar, 1994; Liba et al, 1996; Alcocer and Zepeda, 1999). The overall effect of panel horizontal reinforcement on the seismic performance of CM walls is illustrated in Figure 2-13.

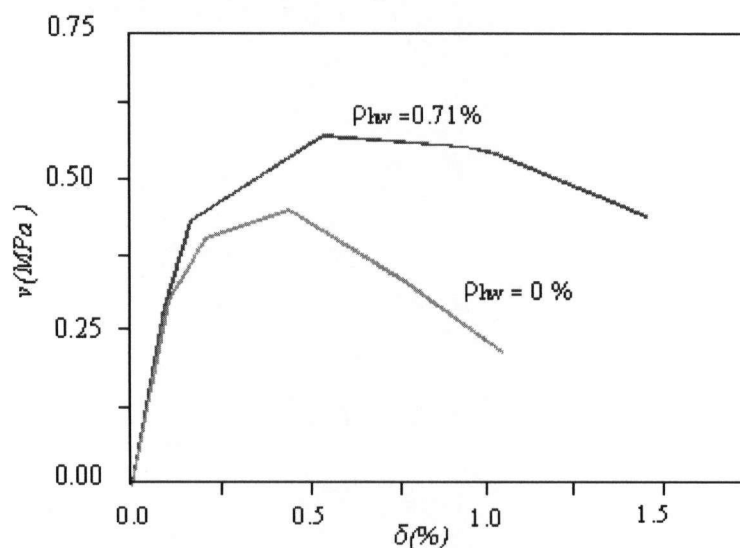


Figure 2-13: The effect of panel horizontal reinforcement on the seismic performance of CM walls (Aguilar et al, 1996)

Chapter 2: Literature review

Efficacy of panel horizontal reinforcement is substantially influenced by two key factors; its amount and type. The amount of panel horizontal reinforcement should be determined to allow yielding of rebar prior to the occurrence of masonry crushing, and to avoid premature rebar rupture before yielding (Flores and Alcocer, 1996). Furthermore, the ratio of horizontal reinforcement to tie column longitudinal reinforcement should always be precisely controlled in order to avoid the predominance of flexural failure mode for over-reinforced CM walls (Casabonne, 2000; Zabala, 2004).

The results of analytical and experimental studies suggest that, in the event of severe earthquakes, heavily reinforced walls will either remain elastic, or will experience a brittle failure mode resulting from masonry crushing prior to yielding of horizontal reinforcement. However, when first-story panels are provided with insufficient reinforcement, fracture of rebar usually occurring near shear cracks and in the middle zones of the wall (where maximum strains are reached) will give rise to sliding of upper stories over these cracks (Aguilar et al, 1996).

As the experimental results suggest, horizontal reinforcement ratio should be kept in the range of 0.005 to 0.017, with an optimum value being about 0.01. (Casabonne, 2000; San Bartolome et al, 2004; Alcocer and Zepeda, 1999; Bingzhang, 1991). In order to account for both panel and rebar characteristics, however, Alcocer and Flores (1996) confined the upper limit to $0.3 f_m/f_{yhv}$.

Horizontal reinforcement may either be embedded in mortar joints (bed-joint reinforcement), or implemented in the form of wire mesh covered with thin layers of mortar (external reinforcement). The use of prefabricated ladder-shape reinforcement in bed joints, however, is not highly favoured due to its tendency to fracture at the welding points of cross-wires and longitudinal rebar (Alcocer et al, 2003). As experimental results suggest, external reinforcement is superior to bed-joint reinforcement in terms of strength characteristics, simply because cover mortar also contributes to shear capacity. However, deformation capacity of reinforced panels is almost independent of the type of reinforcement being used, provided that mortar quality and anchorage spacing are precisely controlled when external reinforcement is employed to fortify the wall (Alcocer et al, 1996).

Top-quality mortar and high-strength masonry units should be utilized, in order to avoid the dominance of premature masonry crushing when panels are provided with bed joint reinforcement (Radovanic, 1998). Corrosion of rebar should also be controlled to prevent them from adversely affecting the bond at the masonry-mortar interface (Cassabone, 2000). Furthermore, to accommodate the installation process, masonry units are recommended to be grooved on their top faces (Mercado, 2004).

Reinforcing the panels in both directions, although not common for CM walls that are provided with lumped reinforcement at their extremes, would further improve the seismic performance of CM walls, especially when hollow units are utilized to construct the panels. The contribution of vertical reinforcement to seismic response is more pronounced for slender panels or any CM wall whose response is governed by flexural deformations (Yoshimura et al, 2000).

2.11 Existing models

The few existing models which predict the seismic behaviour of CM walls have either been developed on the basis of models for URM/RM or are empirically proposed using the results of a small number of experiments. These equations, shown in Table 2-1, simulate only strength characteristics of CM walls.

Cracking shear strength of CM walls, according to these models, is related to panel shear strength (f_m or v_m) and axial load (σ_v) imposed on the walls. However, the effect of panel aspect ratio (H/L), despite its importance, is considered only in the equation developed by Matsumura, 1988. In addition, the contribution of tie columns to post-cracking seismic performance of CM walls is included only in the models proposed by Marrinilli and Castilla, 2006; Tomazevic and Klemenc, 1997(a); and AIJ, 1999. Tie column longitudinal reinforcement ratio, concrete compressive strength and the number of tie columns are among the key design variables that reflect the effect of confinement on the shear capacity of CM walls. However, the other four equations only rely on panel characteristics to predict maximum shear strength of CM walls and overlook the crucial role that tie columns play beyond cracking.

Figure 2-14 compares these models for a typical CM wall ($\sigma_v = 0.55$ MPa, $H/L = 0.97$, $f_m = 5.25$ MPa, $v_m = 0.42$ MPa, $f'_c = 23.05$ MPa, $\rho_{vc} f_{yvc} = 4.29$ MPa, Unit type = Concrete,

$N_{tc}=2$) and for both cracking and maximum shear strengths. It is worth noting that $V_{max-TK97}$ was not included in this figure, due to its direct dependence on cracking shear strength. As is evident from the graphs, strength characteristics of this CM wall vary considerably depending on the utilized model. Therefore, appropriate cracking and maximum shear strength models for CM walls should be proposed.

Table 2-1: Existing models for cracking and maximum shear strength of CM walls

	Notations	Equations	Remarks	References
Cracking Shear Strength	V_{cr-M88}	$V_{cr} = \left(\frac{k_u}{\frac{h_o}{d} + 2} \cdot \sqrt{f_m} + 0.3 \cdot \sigma_v \right) \cdot t_w \cdot j \cdot 10^3$ (Units: N, m)	k_u : reduction factor =0.64 for partially grouted walls and 1 for the rest of the specimens	Matsumura, 1988
			$h_o = 2 h'$	
			$j : 7/8 d, d = L_w - w_{tc}/2$	
	$V_{cr-CC97}$	$V_{cr} = \text{Min}(0.23 \cdot v_m + 0.12 \cdot \sigma_v, 0.35 v_m) \cdot A_w$	---	INN, 1997
	$V_{cr-MAT94}$	$V_{cr} = (0.19 \cdot v_m + 0.12 \cdot \sigma_v) \cdot A_w$	---	Moroni et al, 1994
Maximum Shear Strength	$V_{max-MC04}$	$V_{max} = \text{Min}(0.5 \cdot v_m + 0.3 \cdot \sigma_v, v_m) \cdot A_w$	---	NTC-M, 2004
	$V_{max-CC93}$	$V_{max} = \text{Min}(0.45 \cdot v_m + 0.3 \cdot \sigma_v, 1.5 v_m) \cdot A_w$	---	INN, 1993
	$V_{max-AIJ99}$	$V_{max} = \left[K_u \cdot K_p \cdot \left(\frac{0.76}{\frac{h_o}{d} + 0.7} + 0.012 \right) \cdot \sqrt{f_m} + 0.2 \sigma_v \right] \cdot t_w \cdot j \cdot 10^3$ (Units: N, m)	k_u : the same as V_{cr-M88}	AIJ, 1999
			$k_p = 1.16 \cdot \rho_t^{0.3}$ $\rho_t = A_{s\ tc} / t_w \cdot d$ $A_{s\ tc}$: cross sectional area of column longitudinal reinforcement	
	$V_{max-PC98}$	$V_{max} = (0.5 \cdot \alpha \cdot v_m + 0.23 \cdot \sigma_v) \cdot A_w$	$\alpha = \frac{H}{L}, \frac{1}{3} \leq \alpha \leq 1$	E-070, 1998
	$V_{max-MC06}$	$V_{max} = (0.47 \cdot v_m + 0.29 \cdot \sigma_v) \cdot (A_w - N \cdot A_{tc}) + 4200N$ (Units: kg, cm)	N : number of tie columns	Marinilli and Castilla, 2006
	$V_{max-AC83}$	$V_{max} = (0.6 \cdot v_m + 0.3 \cdot \sigma_v) \cdot A_w$	---	Inspres Cirsoc, 1983
$V_{max-TK97}$	$V_{max} = V_{cr} + 0.806n \cdot d_b^2 \cdot \sqrt{f_c \cdot f_{yv}}$ (Units: N, mm)	d_b : Longitudinal reinforcement diameter	Tomazevic and Kelemence, 1997	
		n : number of longitudinal rebar		

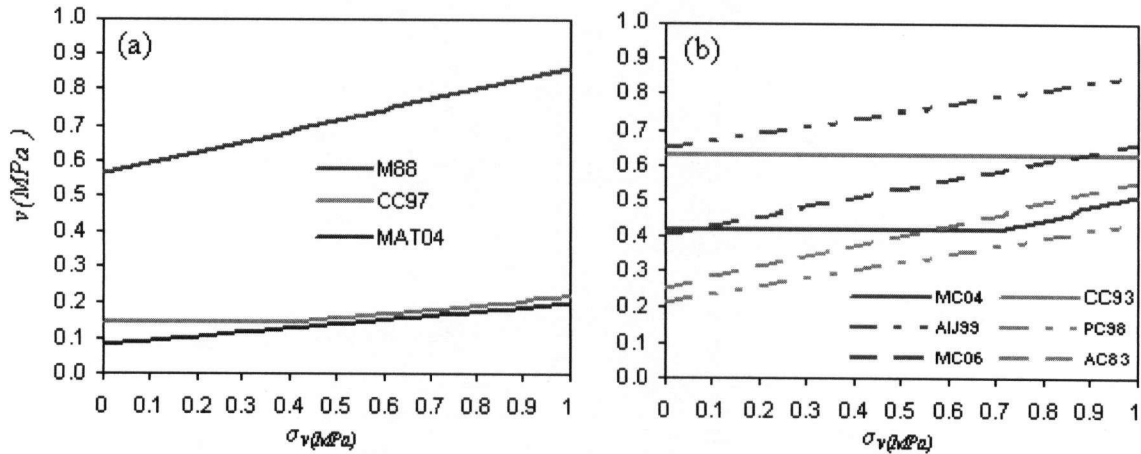


Figure 2-14: Comparison between existing models for a typical CM wall (a) Cracking shear strength, (b) Maximum shear strength

Deformation capacity of CM walls, on the other hand, has been only addressed in a few studies (Astroza and Schmidt, 2004; Urzua et al, 2001) that used the results of experimental tests to impose some practical limits on the deformation capacity at different performance levels. However, no current model addresses this issue which is of great importance to implementation of performance-based earthquake engineering.

According to the findings of these studies and as is shown in Table 2-2, deformation capacity of CM walls is far less than the Chilean code (INN, 1997) stipulated values even considering a 50% probability of failure.

Table 2-2: Deformation capacity of CM walls at 50% probability of failure

$\delta_{\text{cracking}}(\%)$	$\delta_{\text{maximum load}}(\%)$	$\delta_{20\% \text{ strength loss}}(\%)$	Reference
0.13	0.40	0.73	Astroza and Schemidt, 2004
–	0.41	0.69	Urzua et al, 2001
0.62	1.00	<2.50	INN, 1997

The Chilean code figures, however, have been derived on the basis of the seismic performance of masonry infill (MI) walls whose deformation capacities are significantly large considering the ductile behavior of RC frames. In addition, in constructing their fragility curves, Astroza and Schemidt (2004) considered all the 52 data points in their database regardless of the reinforcement detailing of the wall, panel aspect ratio, and the

level of axial stress. As a result, their reported deformation capacities are not representative of the capacity of CM walls with specific characteristics (e.g. with no panel reinforcement or $H/L \leq 1$).

Mexican code (NTC-M, 2004) also calls for some allowable lateral drifts for CM walls with different characteristics as follows;

- 0.35 %: for CM walls with solid units and panel reinforcement
- 0.25%: otherwise

As is apparent from Figure 2-15, these limits, however, are only conservative estimations of the inelastic drift capacity of CM walls which normally have higher capacities according to the conducted experimental tests.

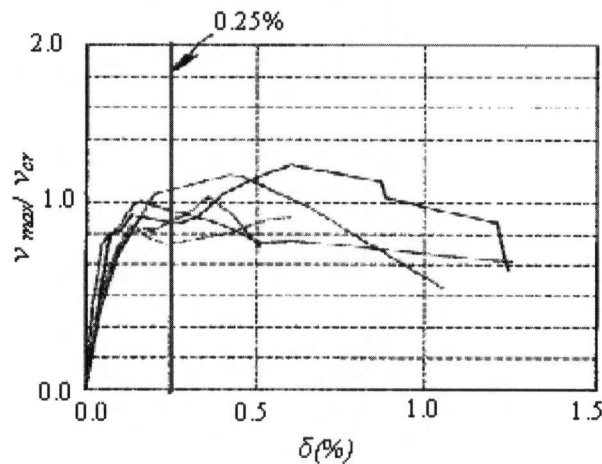


Figure 2-15: Deformation capacity of CM walls made of solid units (Alcocer et al, 2003)

2.12 Closing remarks

Different aspects of CM, as a feasible alternative to URM, its merits and limitations compared to other structural systems, and the seismic performance of this class of structural walls in earthquakes and laboratory tests are among topics addressed by both analytical and experimental studies in this field. The effect of different reinforcement methods, the characteristics of masonry units and mortar as panel constituent materials, and reinforcement detailing of the panel and tie columns have been examined to identify both deficiencies, and the solutions that could be proposed to overcome them.

Out-of-plane seismic behaviour of CM walls, despite its significance for tall thin walls, and characteristics of bond beams are, however, much less discussed in the literature, and

only tie columns and in-plane behaviour have received significant attention. Furthermore, although some research has stressed the effectiveness of opening confinement in improving the seismic performance of CM walls, the size and shape of openings which require confinement has not clearly been expressed. Moreover, masonry codes are not consistent over the question of opening confinement. While the stringent regulations of Mexican code (NTC-M, 2004) calls for confining all openings greater than 600 mm in width, Eurocode-8 (2002) only requires the inclusion of confining elements at the borders of openings whose areas exceed 1.5 m^2 .

The lack of precise analytical models capable of predicting the nonlinear response of CM walls up to large deformation levels is another gap in the literature. The few existing forced-based models have been developed either on the basis of the results of a handful of experiments or were originally proposed for URM/RM walls. The deformation capacity of CM walls was not also addressed properly by masonry codes which either rely on the performance of other structural systems (MI/RM) to propose their practical limits, or are conservative due to the lack of suitable data. In addition, no model exists to predict the deformation capacity of CM walls on the basis of panel and confining element characteristics. Models that are able to simulate the seismic behavior of CM walls in both linear and nonlinear ranges, however, are crucially important for performance-based seismic applications.

2.13 References

Alcocer, S. M., (1996)"Implications derived from recent research in Mexico on confined masonry structures." Proceedings of Structures, Worldwide Advances in Structural Concrete and Masonry, 82-92

Alcocer, S.M., Arias, J.G. Vazquez, A.(2003)."The new Mexico City building code requirements for design and construction of masonry structures" The proceedings of the Ninth North American Masonry Conference, Clemson, South Carolina, 656-667

Alcocer, S.M., Arias, J.G., and Vazquez, A. (2004)."Response assessment of Mexican confined masonry structures through shaking table tests." 13th world conference on earthquake engineering, Vancouver, B.C., Canada, No. 2130

Alcocer, S.M and Meli, R. (1993) "Experimental program on the seismic behaviour of confined masonry structures." Proceedings of the sixth North American masonry conference, Philadelphia, PA ,Vol. 2

Aguilar, G., Meli, R., Diaz, R., Vazquez-del-Mercado, R., (1996)."Influence of horizontal reinforcement on the behaviour of confined masonry walls." 11th World Conference on Earthquake Engineering, Acapulco, Mexico, No 1380

Alcocer S.M., Pineda J.A., Ruiz, J., and Zepeda, J.A. (1996) "Retrofitting of confined masonry walls with welded wire mesh," 11th World Conference on Earthquake Engineering, Acapulco, Mexico, No. 1471

Alcocer S.M., Reyes, C., Bitran, D., Zepeda, O., Flores L.E., and Pacheco M.A. (2002)."An assessment of the seismic vulnerability of housing in Mexico."Proceedings of the 7th US national conference on earthquake engineering, Boston, Massachusetts,USA

Alcocer, S.M, and Zepeda, J.A (1999) "Behaviour of multi-perforated clay brick walls under earthquake-type loading." 8th North American masonry conference, Austin, Texas, USA

Alvarez, J.J (1996) "Some topics on the seismic behaviour of confined masonry structures."11th World Conference on Earthquake Engineering, Acapulco, Mexico, No 180

Arya, A.S. (2000). "Non-engineered construction in developing countries – an approach toward earthquake risk reduction." Proceedings of the 12th World Conference on Earthquake Engineering ,Auckland , New Zealand. No. 2824

Asociacion Colombiana de ingenieria sismics (1998)" Normas Colombianas de diseno y construccion sismo resistente (NSR))

Chapter 2: Literature review

Astroza M.I., and Schmidt A.A. (2004) "Capacidad de deformacion de muros de Albanileria confinada para distintos viveles de desempeno (Deformation capacity of confined masonry for different performance levels)." *Revista de Ingeniería Sísmica* No. 70, 59-75

Bariola, J., and Delgado, C. (1996) "Design of confined masonry walls under lateral loading." 11th World Conference on Earthquake Engineering, Acapulco, Mexico, No.204

Bingzhang, Z. (1991)"Investigation of the seismic design on masonry structural buildings." *Proceedings of the 1991 International Symposium on Building Technology and Earthquake Hazard Mitigation* ,City of Kunming, Yunnan Province, China, 412-418

Bourzam, A. (2002) "Structure behaviour of confined masonry in using solid brick" *Individual Studies by Participants at the International Institute of Seismology and Earthquake Engineering*. Vol. 38, 179-192

Casabonne, C., (2000) "Masonry in the seismic areas of the Americas, recent investigation and developments." *Journal of Progress in Structural Engineering and Materials*. Vol. 2, No. 3, 319-327

Castilla, E., and Marinilli, A. (2000) "Recent experiments with confined concrete block masonry walls." 12th international Brick/block masonry conference, Amsterdam, Netherlands , 419-431

Chuxian, Sh., and Jianguo L., (1991)" Aseismic performance of brick masonry building with RC weak-frame and reinforced masonry wall." 9th International Brick/Block masonry conference, Berlin ,Germany, 498-503

Earthquake engineering research institute (2005)" EERI special earthquake reports"
www.eeri.org/lfe.html

Eshghi, S., and Naserasadi, K. (2005)"Performance of Essential Buildings in the 2003 Bam, Iran, Earthquake." *Earthquake Spectra*, Vol. 21, No. S1, S375-S393

European committee for standardization (2002)" European standard."

Flores, L. E., and Alcocer, S. M. (1996) "Calculated response of confined masonry structures." 11th World Conference on Earthquake Engineering, Acapulco, Mexico, Paper No. 1830

Flores, L.E., Mendoza, J.A., and Carlos Reyes Salinas (2004) "Ensayo de muros de mamposteria con y sin refuerzo alrededor de la abertura." XIV Congreso Nacional de Ingeniería Estructural, Acapulco, Gro, Mexico

Chapter 2: Literature review

Gibu, P., and Zavala C. (2002) " The current state-of -the-art of masonry and adobe buildings in Peru." Japan Peru Center for Earthquake Engineering Research and Disaster Mitigation

Gomez, C., Astroza, M., and Moroni O. (2002) " Confined block masonry building." World housing encyclopedia ([www.world-housing.net/ reports](http://www.world-housing.net/reports))

Gostic, S., and Zarnic, R. (1999) " Cyclic lateral response of masonry infilled RC frames and confined masonry walls." Proceedings of the eighth North American masonry conference, Austin, Texas, USA, 477-488

Grumanazescu, I.P., and Gavrilesco, I.C. (1999) "Different behaviour aspects of confined masonry piers subjected to cyclic reversal and dynamic loads." Proceedings of the Fourth European Conference on Structural Dynamics, EURODYN 919-924

Hernandez , O., and Meli, R. (1976) "Modalozdades de refuerzo para mejorar el comportamiento sismico de muros de mamposteria." Engineering institute, U.N.A.M, Report No. 382, Mexico

Iiba, M., Mizuno, H., Goto, T., and Kato, H. (1996) "Shaking table test on seismic performance of confined masonry wall." World Conference on Earthquake Engineering, Acapulco, Mexico, No 659

INN (1997)" Norma Chilena NCh2123.Of 97 (1997) Albanileria confinada-requisitos de deseno y calculo." Instituto nacional de normalizacion, Santiago, Chile

Inpres-Cirsoc 103. (1983) "Normas Argentinas para construcciones sismorresistentes". Parte III.Construcciones de Mampostería

Irimies, M.T., (2002) "Confined Masonry Walls: the influence of the tie-column vertical reinforcement ratio on the seismic behaviour." The proceedings of the Twelfth European Conference on Earthquake Engineering , No. 7

Ishibashi, K., Meli, R., Alcocer, S.M., Leon, F., and Sanchez, T.A. (1992) "Experimental study on earthquake-resistant design of confined masonry structures." Proceedings of the Tenth World Conference on Earthquake Engineering, Madrid, Spain , 3469-3474

Kato, H.; Goto, T., Mizuno, H., and Iiba, M. (1992)."Cyclic loading tests of confined masonry wall elements for structural design development of apartment houses in the Third World." Proceedings of the Tenth World Conference on Earthquake Engineering, Madrid, Spain, 3539-3544

Kumazava, F., and Ohkubo, M., (2000) "Nonlinear characteristics of confined masonry wall with lateral reinforcement in mortar joints." Proceedings of the 12th World Conference on Earthquake Engineering ,Auckland , New Zealand. No. 743

Chapter 2: Literature review

Liu, D., and Wang, M (2000) "Masonry structures confined with concrete beams and columns." Proceedings of the 12th World Conference on Earthquake Engineering ,Auckland , New Zealand. No. 2720

Marinilli, A., and Castilla, E. (2004). "Experimental evaluation of confined masonry walls with several confining-columns." "13th world conference on earthquake engineering, Vancouver , B.C. , Canada , Accession No. 2129

Marinilli, A., and Castilla, E. (2006) "Seismic behaviour of confined masonry walls with intermediate confining - columns." Proceedings of the 8th U.S. National Conference on Earthquake Engineering, San Francisco, California, USA, No. 607

Meli, Roberto. (1991)"Seismic design of masonry buildings: the Mexican practice." Proceedings of the 1991 International Symposium on Building Technology and Earthquake Hazard Mitigation ,City of Kunming, Yunnan Province, China, 193-210

Moroni, M.O., Astroza, M., and Acevedo, C. (2004) "Performance and seismic vulnerability of masonry housing types used in Chile." Journal of Performance of Constructed Facilities, Vol. 18, No. 3

Moroni M., Astroza M., and Caballero, R., (2000) "Wall density and seismic performance of confined masonry buildings." TMS Journal, July 2000, pp 81-88

Moroni, M., Astroza M., and Mesias, P. (1996)." Displacement capacity and required story drift in confined masonry buildings."11th World Conference on Earthquake Engineering, Acapulco, Mexico, No 1059

Moroni M.O., Astroza, M., and Salinas, C., (1999)." Seismic displacement demands in confined masonry buildings." Proceedings of the eighth North American masonry conference, Austin, Texas, USA, 765-774

Moroni, M. O., Astroza, M., and Tavonatti, S., (1994)."Nonlinear models for shear failure in confined masonry walls." The Masonry Society Journal. Vol. 12, No. 2, 72-78

Norma Peruana de Diseño Sismorresistente E-070 (1998), Capítulo Peruano del ACI.

NTC-M (2004) "Normas tecnicas complementarias para diseno y construccion de estructuras de mamposteria" Gobierno del distriro federal

Radovanovic, Z. (1998)." Nonlinear dynamic analysis of confined masonry buildings according to Yugoslav regulations and Eurocodes." Proceedings of the Eleventh European Conference on Earthquake Engineering , Paris, France

Rodelio Mercado, A. (2004)"Improvement of seismic performance of confined masonry structures." Individual Studies by Participants at the International Institute of Seismology and Earthquake Engineering, vol. 40, 243-255

Chapter 2: Literature review

San Bartolome, A., Quiun, D., and Torrealva, D. (1992) "Seismic behaviour of a three-story half scale confined masonry structure." Proceedings of the 10th World Conference on Earthquake Engineering, Madrid, Spain; 3527-3531

San Bartolome, A., Quiun, D., and Mayorca, P. (2004) "Proposal of standard for seismic design of confined masonry buildings." Bulletin of ERS, No. 37

San Bartolome, A., and Torrealva, D. (1990) "A new approach for seismic design of confined masonry buildings in Peru." Proceedings of the Fifth North American Masonry Conference, University of Illinois at Urbana-Champaign, Vol. 1, 37-44

Sarma, B. S, Sreenath, H.G., Bhagavan, N.G., Ramachandra Murthy, A., Vimalanandam, V. (2003). "Experimental studies on in-plane ductility of confined masonry panels." ACI Structural Journal, Vol. 100, No. 3

Scaletti, H., Chariarse, V., Cuadra, C., Cuadros, G., and Tsugawa, T. (1992). "Pseudodynamic tests of confined masonry buildings Concrete masonry." Proceedings of the 10th World Conference on Earthquake Engineering, Balkema, Rotterdam, Vol. 6, 3493-3497

Tomazevic, M. (1997) "Seismic behaviour of confined masonry buildings, part 1, shaking-table tests of model buildings M1 and M2 : test result." Ljubljana, National Building and Civil Engineering Institute.

^aTomazevic, M., Bosiljkov, V., and Weiss, P.(2004) "Structural behaviour factor for masonry structures." 13th world conference on earthquake engineering, Vancouver, B.C., Canada, No. 2642

^bTomazevic, M., and Klemenc, I. (1997). "Seismic behaviour of confined masonry walls." Earthquake engineering and structural dynamics, Vol. 26, 1059-1071

^cTomazevic, M., and Klemenc, I. (1997). "Verification of seismic resistance of confined masonry buildings." Earthquake engineering and structural dynamics, Vol. 26, 1073-1088

UNIDO/UNDP (1984). "Construction under seismic condition in the Balkan region." Vol. 3: Design and construction of stone and brick masonry buildings.

Urzua, D.A., Padilla, R., and Loza, R. (2001) "Influencia de la carga vertical en la resistencia sismica de muros de albanileria confinada elaborados con materiales pumotocos de guadalajara"

Viridi, S.K., and Raskkoff, D.R. "Low rise residential construction detailing to resist earthquakes: Confined brick masonry"www.staff.city.ac.uk/earthquakes/MasonryBrick/References.htm (December 2005)

Chapter 2: Literature review

Yañez , F., Astroza, M., Holmberg, A.,and Ogaz, O.(2004)"Behaviour of confined masonry shear walls with large openings" 13th world conference on earthquake engineering, Vancouver, B.C., Canada, No. 3438

Yamin, L., and Garcia, L.E. (1997)."Experimental development for earthquake resistance of low-cost housing systems in Colombia." Mitigating the Impact of Impending Earthquakes: Earthquake Prognostics Strategy Transferred into Practice, 377-39

Yoshimura, K., and Kikuchi, K.(1995)." Experimental study on seismic behaviour of masonry walls confined by RC frames." Proceedings of the Pacific Conference on Earthquake Engineering; Melbourne, Australia , Vol. 3, 97-106

Yoshimura, K., Kikuchi, K., Kuroki, M., Nonaka, H., Kim, K.T., Matsumoto, Y., Itai, T., Reezang, W., and Ma, L. (2003)."Experimental study on reinforcing methods for confined masonry walls subjected to seismic forces." Proceedings of the ninth North American masonry Conference, Clemson, South Carolina,USA.

Yoshimura, K. Kikuchi, K. Kuroki, M. Liu, L., and Ma, L.(2000)"Effect of wall reinforcement, applied lateral forces and vertical axial loads on seismic behaviour of confined concrete masonry walls." Proceedings of the 12th World Conference on Earthquake Engineering, Auckland , New Zealand. No. 984

Yoshimura, K., Kikuchi, K., Kuroki, M., Nonaka, H., Tae Kim, K., Wangdi, R., and Oshikata, A. (2004)." Experimental study for developing higher seismic performance of brick masonry walls." 13th world conference on earthquake engineering ,Vancouver, B.C. , Canada , No. 1597

Yoshimura, K., Kikuchi, K., Kuroki, M., Nonaka, H., Tae Kim, K., Wangdi, R., and Oshikata, A. (2004). "Experimental study on effects of height of lateral forces, column reinforcement and wall reinforcement on seismic behaviour of confined masonry walls." 13th world conference on earthquake engineering, Vancouver , B.C., Canada, No. 1870

Yoshimura, K., Kikuchi, k., Okamoto, Z., and Sanchez, T. (1996)."Effect of vertical and horizontal wall reinforcement on seismic behaviour of confined masonry walls." 11th World Conference on Earthquake Engineering, Acapulco, Mexico, No 191

Zabala, F., Bustos, L.J., Masanet, A., and Santalucia, J. (2004)" Experimental behaviour of masonry structural walls used in Argentina." 13th world conference on earthquake engineering, Vancouver, B.C., Canada, No. 1093

Zavala, C., Cabrejos, R., and Tapia, J., (1998)" Aseismic Masonry Building Model for Urban Areas" Structural Engineering World Wide, Paper T209-1

Zavala , C., Honma, C., Gibu, P., Gallardo, P., and Huaco, G. (2004)." Full scale on line test on two story masonry building using handmade bricks" 13th world conference on earthquake engineering, Vancouver, B.C., Canada, No. 2885

Chapter 3

Performance-based Seismic Models for Confined Masonry Walls¹

3.1 Introduction

Performance-based seismic design relies highly on analytical models capable of simulating the performance of structures up to and including the point of failure. Such models must be nonlinear, because almost all structural systems, including confined masonry (CM) walls, are designed to undergo nonlinear behaviour in the event of severe earthquakes. Furthermore, the close relationship between damage and deformation demands, in addition to the necessity to withstand lateral and vertical forces, makes both deformation and strength characteristics equally important.

The evolution of CM walls, as an alternative to unreinforced masonry (URM), whose seismic vulnerability has been repeatedly demonstrated, has been highly influenced by construction practice. Post-earthquake damage observations and laboratory tests provide insight regarding damage patterns, failure modes, and general aspects of seismic performance of CM walls. Backbone response curves – which define the characteristic force-deformation relations from cracking to lateral load failure as a function of design parameters – must, however, be developed and verified to enable the application of performance-based seismic design to CM structures.

¹ A version of this chapter will be submitted for to the Journal of Structural Engineering of the American Society of Civil Engineers for peer-review and publication.

Until now, complete backbone models have not been proposed for CM walls, and past model development, summarized in Table 3-1, has focused only on cracking or maximum shear strength predictions. These predictive equations are either highly influenced by the formulas originally developed for unreinforced and reinforced masonry (RM) walls or are only created on the basis of a limited number of experiments (e.g. Tomazevic and Kelemence, 1997(a)).

Table 3-1: Existing models for cracking and maximum shear strength of CM walls

	Notations	Equations	Remarks	References
Cracking Shear Strength	V_{cr-M88}	$V_{cr} = \left(\frac{k_u}{\frac{h_o}{d} + 2} \cdot \sqrt{f_m} + 0.3 \cdot \sigma_v \right) \cdot t_w \cdot j \cdot 10^3$ (Units: N, m)	k_u : reduction factor =0.64 for partially grouted walls and 1 for the rest of the specimens $h_o = 2 h'$ $j : 7/8 d, d = L_w - w_{lc}/2$	Matsumura, 1988
	$V_{cr-CC97}$	$V_{cr} = \text{Min}(0.23 \cdot v_m + 0.12 \cdot \sigma_v, 0.35 v_m) \cdot A_w$	—	INN, 1997
	$V_{cr-MAT94}$	$V_{cr} = (0.19 v_m + 0.12 \cdot \sigma_v) \cdot A_w$	—	Moroni et al, 1994
Maximum Shear Strength	$V_{max-MC04}$	$V_{max} = \text{Min}(0.5 \cdot v_m + 0.3 \cdot \sigma_v, v_m) \cdot A_w$	—	NTC-M, 2004
	$V_{max-CC93}$	$V_{max} = \text{Min}(0.45 \cdot v_m + 0.3 \cdot \sigma_v, 1.5 v_m) \cdot A_w$	—	INN, 1993
	$V_{max-AIJ99}$	$V_{max} = \left[K_u \cdot K_p \cdot \left(\frac{0.76}{\frac{h_o}{d} + 0.7} + 0.012 \right) \cdot \sqrt{f_m} + 0.2 \sigma_v \right] \cdot t_w \cdot j \cdot 10^3$ (Units: N, m)	k_u : the same as V_{cr-M88} $k_p = 1.16 \cdot \rho_t^{0.3}$ $\rho_t = A_{stc} / t_w \cdot d$ A_{stc} : cross sectional area of column longitudinal reinforcement	AIJ, 1999
	$V_{max-PC98}$	$V_{max} = (0.5 \cdot \alpha \cdot v_m + 0.23 \cdot \sigma_v) \cdot A_w$	$\alpha = \frac{H}{L}, \frac{1}{3} \leq \alpha \leq 1$	E-070, 1998
	$V_{max-MC06}$	$V_{max} = (0.47 \cdot v_m + 0.29 \cdot \sigma_v) \cdot (A_w - N \cdot A_{lc}) + 4200N$ (Units: kg, cm)	N : number of tie columns	Marinilli and Castilla, 2006
	$V_{max-AC83}$	$V_{max} = (0.6 \cdot v_m + 0.3 \cdot \sigma_v) \cdot A_w$	—	Inspres Cirsoc, 1983
	$V_{max-TK97}$	$V_{max} = V_{cr} + 0.806 n \cdot d_b^2 \cdot \sqrt{f_c \cdot f_{yv}}$ (Units: N, mm)	d_b : Longitudinal reinforcement diameter n : number of longitudinal rebar	Tomazevic and Kelemence, 1997(a)

Chapter 3: Performance-based seismic models for confined masonry wall

To be considered robust and indicative of the performance of CM walls with a broad range of design variables, accurate models should be calibrated to data points from extensive databases in a way that analytical predictions closely match experimental results. Such deterministic models can then be implemented in finite element programs or may be extended to consider model uncertainties.

The main objective of this study is to develop the backbone response curve for “typical” CM walls with the following characteristics:

- two tie columns;
- multiple longitudinal rebar per confining element;
- no bed joint reinforcement;
- no openings within the confined panel; and
- height to length ratio of approximately 1.0.

Also evaluated are the effect of openings and panel aspect ratio on the strength characteristics, the validity of the predictive equations for the specimens with bed joint reinforcement, and the capability of existing models to simulate the seismic behaviour of CM walls. The equations, the main outcome of this study, predict mean model parameters. Variability in the model is represented in the coefficients of variation.

The methodology used to produce the final model equations is shown in Figure 3-1. First, model parameters (variables that define the model to be developed), and design variables (those used to predict model parameters) were identified. Additional steps, including setting the functional form of the equations and running the regression analysis, are described in detail in this chapter.

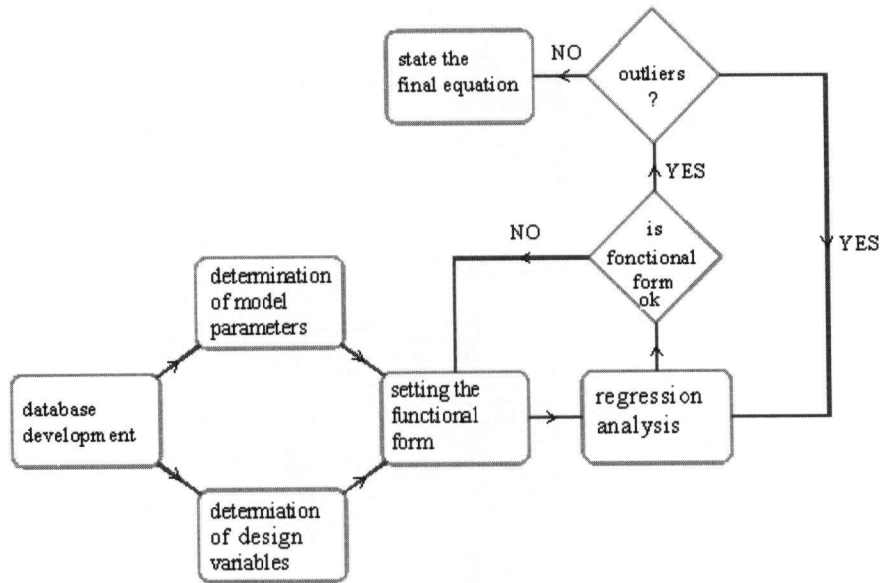


Figure 3-1: The methodology employed to develop the analytical model

3.2 Backbone model and limit states

The shape of the experimental response curve for any structural system is influenced by many factors, including the damage pattern, predominant failure mode, loading protocol, and the number of distinct performance states that can be reliably identified. In this study, limit states (cracking, maximum strength, and ultimate deformation capacity) and their associated model parameters, as shown in Figure 3-2, were identified and measured for any individual test on the basis of these experimental response curves.

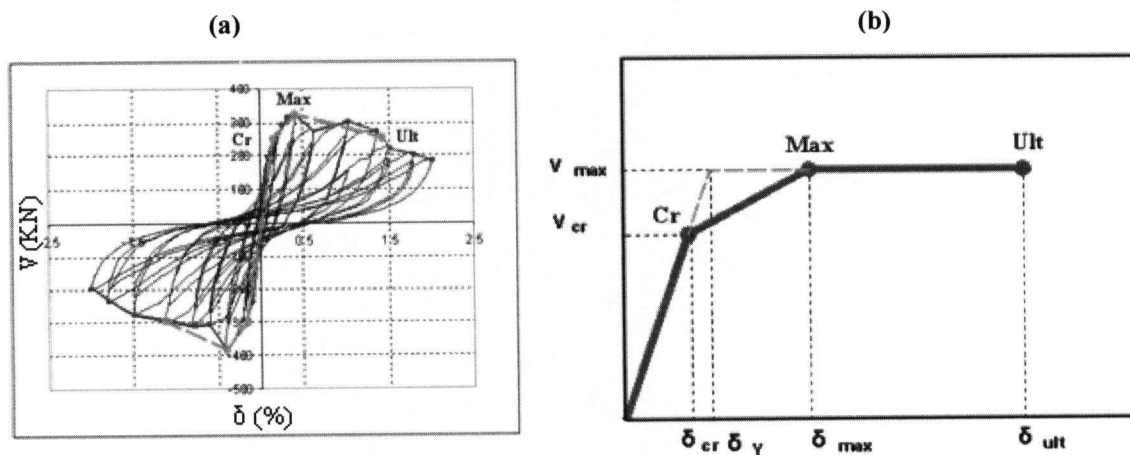


Figure 3-2: (a) Determination of model parameters based on the recorded response, (b) The analytical backbone of the current study

To measure the model parameters, as is shown in Figure 3-2-a, first a smooth backbone was fitted to both positive and negative branches of the recorded response, by implementing the methodology recommended in ASCE/SEI 41 Supplement 1 (Elwood et al, 2007). This backbone (solid line in Figure 3-2-a) was drawn through the peak displacements of the first cycles at each deformation step. A tri-linear backbone (dash line in Figure 3-2-a), was then fit to the smooth backbone for each individual test. This tri-linear curve which passes through the measured model parameters was constructed on the basis of the general aspects of the seismic behavior of CM walls.

As previous studies suggest, for a typical CM wall, whose response is predominately governed by shear deformations, the wall and its confining elements work monolithically at the early stages of loading, and the response is linear-elastic. However, the onset of inclined cracks and their extension towards tie columns reduce the stiffness of the panels. As is evident from Figure 3-2-a, the point at which the first significant cracking occurs is accompanied by approximately 40% decline in the panel stiffness. This point of significant reduction in the effective stiffness was chosen as the cracking point of the analytical model which is defined by two parameters: cracking shear stress (v_{cr}) and its associated drift ratio (δ_{cr}).

Tie columns start to play a role after the cracking limit state is reached. Dowel action of longitudinal reinforcement, which may be augmented by proper detailing of transverse reinforcement, friction, and brick interlock, are the most significant contributors to the shear resistance of confining elements and masonry panel after cracking. As experimental results suggest, the maximum point of the tri-linear backbone (maximum point of the recorded response) is reached when the principal diagonal cracks extend through tie columns ends. This point represents the second limit state of the model, and can be captured with two parameters; the maximum shear stress (v_{max}) and the associated drift ratio (δ_{max}).

Concrete crushing, buckling/rupture of column longitudinal reinforcement, and masonry crushing are the most important factors giving rise to the strength and stiffness deterioration for CM walls. The ultimate drift ratio (δ_{ult}) – the last model parameter – was chosen as the drift ratio at 20% strength loss from the maximum measured shear, or at reported failure load, whichever was reached earlier.

In constructing the analytical model of this study, as is evident from Figure 3-2-b, the only alteration made to the tri-linear backbone was that the value of the maximum strength was kept constant up to the ultimate limit state.

3.3 Proposed empirical equations

3.3.1 Data interpretation and model specification

Several graphical and analytical tools were utilized to select the design variables and to set the functional forms that appropriately relate them to the model parameters. The simplest method of visually searching for relationships between model parameters (e.g. cracking and maximum shear strength) and design variables (e.g. panel aspect ratio, tie column longitudinal and transverse reinforcement, axial stress, etc.) is to plot the parameters versus the variables and search for trends. The major limitation of such a methodology for a large database of CM specimens is that trends are often obscure and hard to detect due to varying loading protocols, testing procedures, and diverse panel and confining element variables. Such plots, in fact, only reveal trends when all variables other than the variable of interest are kept nearly constant. A method for separating data into test series with only a few changing variables was implemented by Haselton (2006), to develop empirical models for reinforced concrete columns. This method was employed in the present study to demonstrate the potentially significant variables, and to identify the trends.

Figure 3-3 depicts the effectiveness of separating the data into test series with one dominantly changing variable. Although several models from Table 3-1 suggest that the shear strength is related to the amount of longitudinal reinforcement in the tie column, no specific trend can be observed in Figure 3-3-a. However, Figure 3-3-b, in which data with the same characteristics are connected with dash lines, indicates that an increase in the normalized longitudinal reinforcement ratio will generally result in an increase in the measured shear strength.

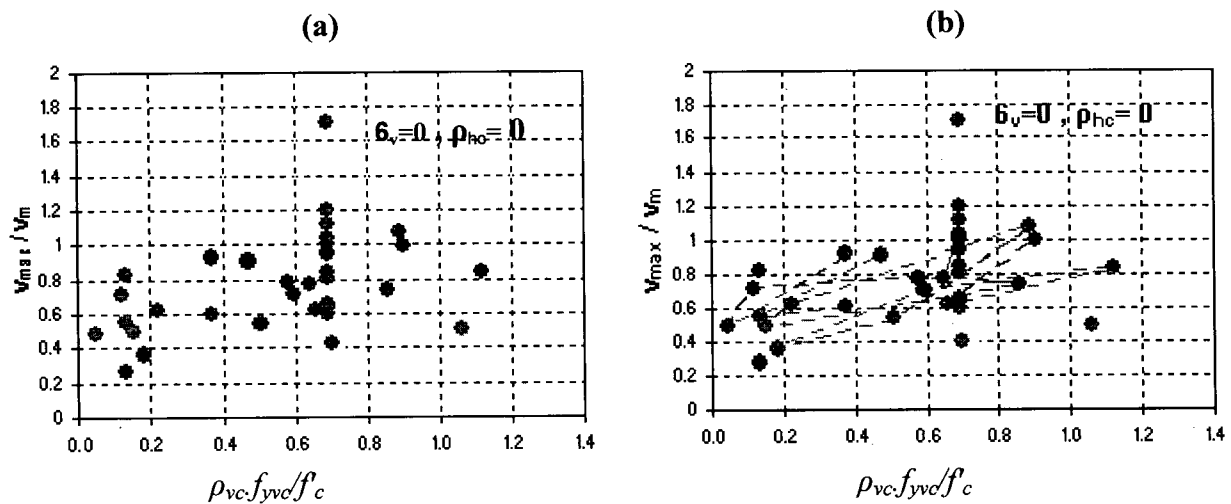


Figure 3-3: (a) Obscure trend between model parameter and design variable, (b) The effectiveness of separating the data into groups with almost the same characteristics to reveal the trends

Existing models, results of previous research, and fundamentals of CM structural behaviour were combined with the previously mentioned visual method to determine the functional form of the analytical equations. Such an iterative procedure began with selecting the most effective design variables, and formulating them into the simplest model form. Performing the first regression analysis and investigating the trends between the residuals (prediction errors) and design variables then assisted in improving these basic functional forms.

Establishing the functional form of the equation, transforming the design variables of interest to fit this specified format, and running the linear regression analysis resulted in determination of the model coefficients. The iterative regression analysis was performed using the statistical software, Stata (Stata press, 2007). After arriving at detailed model equations, those variables whose contribution to the model was insignificant were eliminated, without sacrificing model accuracy. Data inspection, followed by each regression analysis, checking the fitness of the model (R-squared value), and investigating the model overall significance led to the establishment of the final empirical equations.

Detailed information on the regression approach, its fundamental assumptions and the implemented statistical and visual tools, are given in Appendix B. To provide further

insight, general definitions and approaches in this appendix are supplemented with some specific examples from the present study.

3.3.2 Experimental database and criteria for the removal of data

In order to create model equations, a database of 357 CM walls was initially considered. Geometry and reinforcement detailing of the panels and confining elements, loading protocol, the level of axial stress applied to the specimens, scaling factor, recorded hysteretic response, damage pattern and failure mode are among the most important parameters included in the database. Further information on the methodology employed to collect the data and extract the results, the assumptions underlying the development of the dataset, a complete list of the test specimens, anomalies and specific characteristics of each data point, are given in Appendix A.

Prior to focusing on the development of the analytical model, masonry shear strength (v_m) was predicted on the basis of its compressive strength (f_m) considering 197 diagonal compression and masonry compression data from additional testing programs.

In an effort to focus on the behaviour of typical CM walls, however, specimens with the following characteristics were removed from the database and not considered in the development of the models: more than two tie columns, openings in CM walls, simplified reinforcement detailing of tie columns (e.g. single longitudinal rebar and spiral hoops), and panel reinforcement.

Prior to the analysis, initial inspection of the specimens in terms of their characteristics resulted in the elimination of some additional data points. Furthermore, in the process of creating the model equations, some of the data points were also removed from the analysis where they were recognized as having the potential to skew the results of the regression analysis. Leverages (data points with extreme values on single or multiple design variables), and outliers (observations with large prediction errors) were identified and removed from the database if close scrutiny of the references identified test anomalies. Otherwise, the data was kept to avoid any arbitrary removal. The general types of data removed in the process of creating the model equations are described in the list below:

Anomalies in recorded data: Specimens with any anomalies in their response curves for which the determination of some of the model parameters was not accurately possible (e.g. Specimen 117 in Figure 3-4) were taken out, either completely or for the deficient model parameter. The most common anomalies in the response curves that led to the removal of data were: local strength loss, multiple points with 20% loss in strength making the accurate measurement of δ_{ult} impossible, having a large plateau after yielding making the determination of δ_{max} unreliable, and strikingly different response in positive and negative loading.

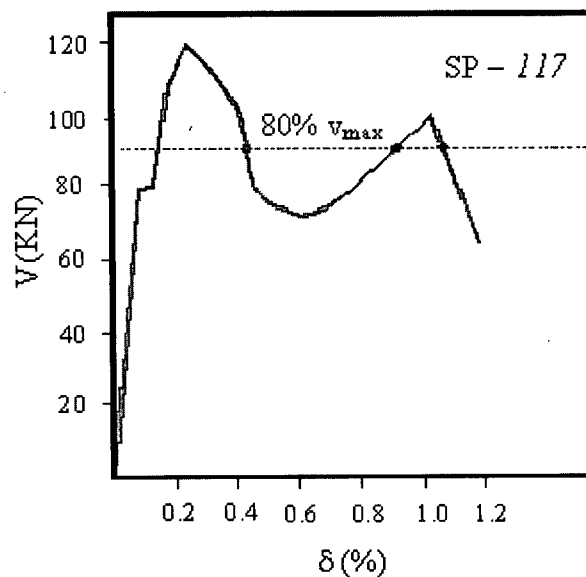


Figure 3-4: Local strength loss and multiple values for δ_{ult} as examples of anomalies that led to the removal of SP-117 for ultimate limit state (Flores et al, 2004)

Complete similitude laws: Small scale specimens were modeled based on two frequently implemented rules: simple similitude and complete similitude laws. While the former keeps the strength characteristics of the model analogous to the prototype, for the latter the strain characteristics coincide. Only four specimens were scaled on the basis of the complete similitude laws and were not comparable with the rest of the data from the stress and strength perspective. As a result, these specimens were eliminated from the model.

Unspecified or unclear parameters: Specimens with unspecified or unclear parameters were removed when these parameters appeared in equations as design variables. For instance, for Specimen 151 (Mercado, 2004) it was not clear whether

the hysteretic curve was given for the panel mid-height or the top. Therefore, the measured drift ratios could not be reliably used for development of the drift models.

Unusual testing procedures: Specimens with anomalies in their testing procedure were left off the list when necessary. For example, specimens which were not pushed far enough to reach 20% loss in strength were not considered for the ultimate limit state. In addition, complex specimens, such as 3D subassemblies, were not used due to the difficulties of comparing their results to typical 2D panel tests.

Diagonal compression loading: Load application in the diagonal direction for a small group of specimens, as shown in Figure 3-5, makes them sustain a predetermined cracking pattern. The substantial difference between the behaviour of these specimens and typical CM walls was also confirmed by the results from the first regression analysis. As a result, these data points were entirely excluded from the model development process.

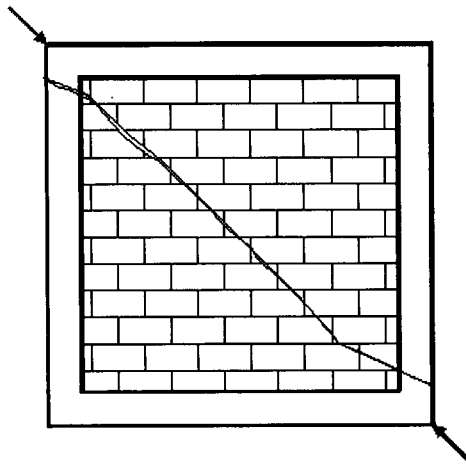


Figure 3-5 : Diagonal compression loading

High axial stress: As previous studies suggest, premature masonry crushing may lead to the occurrence of a significantly brittle failure mode. Therefore, the level of axial stress applied to masonry walls should be restrained to some reasonable portion of the masonry compressive strength. This threshold in many of the current CM codes is suggested to be in the order of $0.12 f_m$. The response of specimens which suffer from premature masonry crushing is not comparable with the rest of data points. However,

to avoid arbitrarily data removal, such specimens were included in the first regression analysis, and their peculiarity resulted in their elimination.

Large aspect ratios: Only ten specimens with panel aspect ratio greater than 2.0 were included in the original database of 357 specimens, and therefore, explicit formulation of their model equations was not accurately possible. In fact, an increase in panel aspect ratio raises the contribution of flexural deformations until these deformations may be controlling the response. Close examination of data and the results of the regression analysis confirmed that these specimens exhibit bilinear behaviour, in contrast to the tri-linear response of typical squat CM walls. As a result, these data points were excluded from the regression analysis. It is also noted, that panels with an aspect ratio greater than 2.0 are rarely seen in CM construction.

Low column reinforcement: Specimens with column longitudinal reinforcement ratio less than 1% were excluded from the final regression analysis when their responses were dominated by flexural failure. It is worth noting that such low reinforcement ratios, however, are not common in practice.

Other specimens: CM walls with concrete units, interior tie columns, and no column transverse reinforcement were not considered in the development of the model. This is also the case for specimens with hollow clay units since they indicate substantially different ultimate deformation capacities compared to the rest of the specimens.

Detailed information on the data that were not included in the final process of model creation, and the type of the problems that resulted in their elimination, is given in Appendix B.

Following data removal, 102 specimens were considered in the development of the analytical model. A complete list of these data points and their most important design variables and model parameters are documented in Table 3-2. Owing to the lack of information on some design variables and model parameters, each equation, however, was developed on the basis of a subcategory of this dataset. The number of data points considered in the prediction of v_{cr} , v_{max} , δ_{cr} , δ_{max} , and δ_{ult} were 80, 39, 52, 37, and 38, respectively. To demonstrate the variability that CM walls inherently possess, the most

important design variables, and their ranges/subcategories are presented in Table 3-3 for the specimens that were considered in the model development.

Table 3-2: The characteristics of Data considered for model development

ID	Loading Protocol	Unit Type	H/L	V_m (MPa)	f_m (MPa)	$\bar{\sigma}_v$ (MPa)	f_c (MPa)	$P_{vc} \cdot f_{yvc}$ (MPa)	$P_{hc} \cdot f_{yhvc}$ (MPa)	V_{cr} (MPa)	V_{max} (MPa)	δ_{cr} (%)	δ_{max} (%)	δ_{ult} (%)
62	RC	Co	0.76	0.52	6.93	0.300	24.26	10.269	3.602	0.32	0.43	0.115	0.271	0.371
74	RC	Cl	1.00	0.38	3.63	0.490	27.47	6.807	0.588	0.31	0.45	0.117	0.426	0.639
99	RC	Cl	0.92	1.11	5.64	0.200	NG	1.056	0.237	0.40	0.49	0.222	0.382	0.397
105	RC	Cl	1.24	1.5	12	0.408	20	8.244	1.488	0.68	0.74	0.086	0.467	0.746
111	RC	Cl	0.70	0.44	2.55	0.000	NG	NG	NG	0.35	0.39	0.050	NG	NG
114	RC	Cl	0.70	0.44	2.55	0.000	NG	NG	NG	0.23	0.28	0.105	0.253	0.599
115	RC	Cl	0.70	0.44	2.55	0.000	NG	NG	NG	0.14	0.16	0.171	0.274	0.800
117	RC	Cl	0.70	0.68	12.75	0.000	NG	NG	NG	0.29	0.32	0.160	0.237	NG
131	M	Co	0.81	0.24	2.44	0.343	13.83	5.136	0.746	0.21	0.26	0.044	0.152	0.176
132	M	Co	0.81	0.24	2.44	0.343	13.83	5.136	0.746	0.33	0.42	0.041	0.163	0.178
135	RC	Cl	0.61	0.55	6.89	0.000	23.9	6.205	1.488	0.29	0.32	0.118	0.535	1.132
136	RC	Cl	0.61	0.55	6.89	0.000	23.9	6.205	1.488	0.25	0.38	0.078	0.634	1.030
137	RC	Co	0.62	0.49	6.04	0.000	23.9	6.205	1.488	NG	0.23	NG	0.231	1.168
138	RC	Co	0.62	0.49	6.04	0.000	23.9	6.205	1.488	0.13	0.25	NG	0.378	1.065
155	RC	Co	0.96	0.57	10.33	0.000	29.43	10.885	0.000	0.24	0.35	0.225	0.428	NG
156	RC	Co	0.96	0.57	14.28	0.233	14.72	10.885	0.000	0.31	0.44	0.078	0.260	NG
158	RC	Co	0.96	0.57	14.28	0.000	19.62	10.885	0.925	0.23	0.38	0.243	0.348	NG
160	RC	Co	0.96	0.57	14.28	0.350	14.72	1.960	0.000	0.29	0.37	0.245	0.523	NG
161	RC	Co	0.96	0.57	14.28	0.000	14.72	1.960	0.000	0.25	0.47	0.114	0.316	NG
162	RC	Co	0.96	0.57	14.28	0.350	14.72	1.960	0.000	0.48	0.62	0.217	0.335	NG
165	M	Co	1.00	0.57	18.07	0.000	29.33	10.885	0.000	0.26	0.53	0.118	0.401	0.616
166	M	Co	1.00	0.57	18.07	0.000	41.2	1.960	0.000	0.20	0.28	0.347	0.865	0.962
167	M	Co	1.00	0.57	18.07	0.000	29.72	3.481	0.000	0.24	0.41	0.076	0.482	0.530
168	M	Co	1.00	0.57	18.07	0.164	33.06	10.885	0.000	0.36	0.49	0.089	0.284	0.372
169	M	Co	1.00	0.57	25.3	0.327	13.34	10.885	0.000	0.43	0.79	0.186	0.500	0.633
170	M	Co	1.00	0.57	25.3	0.654	15.89	10.885	0.000	0.56	0.95	0.215	0.497	0.577
171	M	Co	1.00	0.57	25.3	0.000	18.84	10.885	0.000	0.28	0.45	0.203	0.317	0.795
173	M	Co	1.00	0.57	25.3	0.000	8.14	6.962	0.000	0.40	0.43	0.219	0.334	0.512
175	M	Co	1.00	0.57	25.3	0.981	14.52	10.885	0.000	0.60	1.12	0.147	0.524	0.524
176	M	Co	1.00	0.57	25.3	0.327	13.34	1.960	0.000	0.37	0.47	0.375	0.647	0.767
177	M	Co	1.00	0.57	25.3	0.654	16.48	1.960	0.000	0.55	0.70	0.402	0.879	1.094
181	M	Co	1.00	0.57	25.3	0.000	12.95	1.960	0.000	0.19	0.28	0.165	0.530	0.632
182	M	Co	1.00	0.57	25.3	0.000	15.79	3.481	0.000	0.29	0.36	0.318	0.897	NG
183	M	Co	1.00	0.57	25.3	0.000	12.26	10.885	0.000	0.28	0.61	0.148	0.555	0.583
184	M	Co	1.00	0.57	25.3	0.000	21.48	10.885	0.000	NG	0.31	NG	0.543	0.844
185	M	Cl	1.00	0.33	22.94	0.000	19.23	3.499	0.000	0.11	0.12	0.138	0.285	0.966
186	M	Cl	1.00	0.33	22.94	0.000	32.77	19.429	0.000	0.16	0.24	0.053	0.220	0.898
187	M	Cl	1.00	0.33	22.94	0.000	17.36	19.429	0.000	0.22	0.28	0.107	0.320	0.911
188	M	Cl	1.00	0.33	22.94	0.613	15.3	19.429	0.000	0.45	0.52	0.160	0.266	0.449
189	M	Cl	1.00	0.33	22.94	1.226	12.56	19.429	0.000	0.49	0.80	0.160	0.345	0.400
190	M	Cl	1.00	0.33	22.94	0.000	14.72	9.715	0.000	0.18	0.21	NG	0.448	0.583
191	M	Cl	1.00	0.33	22.94	0.613	13.83	3.499	0.000	0.54	0.65	0.274	0.398	0.583
194	M	Cl	1.00	0.33	22.94	0.000	21.58	19.429	0.000	0.29	0.33	0.122	0.280	NG
195	M	Cl	1.00	0.69	10.01	0.000	10.2	20.289	0.931	0.18	0.24	0.088	0.295	0.582
196	M	Cl	1.00	0.69	10.01	0.286	15.6	20.289	0.931	0.47	0.55	0.234	0.856	1.321
197	M	Cl	1.00	0.69	10.01	0.000	23.25	17.812	0.544	0.26	0.45	0.111	1.340	1.497

Chapter 3: Performance-based seismic models for confined masonry wall

Table 3-2 (Cont.)

ID	Loading Protocol	Unit Type	H/L	V_m (MPa)	f_m (MPa)	$\bar{\sigma}_v$ (MPa)	f'_c (MPa)	$P_{vc} f_{yvc}$ (MPa)	$P_{nc} f_{ync}$ (MPa)	V_{cr} (MPa)	V_{max} (MPa)	$\bar{\delta}_{cr}$ (%)	$\bar{\delta}_{max}$ (%)	$\bar{\delta}_{ult}$ (%)
199	RC	Cl	1.04	0.69	10.01	0.000	14.72	11.835	0.544	0.13	0.17	0.072	0.139	NG
200	RC	Cl	1.04	0.69	10.01	0.472	14.72	11.835	0.544	0.34	0.37	0.397	0.568	NG
219	RC	Co	3.13	0.53	3.46	0.245	19.11	5.998	1.458	0.20	0.21	0.287	0.345	NG
220	RC	Co	2.08	0.43	3.60	0.245	19.11	5.998	1.458	0.15	0.24	0.105	0.285	NG
223	RC	Co	3.13	0.48	3.16	0.123	18.23	5.998	1.458	0.16	0.22	0.117	0.277	NG
224	RC	Co	2.08	0.71	3.13	0.123	18.23	5.998	1.458	0.19	0.28	0.107	0.675	NG
225	RC	Co	1.00	0.47	5.19	0.361	NG	5.998	1.619	0.23	0.37	NG	0.424	NG
226	RC	Co	1.00	0.56	4.31	0.361	NG	5.998	1.619	0.29	0.33	0.175	0.296	NG
227	RC	Co	1.00	0.33	3.06	0.361	NG	5.998	1.619	0.28	0.37	0.142	0.454	NG
228	RC	Co	1.00	0.51	2.72	0.361	NG	5.998	1.619	0.29	0.40	0.203	0.554	NG
229	RC	Cl	1.00	0.38	5.13	0.000	NG	11.835	1.660	0.19	0.27	0.106	0.975	0.975
235	RC	Cl	1.00	0.38	5.13	0.000	NG	12.427	3.500	0.22	0.22	0.074	NG	1.229
238	RC	Co	1.00	0.37	4.05	0.000	NG	6.498	0.000	0.18	0.28	0.063	0.761	1.027
239	RC	Co	1.00	0.37	4.05	0.000	NG	14.728	1.747	0.21	0.22	0.075	0.250	0.372
250	RC	Co	0.97	0.42	5.25	0.549	23.05	5.933	0.551	0.34	0.43	0.087	0.383	0.445
251	RC	Co	0.97	0.42	5.25	0.549	23.05	5.933	0.551	0.29	0.44	0.098	0.334	0.502
252	RC	Co	0.97	0.42	5.25	0.549	23.05	5.933	0.551	0.35	0.54	0.068	0.336	0.502
253	RC	Co	0.97	0.42	5.25	0.549	23.05	5.933	0.551	0.41	0.50	0.075	0.292	0.443
254	RC	Co	0.97	0.42	5.25	0.549	23.05	4.288	0.794	0.42	0.46	0.099	0.252	0.494
255	RC	Co	0.97	0.42	5.25	0.549	23.05	4.288	0.794	0.41	0.46	0.082	0.158	0.362
256	RC	Co	0.97	0.42	5.25	0.549	23.05	4.288	0.794	0.44	0.47	0.070	0.208	0.473
257	RC	Co	0.97	0.42	5.25	0.549	23.05	4.288	0.801	0.45	0.45	0.103	0.103	0.407
265	RC	Cr	1.00	1.08	14.03	0.000	23.69	NG	NG	0.34	0.42	0.125	0.292	0.655
266	RC	Cr	1.00	1.08	14.03	0.000	24.88	NG	NG	0.35	0.56	0.110	0.292	0.580
293	RC	Co	1.00	0.72	9.34	0.430	NG	NG	NG	0.37	0.57	0.260	0.506	NG
294	RC	Co	1.00	0.71	12.65	0.430	NG	NG	NG	0.43	0.54	NG	0.490	NG
295	RC	Co	1.00	0.74	15.52	0.430	NG	NG	NG	0.34	0.49	0.130	0.408	NG
296	RC	Co	1.00	0.74	15.52	0.000	NG	NG	NG	0.19	0.45	0.130	0.558	NG
297	RC	Cl	1.00	0.9	8.29	0.000	NG	NG	NG	0.48	0.64	NG	NG	0.833
301	RC	Cl	1.07	0.8	6.86	0.907	NG	NG	NG	0.75	0.83	NG	NG	0.543
304	RC	Cl	1.00	1.06	7.66	0.000	NG	NG	NG	0.46	0.60	NG	NG	NG
305	RC	Cl	1.00	0.98	7.77	0.000	NG	NG	NG	0.48	0.64	NG	NG	NG
306	RC	Cl	1.00	1.09	10.07	0.000	NG	NG	NG	0.56	0.68	NG	NG	NG
307	RC	Cl	1.00	1.07	9.42	0.000	NG	NG	NG	0.50	0.66	NG	NG	NG
308	RC	Co	0.74	0.78	7.85	0.000	36.7	5.736	3.573	NG	NG	NG	0.190	0.310
313	RC	Co	0.97	0.78	7.85	0.820	36.7	10.186	3.573	NG	NG	NG	0.425	0.450
317	RC	Cr	1.00	0.78	11.96	0.000	NG	NG	NG	0.35	NG	0.150	0.319	NG
318	RC	Cr	1.00	0.78	11.96	0.240	NG	NG	NG	0.54	NG	0.381	0.410	NG
319	RC	Cr	1.00	0.78	11.96	0.480	NG	NG	NG	0.48	NG	0.186	0.189	NG
320	RC	Cr	1.00	0.78	11.96	0.480	NG	NG	NG	0.44	NG	0.107	0.147	NG
321	RC	Cr	1.00	0.78	11.96	0.480	NG	NG	NG	0.57	NG	0.135	0.155	NG
322	RC	Cr	1.00	0.24	2.41	0.000	NG	NG	NG	0.13	NG	0.067	0.212	NG
326	RC	Cr	1.00	0.24	2.41	0.220	NG	NG	NG	0.26	NG	NG	0.531	NG

ID = Identification number, RC = Reversed Cyclic, M = Monotonic, Co = Concrete, Cr = Ceramic, Cl = Clay, NG = Not Given,
 Bold numbers refer to measured model parameters that were considered in the development of model equations at each limit state.

Table 3-3: Important CM design variables considered in model development

Important parameters	Range or subcategories	Important parameters	Range or subcategories
Loading Protocol	Monotonic	f_m (MPa)	2.25 — 25
	Reversed cyclic	δ_v (MPa)	0 — 1
Unit Type	Industrialized solid	f'_c (MPa)	8.14 — 41.20
	Handmade solid	v_m (MPa)	0.25-1.1
	Hollow	Tie Column type	* Exterior
	Multi-perforated		Interior
Unit Material	Concrete	# column longitudinal bars	2 — 6
	Clay	$\rho_{vc} \cdot f_{yvc}$ (MPa)	1.06 — 20.20
	Ceramic	$\rho_{hc} \cdot f_{yhc}$ (MPa)	0 — 4.70
H/L	0.6 — 2	Failure Mode	Shear
* Exterior tie columns refer to reinforced concrete columns cast against masonry, whereas, the interior tie columns are grouted reinforced hollow blocks.			

3.3.3 Prediction of masonry shear cracking strength using f_m

To predict masonry shear strength on the basis of its compressive strength, a simple regression analysis was performed and Equation 3-1 was derived. Prediction of v_m on the basis of f_m is useful from a design perspective, since compressive strength of masonry, not its shear strength, is normally specified in design.

$$v_m = 0.184 \cdot \sqrt{f_m} \quad \text{(Equation 3-1)}$$

Appearance of $\sqrt{f_m}$ in this equation could be taken as an indicator that masonry shear strength is dominantly controlled by its tensile strength. Equation 3-1 predicts the mean shear strength with a coefficient of determination, R^2 , equal to 0.89. While the proposed equation does capture the general trend of increasing shear strength with increasing masonry compressive strength, Figure 3-6 indicates there is still considerable scatter in the data.

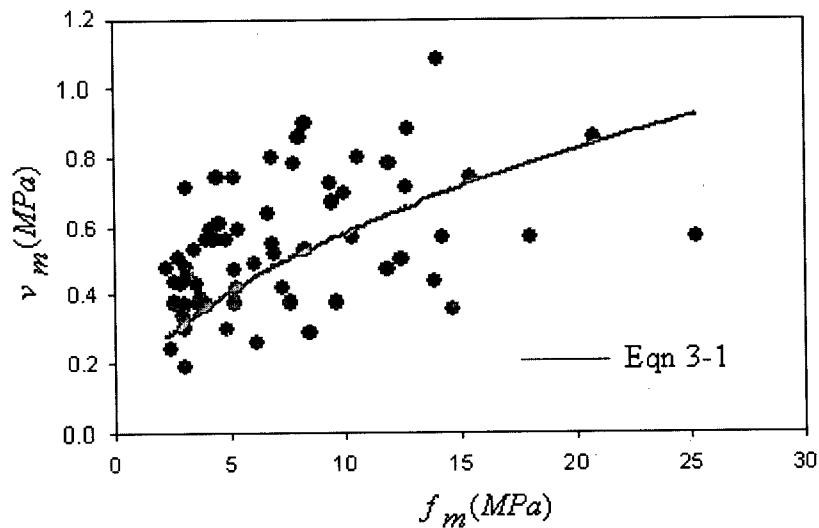


Figure 3-6: The ability of the proposed equation to predict v_m

In the development of the analytical model Equation 3-1 was not used to predict v_m where masonry shear strength was not reported from compression diagonal tests. However, for the specimens that were considered in the model creation the predicted and measured masonry shear strengths were compared not to be substantially different.

3.3.4 Equations for shear cracking strength

3.3.4.1 Equation development

As noted in Chapter 2, CM cracking shear strength (v_{cr}) is governed by panel characteristics, whereas tie column contribution in this linear-elastic portion is almost negligible. On the basis of existing models, visual trends, and formulation of the linear elastic behaviour (idealizing masonry panel as a cantilever shear beam for nearly squat walls (Appendix C)), design variables were selected and functional form of the equation determined. Since slender panels comprise only a small portion of the database, Equation 3-2 was developed only for walls with aspect ratios equal to or less than 1.2

$$v_{cr} = \text{Min}\left(0.424 \cdot v_m + 0.374 \cdot \sigma_v, v_m\right) \quad \text{(Equation 3-2)}$$

As statistical measures indicate, v_m and σ_v contribute equally to this equation, and therefore, both masonry shear strength and axial load are of paramount importance to the strength characteristics of CM walls at the cracking limit state. Figure 3-7 compares v_{cr}

with these two design variables and the capability of the proposed equation to simulate the observed behaviour of CM walls.

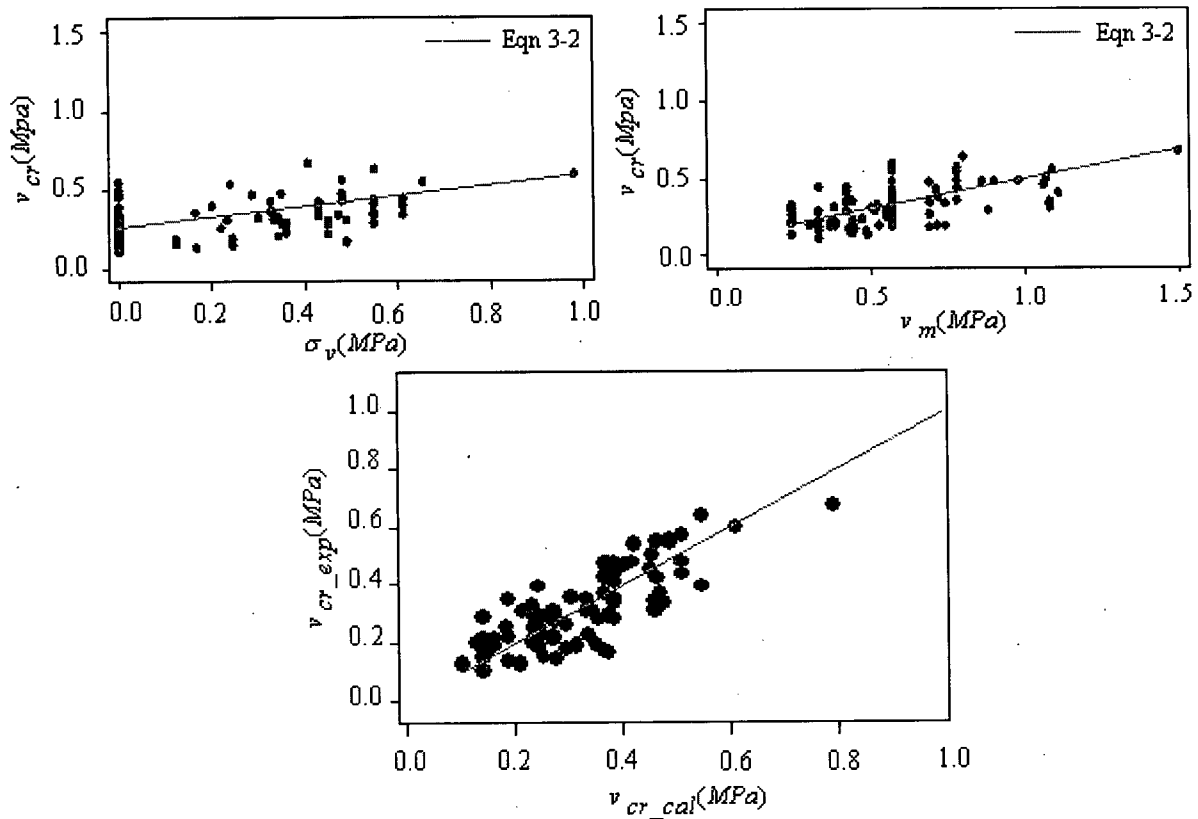


Figure 3-7 : Fitness of the proposed model to the experimental data

3.3.4.2 Comparison with existing models

As is apparent from Table 3-1, the proposed equation to predict v_{cr} is quite similar to the existing cracking models in its form and constituent variables. However, among these models, *M88* was originally developed for RM, and as is illustrated in Figure 3-8-a, greatly overestimates the shear cracking strength of CM walls. The other two equations for the cracking shear strength (*CC97* and *MAT94*), on the other hand, are highly conservative, and as shown in Table 3-4, are not appropriate for design purposes.

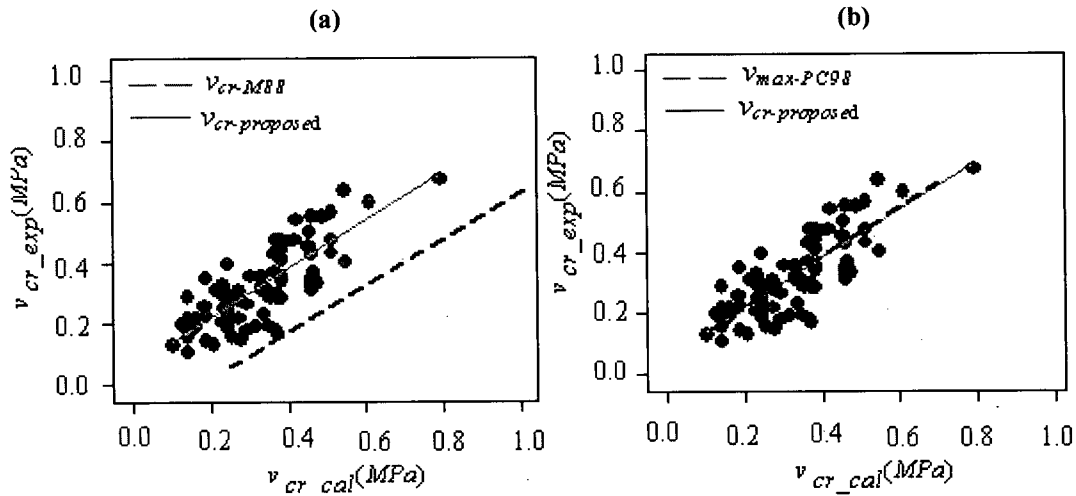


Figure 3-8: Ability of the proposed equation and existing models to predict v_{cr}

Since 4 of the 7 existing models for maximum shear strength rely only on panel characteristics (Table 3-1), they were compared with the proposed cracking shear equation of this study. While *MC04* slightly departs from the proposed equation, *CC93* and *PC98* (Figure 3-8-b) closely match both experimental data and the developed model. However, *PC98* is superior, in that it takes into account the effect of panel aspect ratio, and may be reliably used for slender CM walls.

Among the remainder of the models listed in Table 3-4, *AC83* with much higher v_m coefficient, and *AIJ99*, *MC06*, and *TC07* which incorporate the confinement effects of tie columns in their equations, fail to properly predict v_{cr} .

Table 3-4: Comparison between existing models and actual response of CM walls

Notations	$v_{cr(exp)} / v_{cr(cal)}$	$v_{max(exp)} / v_{max(cal)}$	References
$V_{cr-proposed}$	1.05	—	—
V_{cr-M88}	0.51	—	Matsumura, 1988
$V_{cr-CC97}$	2.24	—	INN, 1997
$V_{cr-MAT94}$	2.52	—	Moroni et.al, 1994
$V_{max-proposed}$	—	1.00	—
$V_{max-MC04}$	0.97	1.39	NTC-M, 2004
$V_{max-CC93}$	1.05	1.27	INN, 1993
$V_{max-AIJ99}$	—	0.96	AIJ, 1999
$V_{max-PC98}$	1.01	1.29	E-070, 1998
$V_{max-MC06}$	—	0.75	Marinilli and Castilla, 2006
$V_{max-AC83}$	0.83	0.97	Inspres Cirsoc, 1983
$V_{max-TK97}$	—	0.69	Tomazevic and Klemence, 1997

3.3.4.3 The effect of openings

Openings are believed to adversely affect the seismic performance of CM walls, and therefore, their size, location, and number in addition to their confinement detailing, have recently received considerable attention (Ishibashi et al, 1992; Yañez, et al, 2004; and Flores et al, 2004). These specimens, however, comprise only a small portion of the database. Keeping the size of the opening as the only varying factor between typical CM walls and those with openings, resulted in consideration of only 14 specimens tested by Yañez et al (2004) to assess the opening effects.

To identify the effect of openings, a plot of v_{cr} versus β (the ratio of the opening area to HL) was drawn and a linear relationship was fitted to the experimental data. As Figure 3-9 illustrates, an increase in the size of openings results in a relatively sharp decline in the cracking shear strength of the intact specimen with the same panel and confining element characteristics. Being developed on the basis of only a few specimens, Equation 3-4 has its own limitations, and therefore, should be utilized with caution.

$$\frac{v_{cr}(\beta \neq 0)}{v_{cr}} = -2.2 \cdot \beta + 1 \quad \text{(Equation 3-4)}$$

v_{cr} should be determined on the basis of Equation 3-2.

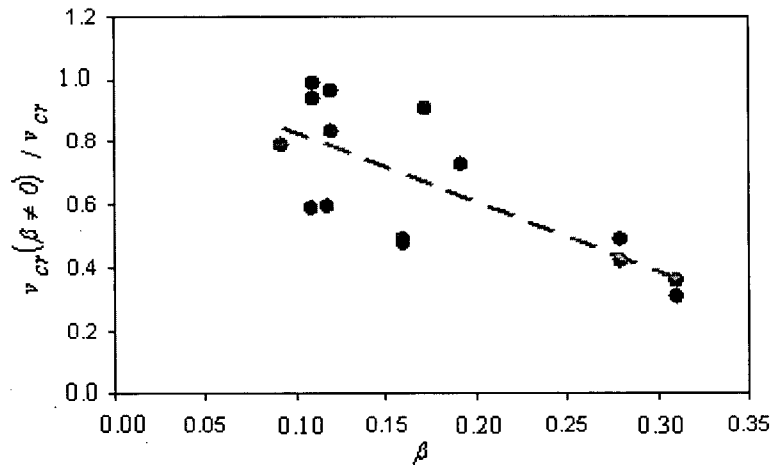


Figure 3-9: The effect of openings on cracking shear strength of CM walls

3.3.5 Equations for maximum shear strength

3.3.5.1 Equation development

The database results indicate that the maximum shear strength is, on average, 1.3 times the cracking strength of the panels, suggesting that the post-cracking contribution of tie columns to the seismic performance of CM walls is of significance. However, only a few existing models (*MC06, AIJ99, and TK97*) rely on such column design variables as longitudinal reinforcement ratio, concrete compressive strength and the number of tie columns in order to predict the maximum shear capacity of CM walls. These studies, as was noted in Chapter 2, attribute the effect of tie columns to dowel action of longitudinal reinforcement, which is augmented by the proper detailing of transverse reinforcement. As a result, both panel characteristics (v_m , and σ_v) and tie column design variables ($\rho_{vc} \cdot f_{yvc}$, $\rho_{hc} \cdot f_{yhc}$, and f'_c), along with the type of masonry units (clay, concrete and ceramic), were considered in the prediction of the maximum shear strength of CM walls. In fact, when the maximum shear strength is attained for a CM wall, cracks will develop in the tie columns at the ends of the diagonal compression strut (see Figure 2-2). Shear forces must be transferred across these cracks and can be appropriately modeled by shear

friction. Loov et al (1994) proposed that shear friction may be represented by two components: $C_1 + C_2\sqrt{\sigma f'_c}$. In this model, σ – the normal stress acting on the crack – is primarily influenced by column longitudinal reinforcement, and to a lesser degree by transverse reinforcement detailing (Loov et al, 1994). Hence, a term in the form of $C_2\sqrt{\rho_{vc}f_{yvc}f'_c}$ was considered in the development of the maximum shear strength model to reflect the effect of tie columns. Note that, the cohesion term (i.e. C_1) was found to be insignificant for the formulation of the maximum shear strength for CM walls, and hence, was eliminated without sacrificing the model accuracy.

Unit type and tie column transverse reinforcement, based on statistical tests and the results of regression analysis, also proved insignificant and were therefore excluded from the process at an early stage. Furthermore, improvement of the model statistical significance using the functional form of the equation proposed by Loov et al (1994) demonstrated the accuracy of considering the effect of tie columns through shear friction. Running the regression analysis for panels with aspect ratios equal to or less 1.2 resulted in Equation 3-5 for the maximum shear capacity of CM walls.

$$v_{max} = 0.21 \cdot v_m + 0.363 \cdot \sigma_v + 0.0141 \cdot \sqrt{\rho_{vc} \cdot f_{yvc} \cdot f'_c} \geq v_{cr} \quad \text{(Equation 3-5)}$$

Maximum shear strength from this equation should always be equal to or greater than the cracking shear strength determined from Equation 3-2. No specific trend with transverse reinforcement is evident from Figure 3-10, used to show the ability of the proposed model, thus supporting the exclusion of transverse reinforcement from Equation 3-5.

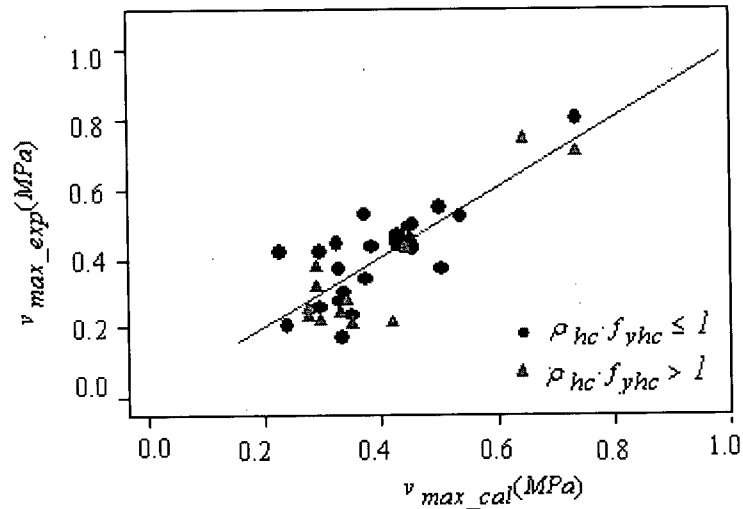


Figure 3-10: Fitness of the proposed model to the experimental data

Based on statistical measures, axial stress is the most significant variable in this equation, followed by the term that accounts for the contribution of tie columns. However, the contribution of panel shear strength, v_m , to maximum shear capacity is minimal compared to other variables.

3.3.5.2 . Comparison with existing equations

MC06, *AIJ99*, and *TK97* are the only existing models that consider column design variables to predict the maximum shear strength of CM walls (Table 3-1). As shown in Figure 3-11, however, these models fail to match the experimental results closely, and are therefore incapable of simulating the actual response at this limit state. As is apparent from this figure, in spite of being very similar in its formulation to the empirical model of this study, *TK97* overestimates the contribution of tie columns by over three times. This could be attributed to the fact that this model was developed on the basis of a few experimental tests that were scaled using complete similitude laws, and, as noted previously, these specimens exhibited different response characteristics compared to other panels in the database.

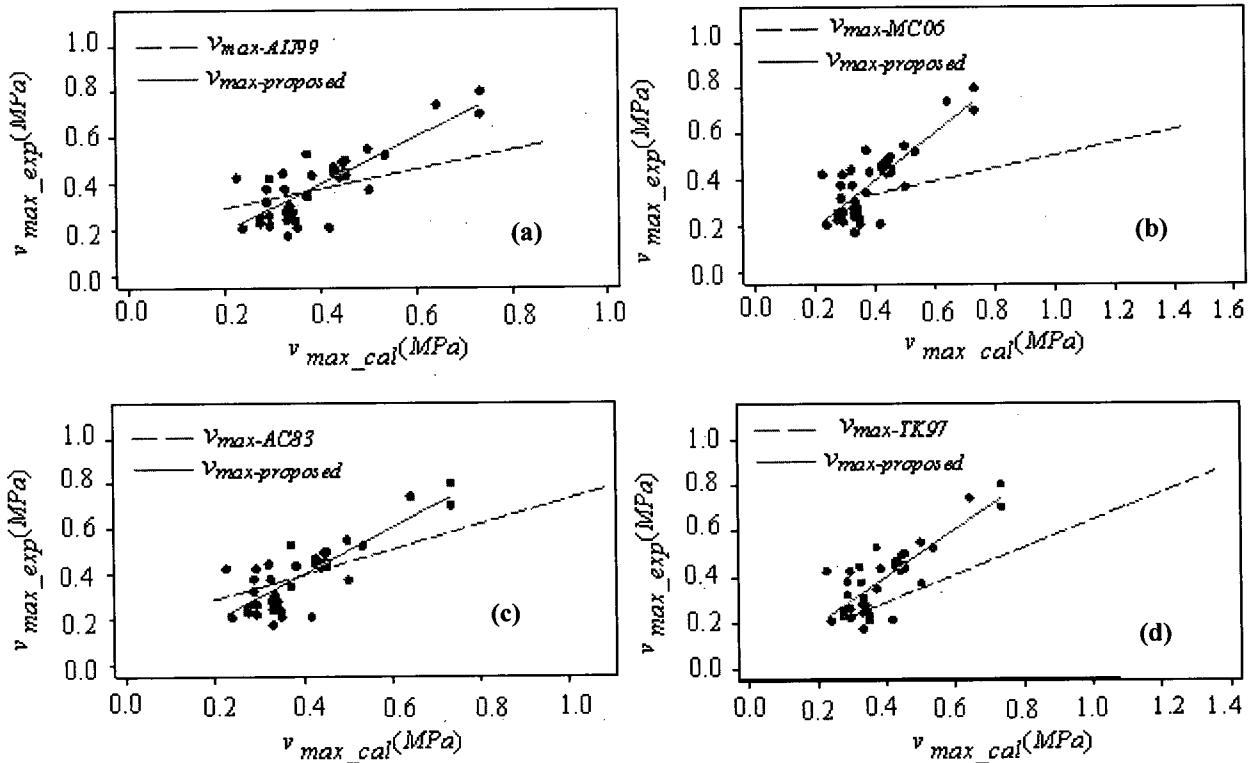


Figure 3-11: Comparison between the proposed and existing models to predict v_{max}

As shown in Table 3-4 and Figure 3-11, *AC83*, despite not considering column design variables, on average, provides a good estimate of the maximum shear capacity of CM walls. However, accentuating the contribution of panel shear strength which, compared to other variables, is minimal at this stage, may be considered its weakness. The effect of tie columns should have been incorporated in axial stress, if simplicity were the goal.

3.3.6 The effect of panel aspect ratio on strength characteristics

Assuming CM walls as homogeneous cantilever beams which behave linearly up to cracking limit state, and considering the relationship that most of the masonry codes assume between masonry elastic modulus and its compressive strength (E_m is proportional to f_m^c) Equation 3-3 was derived as follows:

$$V_{cr} = k_{cr} \cdot \Delta_{cr} \quad , \quad K_{cr} = \beta_1 \cdot K_{int} \quad , \quad G_m = \beta_2 \cdot f_m^c$$

$$K_{int} = \left(\frac{H_w^3}{3 \cdot E_m \cdot I_w} + \frac{H_w}{G_m \cdot A_w} \right)^{-1}$$

$$v_{cr} = \frac{\delta_{cr} \cdot f_m^c}{\gamma \left(\beta_3 \cdot \left(\frac{H}{L} \right)^2 + 1 \right)} \quad \text{(Equation 3-3)}$$

The term in the denominator of this equation accounts for the panel stiffness and γ and β_3 are constants.

For typical CM walls whose response is dominated by shear deformations, the first term in the stiffness equation which accounts for the contribution of flexural deformations may be ignored. Therefore, panel aspect ratio appears insignificant for squat CM walls with aspect ratios close to one. This is also confirmed by the results of the regression analysis, where H/L appears insignificant to the cracking shear strength model for CM walls with $H/L \leq 1.2$. However, as panel aspect ratio increases, the contribution of flexural deformations, and in turn, panel aspect ratio to the response becomes more significant, and for really slender walls this type of deformation would control the response. As a result, the term indicative of the role of aspect ratio in Equation 3-3 should be considered for slender panels to come up with accurate cracking and maximum shear strength models.

In order to incorporate the effect of panel aspect ratio into cracking and maximum shear strength equations, fundamentals of the CM behaviour for slender walls discussed above, and previous models were consulted. The coefficient α which is multiplied by v_m in Equation 3-2 and 3-5 was determined on the basis of a few data points since slender CM walls comprise only a small portion of the database.

$$\alpha = \left[1, \frac{H}{L} \leq 1.2 \quad \frac{L}{H}, 1.2 < \frac{H}{L} \leq 1.5 \quad \left(\frac{L}{H} \right)^2, 1.5 < \frac{H}{L} \leq 2 \right]$$

Although α is utilized consistently to reflect the effect of panel aspect ratio in both cracking and maximum shear strength models, the significance of H/L to Equation 3-5 is far less simply because it is multiplied by a smaller factor.

Being only developed on the basis of a few experimental tests (7 specimens altogether), this coefficient should be utilized with caution for CM walls with aspect ratios greater than 1.5 and its accuracy should be improved by conducting more experimental tests. However, such slender walls are not commonly used in CM practice.

3.3.7 Equation development for drift capacity at cracking limit state

Idealization of typical CM walls as cantilever shear beams, assuming a linear relationship between cracking shear capacity and its corresponding drift ratio (Appendix C), and comparison between various design variables all assisted in the formulation of cracking drift capacity equation, for which no previous model existed. Shear modulus of masonry (G_m), as was noted in the previous section, could be related to its elastic modulus (E_m) assuming masonry as an approximately homogeneous material prior to cracking. Elastic modulus, however, in many masonry codes and regulations is proportioned to its compressive strength. As a result, f_m and unit material – clay, concrete and ceramic – were initially selected as representatives of the masonry shear modulus, and v_{cr} (from Equation 3-2), composed of three independent variables itself, was chosen as the third contributing design variable. The presence of a clear trend in the plot of residuals versus the predictor variable after the first regression analysis, however, resulted in a square root transformation of f_m . The type of unit materials, also proved significant, and was therefore included in the final formulation of the model (Equation 3-6).

$$\delta_{cr} = \gamma \cdot \frac{v_{cr}}{\sqrt{f_m}} \quad \gamma = \begin{pmatrix} 1.128, \text{clay} \\ 0.717, \text{concrete} \\ 0.949, \text{ceramic} \end{pmatrix} \quad \text{(Equation 3-6)}$$

v_{cr} and f_m should be incorporated in MPa in this equation.

Due to the lack of data for slender walls, Equation 3-6 was also developed for panels with aspect ratios less than 1.2. The number of specimens included in the model was 18, 23, and 11 for clay, concrete and ceramic units respectively, and their corresponding R^2 were 0.811, 0.887, and 0.936.

The value of γ for clay units, which are believed to possess the most ductile behaviour among considered unit materials, seems reasonable. However, since ceramic is generally more brittle than concrete, one may expect the gamma for ceramic to be lower. This discrepancy may be related to the number of ceramic specimens available to develop the model, and therefore, more experimental tests of CM walls made of these units may be required.

3.3.8 Equation development for ultimate drift capacity of CM walls

Lack of empirical/analytical models for predicting the deformation capacity of CM walls, nonlinearity, and contribution of both panel and tie column design variables to the ultimate drift capacity, made variable selection and model specification very difficult at the ultimate limit state. However, since shear strength degradation is mainly ascribed to concrete and masonry crushing, and rebar rupture/buckling, concrete compressive strength (f'_c), both column longitudinal and transverse reinforcement ($\rho_{vc}, f_{yvc}, \rho_{hc}, f_{yhc}$), and axial stress to masonry compressive strength ratio (σ_v/f_m) were initially considered as significant variables. The dependence of stiffness degradation on unit materials, as was noted in the calculation of δ_{cr} , also resulted in the inclusion of this variable in the development of the model.

The yield drift capacity (δ_y) defined by cracking stiffness and maximum shear capacity (Figure 3-2-b) was multiplied by a ductility factor (μ) to determine the ultimate drift capacity of CM walls. In fact, δ_y was first determined by substituting v_{max} for v_{cr} in Equation 3-6. All that remained therefore was to determine the ductility factor.

Selecting v_{max} from Equation 3-5 (which reflects the influence of v_m , σ_v , ρ_{vc}, f_{yvc} and f'_c) on the basis of an iterative process, and including unit material in the calculation of δ_y , column transverse reinforcement remained the only variable to be considered. This design variable, however, appeared insignificant to the model, and as depicted in Figure 3-12, even after separating the data into groups with almost the same characteristics, the trend in the plot remained highly obscure. Therefore, column transverse reinforcement was excluded from the final model (Equation 3-7).

$$\delta_{ult} = \mu \cdot \gamma \cdot \frac{v_{max}}{\sqrt{f_m}} \quad \mu = \frac{0.5}{2} + 1.3 \leq 6 \quad \text{(Equation 3-7)}$$

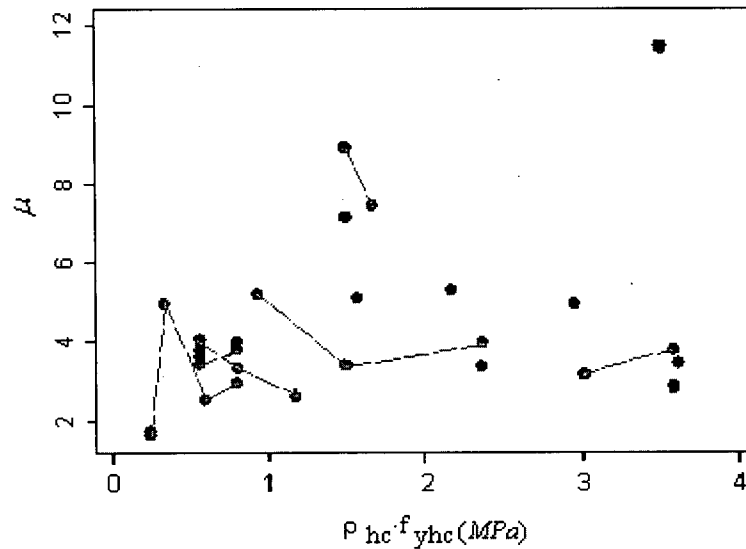


Figure 3-12: Lack of distinct relationship between μ and $\rho_{hc}f_{yh}$

Equation 3-7 was likewise developed for specimens with $H/L \leq 1.2$. Furthermore, removal of outliers resulted in only two specimens with ceramic units remaining, and therefore, the model should not be applied to CM walls with ceramic units.

Figure 3-13 illustrates the measured ductility factor as a function of v_{max} (from Equation 3-5). The value of μ is recommended to be cut off at 6, since only limited data is available above this limit and ductility demands larger than 6 are expected to result in excessively large diagonal cracks in CM walls which may impact the integrity of the panel.

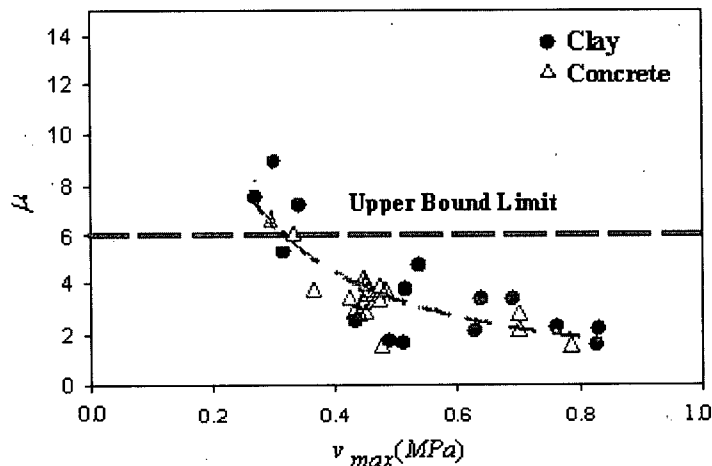


Figure 3-13: The capability of the proposed equation to predict the ductility factor

Despite inclusion of all potentially important predictors, individually or in combination with other variables, and verification of the model specification and its statistical

significance, the presence of a constant in the estimation of the ductility which appears statistically significant to the model, could be taken as an indicator of unknown variables that are contributing to the response. This constant may also be interpreted as implying that typical CM walls, regardless of the reinforcement detailing of their tie columns, have an intrinsic ductility of approximately 1.8. Further research is required to assess the contribution of other design variables and the minimum ductility achieved by CM walls. The expected ductility factors for different unit materials are presented in Table 3-5. Hollow clay units, in general, indicate higher than normal ductility factors compared to the values of this table, and therefore, Equation 3-7 should be utilized for such specimens with caution. This could be attributed to the elimination of specimens with hollow clay units, interior tie columns and $\rho_{hc} = 0$ from the process of model development.

Table 3-5 : Mean ductility factor for different unit materials

Unit Material	$\mu_{avg} \pm \sigma$
Clay	2.90 ± 1.20 *
Concrete	3.60 ± 0.40
Ceramic	NG
* use with caution for hollow clay bricks	

3.3.9 Prediction of drift capacity at maximum limit state

Determination of maximum shear strength on the basis of recorded response curves was a relatively easy task. However, such problems as local strength loss, and the presence of a plateau in the force-deformation response after yielding point made it difficult to determine the drift ratio at maximum strength with acceptable accuracy. In addition, this parameter, in spite of its necessity for constructing the analytical backbone curve, is not of paramount importance from a performance-based design perspective. In fact, as the database results indicate, δ_{max} might fall anywhere between the cracking and ultimate drift ratios.

Considering all these issues, drift capacity at maximum limit state was determined as a portion of the ultimate drift capacity of CM walls. To achieve this, the empirical model for δ_{ult} was first proposed (Equation 3-7), in order to identify the outliers and deficient

data points. Considering 37 specimens, mean and standard deviation of $\delta_{max}/\delta_{ult}$ were found to be 0.653 and 0.203 respectively. Since tighter limits might be sought in practice, the lognormal distribution of $\delta_{max}/\delta_{ult}$ is presented in Figure 3-14, in order to facilitate determination of this ratio at any confidence level.

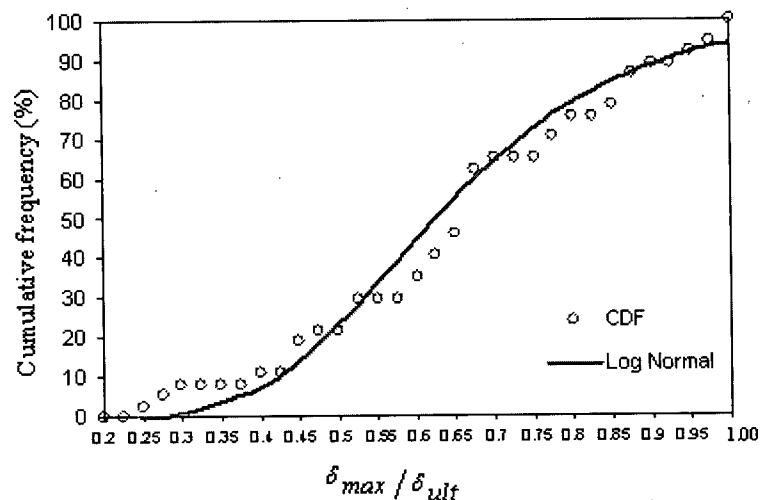


Figure 3-14: Lognormal distribution of $\delta_{max}/\delta_{ult}$

3.3.10 Comparison of drift models with existing empirical limits

As was noted in Chapter 2, no previous model for prediction of drift capacity of CM walls on the basis of panel and tie column design variables has been developed. However, the few studies that imposed some practical limits on the drift capacities at different performance levels along with Chilean (INN, 1997) and Mexican (NTC-M, 2004) codes are compared in Table 3-6 with the results of drift models of this study considering a 50% probability of failure.

Table 3-6: Comparison between the proposed drift models and existing limits

ID	Unit material	$\delta_{cr}(\%)$	$\delta_{max}(\%)$	$\delta_{ult}(\%)$	Reference
-	Clay	0.105	0.455	0.697	Present study
	Concrete	0.106	0.382	0.586	
	Ceramic	0.128	NG	NG	
AS04	Ceramic and concrete	0.130	0.400	0.730	Astroza and Schemidt, 2004
U01	Pumice	-	0.410	0.690	Urzua et al, 2001
INN97	All	0.620	1.000	<2.500	INN, 1997
NTCM04	All	0.250 (allowable inelastic drift)			NTC-M, 2004

As is evident from this table, *AS04* provides a good estimate of the cracking drift capacity. However, it over-predicts the drift capacities at maximum and ultimate limit states by 4.5% and 19% considering the results of the proposed models for concrete units. Although *U01* limits are suggested for CM walls made of pumice bricks it still provides a slightly better estimate of both δ_{max} and δ_{ult} compared with *AS04*.

INN97 which was developed on the basis of the seismic performance of masonry infill walls substantially overestimates the drift capacity of the CM walls at all limit states due to the ductile behavior of RC frames. However, the allowable inelastic drift of *NTCM04* is highly conservative even after considering the inherent variability that CM walls suffer from.

3.4 Discussion

3.4.1 Summary of the proposed equations

The main objective of this research is to create a comprehensive set of equations for predicting the model parameters of the analytical backbone curve simulating the nonlinear behaviour of CM walls in the event of severe earthquake. The equations are developed on the basis of both cyclic and monotonic experiments of an extensive database compiled by the author (Appendix A). This model could be utilized to track the nonlinear behaviour of CM walls up to ultimate limit state corresponding to 80% of the measured maximum strength.

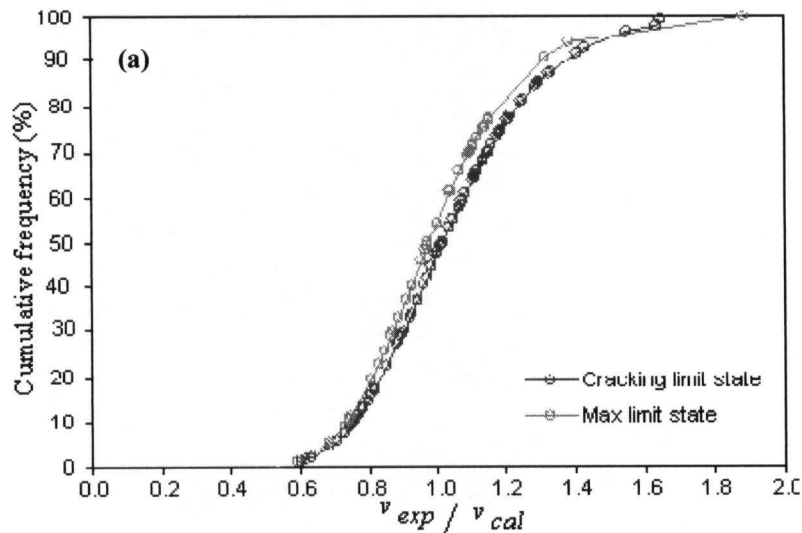
The empirical equations, 3-1 to 3-7, are presented for all model parameters characterizing three different limit states: cracking, maximum strength, and ultimate deformation capacity. These predictive equations are proposed on the basis of the important tie column and panel characteristics, and are specified and developed through an iterative linear regression analysis. The most important variables included in the model are: axial stress (σ_v), panel aspect ratio (H/L), masonry compressive strength (f_m), shear strength of the masonry (v_m), column longitudinal reinforcement ($\rho_{vc}f_{yvc}$), and masonry unit type (clay, concrete, and ceramic). Table 3-7 summarizes the mean, median, coefficient of variation, coefficient of determination, and the number of data points included in the development of the equation for each model parameter.

Table 3-7: Statistical characteristics of the proposed equations for panels with $H/L \leq 1.2$

Model Parameter	Unit Type	Mean (exp/cal)	Median (exp/cal)	COV (exp/cal)	N	R ²	Equation No
v_m	All	1.111	1.085	0.347	197	0.89	3-1
v_{cr}	All	1.046	1.067	0.245	80	0.958	3-2
v_{max}	All	1.001	0.976	0.223	39	0.96	3-5
δ_{cr}	Clay	1.240	1.249	0.553	18	0.811	3-6
	Concrete	1.065	1.148	0.303	23	0.887	
	Ceramic	1.061	1.077	0.296	11	0.936	
δ_{ult}	Clay	1.036	1.040	0.329	27	0.801*	3-7
	Concrete	0.937	0.961	0.189	11		
	Ceramic	N/A	N/A	N/A	N/A		

* Based on results shown in Figure 3-13 for ductility. One ductility model for all unit types.

The lognormal fragility curves of experimental to calculated model parameters are presented in Figure 3-15 to further depict the variability of the proposed model. Such curves are also useful in practice where, due to the inherent variability of CM walls and economic constraints, higher margins of safety might be sought.



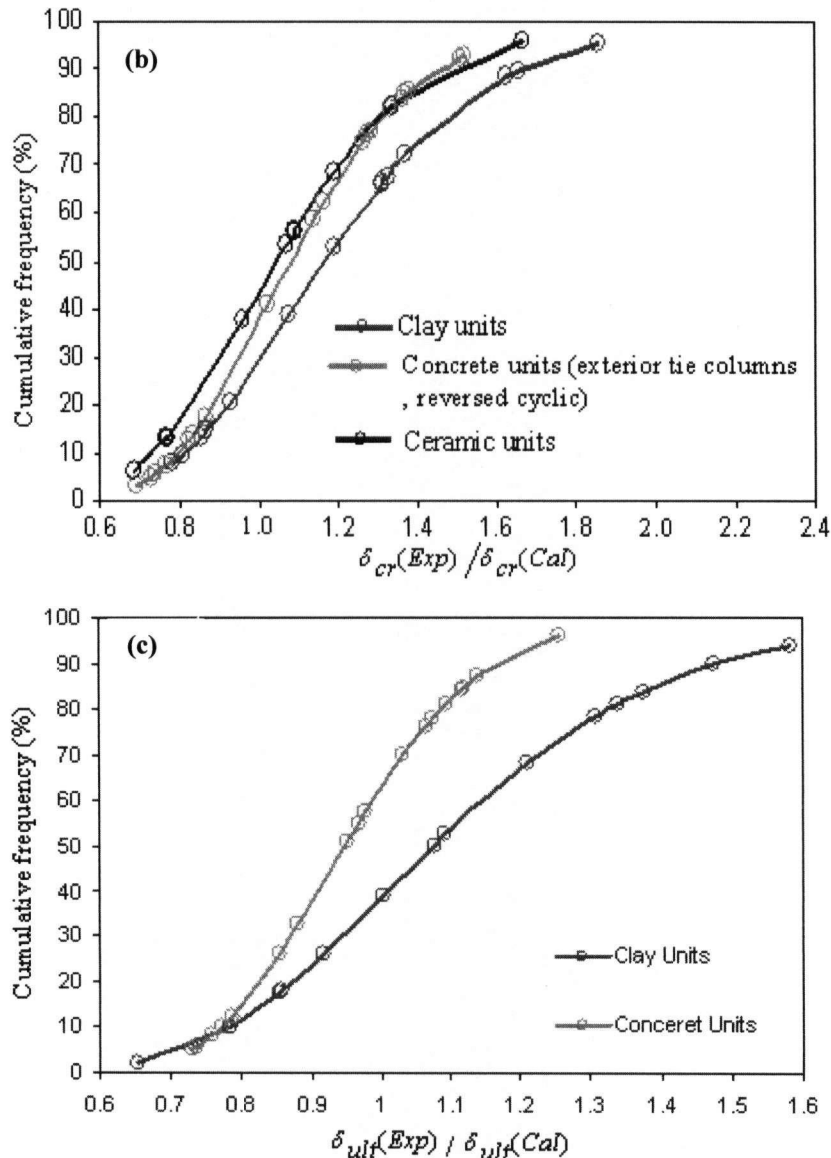


Figure 3-15: Fragility curves for model parameters at different limit states

As is evident from these graphs, the model parameters are suffering from high variability which should be lowered through collection of more suitable data and improvement of the model itself. These fragility curves are also shown in Figure 3-16 for a typical CM panel which fits in all the constraints of the proposed model ($\sigma_v=0.55$ MPa, $H/L=0.97$, $f_m=5.25$ MPa, $v_m=0.42$ MPa, $f'_c=23.05$ MPa, $\rho_{vc}f_{yvc}=4.29$ MPa, Unit type = Concrete) . For such a specimen the ratio of the experimental to calculated mean model parameters approach to unity.

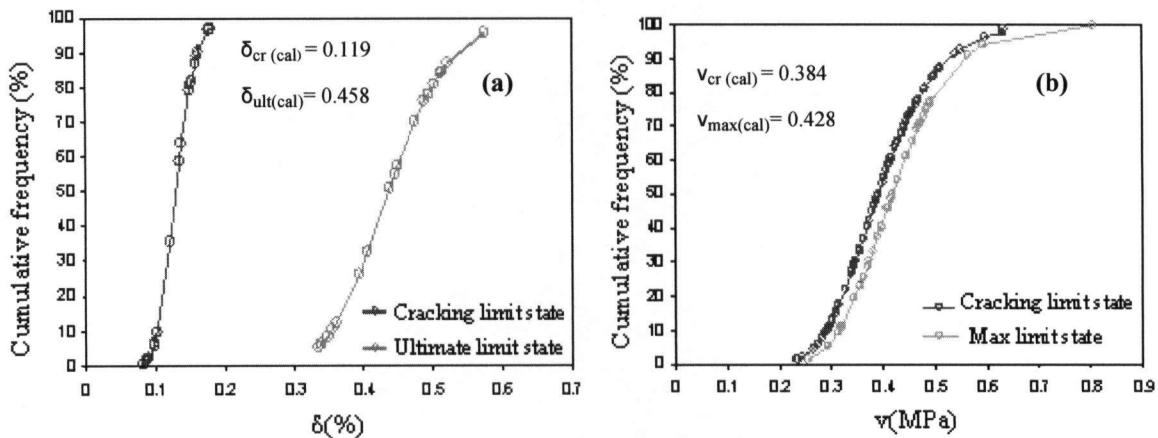


Figure 3-16: Fragility curves for Specimen 254 (Flores, 2004)

The curves of Figure 3-16, constructed on the basis of fragility curves of Figure 3-15 and proposed equations, may be used for the determination of model parameters at any desirable confidence level. For example, model parameters at different limit states for 10% probability of failure would be: $v_{cr} = 0.28$ MPa, $\delta_{cr} = 0.1$ %, $v_{max} = 0.33$ MPa, $\delta_{max} = 0.14\%$, $\delta_{ult} = 0.33\%$.

3.4.2 Limitations of the backbone model

The empirical equations developed in this study relate CM design variables to model parameters required for simulating the performance-based nonlinear behaviour of CM walls. The limitations of these predictive equations in terms of scope and applicability are described below.²

The primary limitation of the proposed model is that the empirical equations are derived for CM walls whose response is mainly governed by shear deformations. This predominance has been repeatedly demonstrated in previous earthquakes and experimental tests. However, shear failure of CM walls, unlike their URM counterparts is not highly brittle, and the contribution of confining elements improve both strength and deformation characteristics of the walls. In general, any violation from this major assumption – predominance of shear deformations – could disturb the accuracy of the model. As noted elsewhere in this report, the applicability of these predictive equations is

² More specific model limitations are described throughout the chapter

further limited by being developed only for “typical” CM walls. That is, the developed model best simulates the seismic performance of:

- panels with identical reinforcement detailing for both tie columns (symmetric reinforcement);
- CM walls with sufficient tie column longitudinal reinforcement for which the response is not dominated by either premature rebar yielding or brittle shear failure of CM walls whose tie columns are heavily reinforced. The database results suggest that the desired behaviour is observed if the tie column longitudinal reinforcement ratio is between 1% and 3%;
- CM walls with panel aspect ratio less than or equal to 1.2; and
- panels with axial stress less than $0.12f_m$ for which the response is not controlled by premature masonry crushing.

The applicability of the derived equations is also limited by the range of design variables included in the development of the model, particularly after removal of leverages. Considering the mentioned constraints, the reasonable ranges for all important variables are as listed in Table 3-8.

Approximately 80% of the specimens considered in developing the backbone model were tested using cyclic loading protocol. However, this loading method with 2-3 cycles per deformation level may not be consistent with earthquake loading that typically results in a few cycles with large deformations before reaching the ultimate limit state. In addition, it should be kept in mind that all the empirical equations are developed on the basis of laboratory tests with highly controlled construction and material qualities. Actual CM walls therefore are likely to have lower performance levels, especially since material properties and workmanship are highlighted as key factors that can substantially affect the seismic performance of these composite structural walls (Alcocer et al, 2003).

Table 3-8: Practical ranges of important design variables for predicting the seismic response of CM walls using the proposed model

Design Variable	Practical Range	Remarks
v_m	0.25 – 1.1 MPa	—
f_m	2.5 – 25 MPa	—
$\bar{\sigma}_v$	0 – 1 MPa	—
$\bar{\sigma}_v / f_m$	0 – 0.12	—
f'_c	10 – 35 MPa	—
ρ_{vc}, f_{yvc}	2 – 15 MPa	—
ρ_{vc} (%)	1–3	—
ρ_{hc} (%)	0–0.8	—
H/L	≤ 1.2	Although the empirical equations for v_{cr} and v_{max} are capable of predicting the response for aspect ratios up to two, the accuracy of these equations should be improved for walls with $H/L > 1.5$ by conducting more experimental tests.
Unit type	Clay, Concrete, Ceramic	Due to the lack of data on ceramic units δ_{ult} is predicted only for concrete and clay units. The predictive equation should also be utilized with caution for hollow clay units.

3.4.3 Evaluation of the proposed equations

Due to the inclusion of all the available data in the development of the proposed backbone curve, evaluation of the model by selecting suitable data points from outside the sample space is not possible in this study. As a result, specimens from the database with a complete set of experimental and analytical model parameters were considered for the purpose of model evaluation, and were selected in a manner that allowed for demonstration of model limitations and underlying assumptions.

The selected data points were separated into three major categories: CM walls that entirely satisfied the constraints of the model, data points that were removed from the statistical regression process as outliers or highly peculiar specimens, and atypical CM walls that were excluded at the outset.

Figure 3-17 illustrates the analytical and experimental backbone curves of two specimens that entirely comply with the limitations of the proposed model. As is evident from both graphs, the empirical model is capable of predicting the observed response with sufficient accuracy.

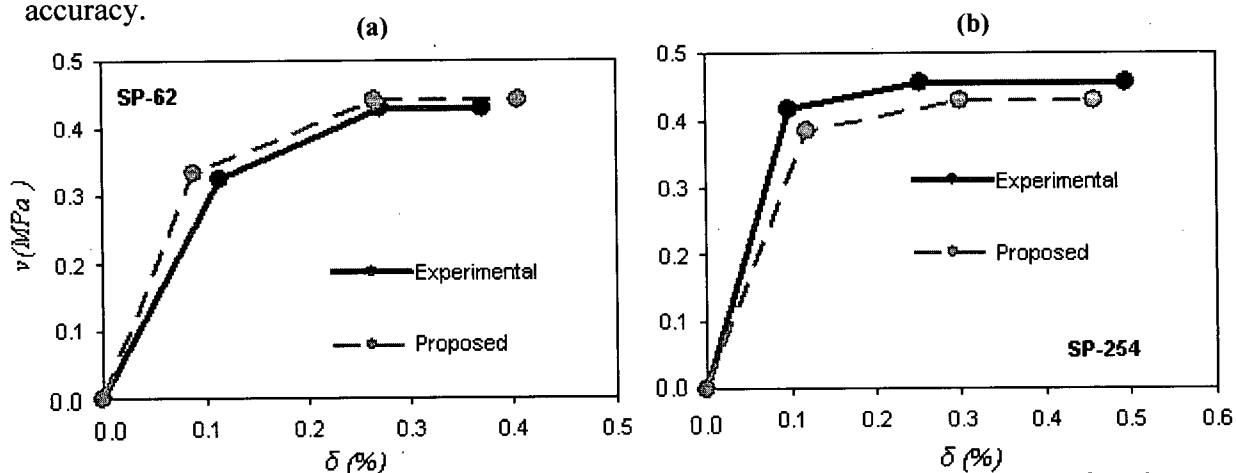


Figure 3-17: Comparison of measured and proposed backbone curves for conforming specimens (a) SP-62: Marrinilli and Castilla, 2006, (b) SP-254: Flores, 2004

Figure 3-18 shows the response curves for a specimen with a very high axial stress compared to its panel compressive strength ($\bar{\sigma}_v/f_m=0.14$). The occurrence of premature masonry crushing, as is clear from the graph, limits the deformation capacity, and therefore, the model over-predicts the ultimate drift capacity by almost 25%.

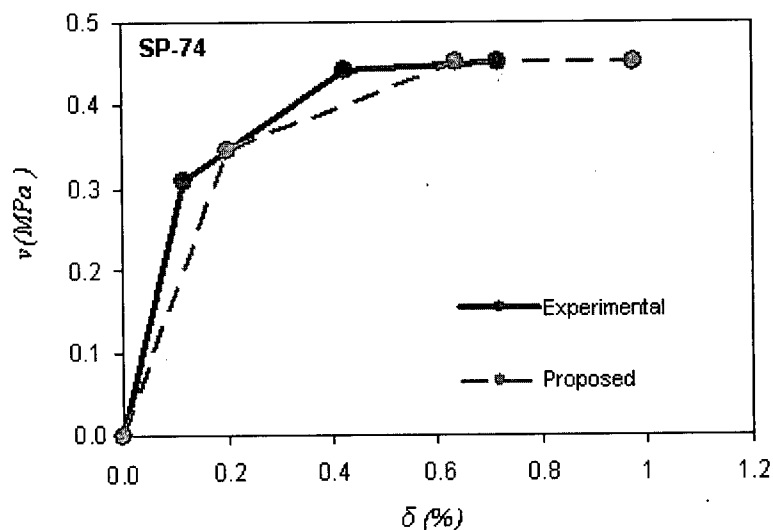


Figure 3-18: Inability of the model to predict the deformation capacity of a CM wall with excessively large axial stress (Aguilar et al, 1996)

Both experimental and proposed response curves of Specimen 195, as a representative of a class of CM walls that greatly deviate from the assumptions of the model, are shown in

Figure 3-19. The proposed model completely fails to track the nonlinear behaviour of this highly deficient specimen (low v_m compared to prediction based on Equation 3-1, high tie column longitudinal reinforcement ($\rho_{vc} f_{yc} = 20.29$ MPa), and very low concrete compressive strength ($f'_c = 10.2$ MPa)).

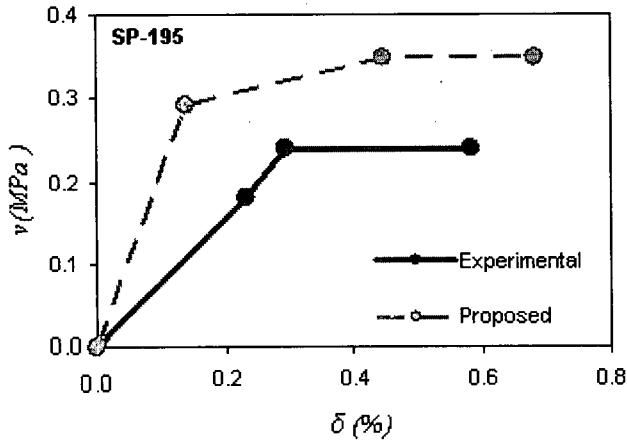


Figure 3-19: Inability of the model in predicting the seismic response of a highly deficient CM wall (Meli and Salgado, 1969)

Response curves of Specimen 76, as a representative of CM walls with bed joint reinforcement ($\rho_{hw} = 0.18\%$), is represented in Figure 3-20 to evaluate the accuracy of the model for a group of atypical CM walls that were removed from the analytical process. Proposed equations adequately predict the model parameters at the cracking limit state that is believed to be independent of reinforcement detailing of the panel and confining elements. However, the response at both maximum and ultimate limit states is under-predicted by the empirical equations, due to the beneficial effects of horizontal reinforcement on both deformation and strength characteristics of the panels.

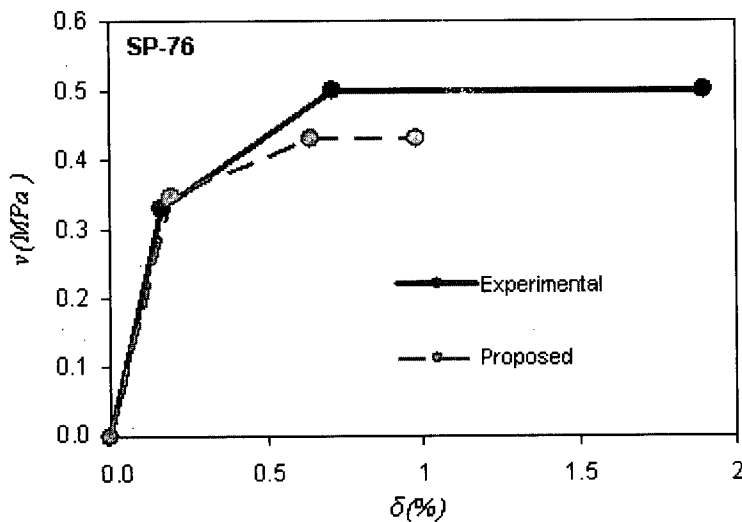


Figure 3-20: The effect of bed joint reinforcement on the seismic behaviour of CM walls, and the inability of the model to predict the maximum and ultimate response parameters (Aguilar et al, 1996)

Finally, the effect of low tie column longitudinal reinforcement ratio (below 1%) on the accuracy of the model is reflected in Figure 3-21. As is evident from the graph, yielding of insufficient longitudinal reinforcement (0.89%) beyond cracking, and its significant contribution to the maximum strength and deformation capacities result in the under-prediction of the measured response which appears to be governed by flexural deformations.

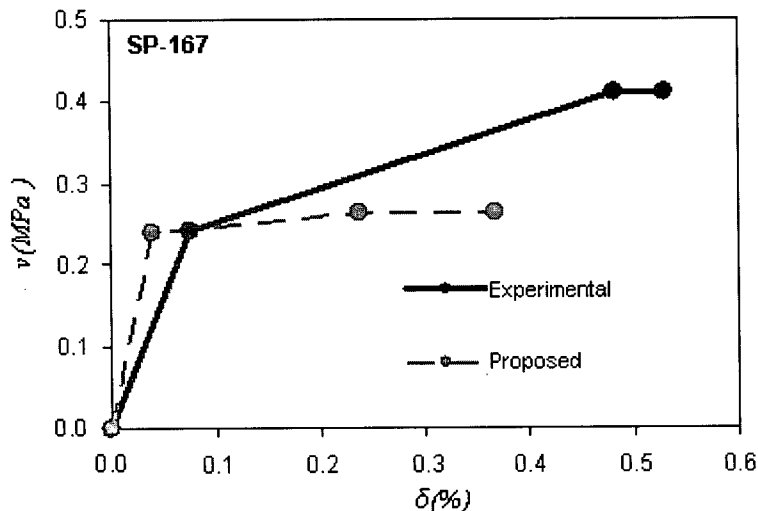


Figure 3-21: Inability of the model to predict the recorded response due to the predominance of flexural deformations (Meli and Salgado, 1969)

Based on the above mentioned points, the model predicts reasonably well the seismic response of CM walls that fit the constraints of the proposed equations, but fails to track the backbone curves of specimens whose characteristics do not conform to the assumptions of the model.

Owing to the lack of proper data, the model has been only adjusted for specimens with openings at cracking limit state. As a result, in order to verify the capability of the model to simulate the measured response of such walls more tests are required.

3.4.4 Recommendations and future directions

As has been mentioned, the proposed model was developed on the basis of 102 CM wall tests. As a result, different types of experiments can be conducted, either to relax some of the currently imposed limitations that stem from the lack of data, or to assess the effects of other contributing factors. Panels with openings of different size, location, and confining details, specimens with panel reinforcement (external/bed-joint reinforcement),

and masonry walls with multiple confining elements are among the specimens whose backbones cannot be predicted, because the small sample size makes them incomparable to the rest of typical specimens included in the database.

CM walls with simplified reinforcement details, (i.e. single longitudinal rebar with spiral hoops/no transverse reinforcement) should also be included in a list of future experimental tests, provided that other aspects of their properties coincide with typical CM walls. Furthermore, because monotonic and cyclic tests were not separated for the purpose of model development, due to the lack of data on the former category, it will also be desirable to conduct future experiments with monotonic loading protocol.

In developing the empirical model, tie column transverse reinforcement was among the predictor variables that proved insignificant to the ultimate deformation capacity. However, due to the presence of a large constant in the proposed equation which is also statistically significant, and the crucial role that transverse reinforcement is believed to have in confining the core concrete and augmenting the dowel action of longitudinal reinforcement, it is highly recommended this factor be studied more closely in future research on the topic.

The proposed equations are all deterministic in nature, and model uncertainties are accounted for using standard deviations. As a result, sensitivity analysis and development of probabilistic models would also enable the applicability of the model to reliability analysis (Zhu et al, 2007).

The current analytical model was developed on the basis of quasi-static laboratory tests with highly controlled material properties and testing conditions. Therefore, both dynamic testing of specimens having almost identical characteristics to typical CM walls and in-situ testing of CM walls are needed for validation of the models under dynamic loading conditions, and for adjustment appropriate in building practice.

Current CM codes, as the basis of design and construction, rely on conventional force-based equations that were originally developed for URM/RM panels, and the effect of confining elements has been overlooked by many of them. As a result, such models are incapable of predicting actual response with high accuracy. In addition, deformation characteristics which are believed to be more closely correlated with sustained earthquake damage, are rarely reflected in the codes. The code stipulated drift capacities

Chapter 3: Performance-based seismic models for confined masonry walls

are either highly conservative (the 0.25% allowable drift in Mexican code) or greatly overestimate the deformation characteristics of CM walls (the 2.5 % ultimate drift capacity of Chilean code). The outcome of this research, however, could contribute to the development of more accurate models and guidelines for improvement of these currently deficient provisions.

3.5 References

- Aguilar, G., Meli, R., Diaz, R., Vazquez-del-Mercado, R., (1996). "Influence of horizontal reinforcement on the behaviour of confined masonry walls, 11th World Conference on Earthquake Engineering, Acapulco, Mexico, No 1380
- AIJ, 1999: Architectural Institute of Japan (AIJ) Committee for Concrete and Masonry Wall Building Structures (1999) "Ultimate Strength and Deformation Capacity of Buildings in Seismic Design.", 592-593,
- Alcocer, S.M., Arias, J.G. Vazquez, A. (2003). "The new Mexico City building code requirements for design and construction of masonry structures" The proceedings of the Ninth North American Masonry Conference, Clemson, South Carolina, 656-667
- Alcocer, S.M and Meli, R. (1993) "Experimental program on the seismic behaviour of confined masonry structures." Proceedings of the sixth North American masonry conference, Philadelphia, PA, Vol. 2
- Alcocer, S.M, and Zepeda, J.A (1999) "Behaviour of multi-perforated clay brick walls under earthquake-type loading." 8th North American masonry conference, Austin, Texas, USA
- Alvarez, J.J (1996) "Some topics on the seismic behaviour of confined masonry structures." 11th World Conference on Earthquake Engineering, Acapulco, Mexico, No 180
- Astroza M.I., and Schmidt A.A. (2004) "Capacidad de deformacion de muros de Albanileria confinada para distintos niveles de desempeno (Deformation capacity of confined masonry for different performance levels)." Revista de Ingenieria Sismica No. 70, 59-75
- Bariola, J., Delgado, C. (1996) "Design of confined masonry walls under lateral loading." Eleventh World Conference on Earthquake Engineering, Acapulco, Mexico, No. 204
- Bourzam, A (2002) "Structure behaviour of confined masonry in using solid brick" Individual Studies by Participants at the International Institute of Seismology and Earthquake Engineering. Vol. 38, 179-192
- Castilla, E., and Marinilli, A. (2000) "Recent experiments with confined concrete block masonry walls." 12th international Brick/block masonry conference, Amsterdam, Netherlands, 419-431
- Chatterjee, S., and Hadi, A.S., (2006) "Regression Analysis by Example." Fourth Edition, John Wiley and Sons Inc., New York, USA.

Chapter 3: Performance-based seismic models for confined masonry walls

Chen, X., Ender, P.B., Mitchell, M., and Wells, C. "Regression with stata"
<http://www.ats.ucla.edu/stat>

Diez, J., Astroza, M., and Delfin, F. (1988) "Estudio experimental de modalidades de refuerzo para muros de albanileria de unidades ceramicas." Colloquia, Madrid, Espana.

Elwood K.J., Matamoros A.B., Wallace J.W., Lehman D.E., Heintz J.A., Mitchell A.D., Moore M.A., Valley M.T., Lowes L.N., Comartin C.D., and Moehle J.P. "Update to ASCE/SEI 41 concrete provisions." Earthquake spectra, 2007, in press

FEMA 356, Prestandard and commentary for the seismic rehabilitation of buildings, Washington, DC, 2000. Chapter - 7

Flores, L. (2004) "UNAM Database." National disaster prevention centre, Mexico

Flores, L.E., Mendoza, J.A., and Carlos Reyes Salinas (2004) "Ensayo de muros de mamposteria con y sin refuerzo alrededor de la abertura." XIV Congreso Nacional de Ingeniería Estructural, Acapulco, Gro, Mexico

Flores, L.E., Ríos, M., and Salinas, C., (2004) "Rehabilitacion con malla y mortero de muros de mamposteria con aberturas." XIV Congreso Nacional de Ingeniería Estructural, Acapulco, Gro, Mexico

Gibu, P. and Serida, C. (1993) "Confined masonry walls subjected to lateral loads (Muros Albanileria confinada sujetos a carga lateral)." National University of engineering (UNI) Lima-Peru

Gibu, P., and Zavala, C. "The current state-of -the art of masonry and adobe buildings in Peru." Japan Peru Center for Earthquake Engineering Research and Disaster Mitigation

Gostic, S., and Zarnic, R. (1999) "Cyclic lateral response of masonry infilled RC frames and confined masonry walls." Proceedings of the eighth North American masonry conference, Austin, Texas, USA, 477-488

Grumanazescu, I.P., and Gavrilesco, I.C. (1999) "Different behaviour aspects of confined masonry piers subjected to cyclic reversal and dynamic loads." Proceedings of the Fourth European Conference on Structural Dynamics, EUROLYN 919-924

Gunst R.F., and Mason R.L. (1980) "Regression analysis and its application; a data oriented approach." A series edited by the department of statistics Southern Methodist University, Dallas, Texas Vol. 34

Haselton, C.B., (2006) "Beam-column element model calibrated for predicting flexural response leading to global collapse of RC frame buildings." Stanford University.

Chapter 3: Performance-based seismic models for confined masonry walls

Hernandez, O., and Meli, R. (1976) "Modalidades de refuerzo para mejorar el comportamiento sismico de muros de mamposteria." Instituto de Ingenieria, UNAM, Report No.382, Mexico

INN (1997) " Norma Chilena NCh2123.Of 97 (1997) Albanileria confinada-requisitos de deseno y calculo." Instituto nacional de normalizacion, Santiago, Chile

Inpres-Cirsoc 103. (1983) "Normas Argentinas para construcciones sismorresistentes". Parte III.Construcciones de Mamposteria

Irimies, M.T., (2002) "Confined Masonry Walls: the influence of the tie-column vertical reinforcement ratio on the seismic behaviour." The proceedings of the Twelfth European Conference on Earthquake Engineering, No. 7

Ishibashi, K., Meli, R., Alcocer, S.M., Leon, F., and Sanchez, T.A. (1992) "Experimental study on earthquake-resistant design of confined masonry structures." Proceedings of the Tenth World Conference on Earthquake Engineering, Madrid, Spain, 3469-3474

James G.MacGregor and F.Michael Bartlett (2000)"Reinforced concrete; mechanics and design." Prentice Hall Canada Inc., Scarborough, Ontario, First edition

Kato, H.; Goto, T., Mizuno, H., and Iiba, M. (1992)."Cyclic loading tests of confined masonry wall elements for structural design development of apartment houses in the Third World." Proceedings of the Tenth World Conference on Earthquake Engineering, Madrid, Spain, 3539-3544

Kumazava, F. and Ohkubo, M. (2000) "Nonlinear characteristics of confined masonry wall with lateral reinforcement in mortar joints." Proceedings of the 12th World Conference on Earthquake Engineering, Auckland, New Zealand. No. 743

Marinilli, A., and Castilla, E. (2004). "Experimental evaluation of confined masonry walls with several confining-columns." 13th world conference on earthquake engineering, Vancouver, B.C., Canada, Accession No. 2129

Marinilli, A., and Castilla, E. (2006) "Seismic behaviour of confined masonry walls with intermediate confining - columns." Proceedings of the 8th U.S. National Conference on Earthquake Engineering, San Francisco, California, USA, No. 607

Matsumura, 1988" Matsumura, A., "Shear Strength of Reinforced Masonry Walls," Proceedings of the 9th World Conference on Earthquake Engineering, Tokyo-Kyoto, Japan, 121-126.

Meli, R., and Salgado, G., (1969) "Seismic Behaviour of Masonry Walls Subjected to Lateral Loading (Comportamiento de Muros de Mamposteria Sujetos a Carga Lateral)." Report N0. 237, Instituto de Ingenieria, UNAM, Mexico City.

Chapter 3: Performance-based seismic models for confined masonry walls

Moroni, M.O., Astroza, M., and Tavonatti, S., (1994). "Nonlinear models for shear failure in confined masonry walls." *The Masonry Society Journal*. Vol. 12, No. 2, 72-78

Norma Peruana de Diseño Sismorresistente E-070 (1998), Capítulo Peruano del ACI.

Pineda J.A (1996)" Comportamiento ante laterales de mamposteria confinada reforzados con malla electrosoldada." Msc Thesis No 171, Mexico

Ramirez Mestas, O. (1994) " Nonlinear finite element analysis of confined masonry walls." *Individual Studies by Participants at the International Institute of Seismology and Earthquake Engineering*

Rodelio Mercado, A. (2004)"Improvement of seismic performance of confined masonry structures." *Individual Studies by Participants at the International Institute of Seismology and Earthquake Engineering*, vol. 40, 243-255

Sanchez, T.A., Alcocer S.M., and Flores, L "Estudio experimental sobre una estructura de mamposteria confinada tridimensional,construida a escala natural y sujeta a cargas laterales." Xth National conference

Sanchez, T., Flores, L, Alcocer, S. M., and Meli, R. (1992)"Respuesta sismica muros de mamposteria confinada con diferentes tipos de refuerzo horizontal.Coordinacion de investigacion." CENAPRED, Mexico

Sánchez, T.A., Flores, L., León, F., Alcocer, S.M and Meli R. (1991) "Seismic response of confined masonry walls with different types of flexural coupling." *National disaster prevention report*

Sarma, B. S, Sreenath, H.G., Bhagavan, N.G., Ramachandra Murthy, A., Vimalanandam, V. (2003)."Experimental studies on in-plane ductility of confined masonry panels." *ACI Structural Journal*, Vol. 100, No. 3

NTC-M (2004) "Normas tecnicas complementarias para diseno y construccion de estructuras de mamposteria" Gobierno del distrito federal

Stata press "Based reference manual."2007

Tomazevic, M., and Klemenc, I. (1997). "Seismic behaviour of confined masonry walls." *Earthquake engineering and structural dynamics*, Vol. 26, 1059-1071

Tomazevic, M., and Klemenc, I. (1997)."Verification of seismic resistance of confined masonry buildings." *Earthquake engineering and structural dynamics*, Vol. 26, 1073-1088

Yañez, F., Astroza, M., Holmberg, A.,and Ogaz, O.(2004)"Behaviour of confined masonry shear walls with large openings" 13th world conference on earthquake engineering, Vancouver, B.C., Canada, No. 3438

Chapter 3: Performance-based seismic models for confined masonry walls

Yamin, L., and Garcia, L.E. (1997). "Experimental development for earthquake resistance of low-cost housing systems in Colombia." *Mitigating the Impact of Impending Earthquakes: Earthquake Prognostics Strategy Transferred into Practice*, 377-39

Yoshimura, K., Kikuchi, K., Kuroki, M., Nonaka, H., Kim, K.T., Matsumoto, Y., Itai, T., Reezang, W., and Ma, L. (2003). "Experimental study on reinforcing methods for confined masonry walls subjected to seismic forces." *Proceedings of the ninth North American masonry Conference, Clemson, South Carolina, USA*.

Yoshimura, K., Kikuchi, K., Kuroki, M., Nonaka, H., Tae Kim, K., Wangdi, R., and Oshikata, A. (2004). "Experimental study for developing higher seismic performance of brick masonry walls." *13th world conference on earthquake engineering, Vancouver, B.C., Canada, No. 1597*

Yoshimura, K., Kikuchi, K., Kuroki, M., Nonaka, H., Croston, T., Koga, S., Kim, K. T. and Ma, L. (2000). "Experimental study for higher seismic performance of masonry walls in developing countries." *Proceedings of 25th Conference on Our World in Concrete & Structures*, 695-702

Yoshimura, K., Kikuchi, K., Kuroki, M., Nonaka, H., Tae Kim, K., Wangdi, R., and Oshikata, A. (2004). "Experimental study on effects of height of lateral forces, column reinforcement and wall reinforcement on seismic behaviour of confined masonry walls." *13th world conference on earthquake engineering, Vancouver, B.C., Canada, No. 1870*

Yoshimura, K., Kikuchi, K., Kuroki, M., Liu, L., and Ma, L. (2000). "Effect of wall reinforcement, applied lateral forces and vertical axial loads on seismic behaviour of confined concrete masonry walls." *Proceedings of the 12th World Conference on Earthquake Engineering, Auckland, New Zealand. No. 984*

Yoshimura, K., Kikuchi, K., Kuroki, M., Liu, L., and Ma, L. (1999). "Effect of vertical axial loads and repeated lateral forces on seismic behaviour of confined concrete masonry walls." *Eighth Canadian Conference on Earthquake Engineering*; 107-112

Zabala, F., Bustos, L.J., Masanet, A., and Santalucia, J. (2004). "Experimental behaviour of masonry structural walls used in Argentina." *13th world conference on earthquake engineering, Vancouver, B.C., Canada, No. 1093*

Zavala, T., Cabrejos R.T., and Tapia, J.G. (1998). "Aseismic Masonry Building Model for Urban Areas" *Structural Engineering World Wide*, T209-1

Zhu, L., Elwood K.J., and Haukaas, T. (2007). "Classification and seismic safety evaluation of existing reinforced concrete columns." *Journal of structural engineering, ASCE, Vol. 133, No. 9*

Summary and Future Research

4.1 Summary

A thorough review of past CM studies, development of an extensive database of 357 monotonic and reversed cyclic tests, removal of anomalous data points, and running the iterative regression analysis all combined to develop the performance-based backbone model of this study.

Based on the thorough literature review, the following key factors have been identified as providing enhancements to the seismic performance of CM walls: constructing the wall with solid units and high-quality mortar with sufficient fluidity; providing the panel with exterior tie columns; ensuring symmetrical distribution of openings and providing them with confining elements able to restrain the extent of damage; providing column-beam joints and corners of openings with tightly spaced stirrups; providing tie columns with multiple rebar to avoid sliding of the panel at wall-foundation interface; and providing CM buildings with sufficient wall density per unit weight in both principal directions.

The backbone model of this study, however, is developed on the basis of the panel and tie column characteristics of 102 monotonic and reversed cyclic experiments, and is only proposed for typical CM walls whose response is mainly governed by shear deformations. As a result, only plain solid CM walls with panel aspect ratio less than or equal to 1.2, tie column longitudinal reinforcement ratio between 1% and 3%, and axial stress to masonry compressive strength ratio less than or equal to 0.12 have been considered in the creation of the model equations. The proposed equations which characterize three different limit states: cracking, maximum strength, and ultimate deformation capacity, are deterministic in nature. Model uncertainties are merely accounted for using standard deviations. The seismic response of the specimens that fit the constraints of the model is predicted by these empirical equations with sufficient

accuracy. However, the proposed model fails to match closely the recorded response of atypical or anomalous CM walls.

As the performance of the developed backbone model and database results confirm, confinement from tie columns and bond beams improves the shear capacity of masonry panels by almost 30%. However, CM walls, compared with their URM counterparts, indicate much higher deformation capacities. Cracking drift capacity of CM walls, on average, is in the range of 0.11% to 0.13%, with clay units having the largest values. The ultimate deformation capacity of typical CM panels, however, is about 0.7%, 0.6%, and 0.5% for clay, ceramic and concrete masonry units; thus making clay units the best unit type for CM structures in highly active seismic regions.

Past CM models with sharp focus on strength characteristics are either developed on the basis of a few experimental tests or are originally developed for URM, RM, or masonry infill walls. The post-cracking role of tie columns in improving the shear capacity of CM walls has been overlooked by many of the forced-based equations. Deformation capacity, on the other hand, has been only addressed through empirically imposed limits which are either highly conservative or largely overestimate the observed capacity of CM walls. Thus, these existing models in general fail to simulate the measured response of typical CM walls with sufficient accuracy.

4.2 Future research directions

As previously noted, the proposed empirical model developed in the present study is deterministic in nature, and prediction errors are accounted for using coefficients of variation. However, model uncertainty stemming mainly from lack of data may be improved by inclusion of more observations, either to enhance model accuracy and alleviate some of its limitations, or to assess the effects of other design parameters not considered in the original model. Parameters recommended for consideration in future experimental tests are: specimens with openings of different size, shape, and confinement details; panels with multiple tie columns; specimens with simplified tie column reinforcement detailing; panels with bed joint reinforcement; and CM walls with varying bond beam design.

Both because assessment of the effect of openings on the seismic response of CM walls has been made on the basis of a handful of specimens, and because recommendations for

Chapter 4: Summary and future research

opening confinement are not consistent in seismic codes, it remains important to conduct experiments with varying opening characteristics.

Similarly important are proper dynamic and in-situ tests to assess effects of loading conditions, material quality, workmanship, and maintenance as key factors affecting the seismic performance of CM walls. To date, the model has been developed on the basis of laboratory monotonic and cyclic quasi-static tests incapable of reflecting seismicity, soil conditions, and ground motion characteristics, and without taking into account the inherent inferiority of in-situ CM walls as compared to laboratory tests with highly controlled construction and material qualities.

When developing the empirical equation for ultimate deformation capacity of CM walls, tie column transverse reinforcement proved insignificant to the model. Owing to the presence of a large constant statistically significant to the model, and to the vital role that transverse reinforcement is believed to have on the post-peak behaviour of CM walls, it is highly recommended that its effects be more closely studied in future research.

Also recommended for future study are experimental and analytical examination of out-of-plane seismic behaviour; and examination of how research outcomes and state-of-knowledge of CM may be used to improve seismic codes and provisions as the basis of the design and construction.

Appendix A

Confined Masonry Database³

A.1 Introduction

Databases may be considered essential tools in evaluation of seismic performance of structural systems; in verification of the accuracy and adequacy of current codes and specifications; and in development of empirical models. The UBC confined masonry database has been assembled primarily as the basis of performance-based seismic models, and consists of two major categories. The first database includes 357 monotonic and reversed cyclic tests; the second set comprises 24 shake table and pseudo-dynamic experiments.

Many resources have been consulted in constructing the databases. The most significant contributor source is previous work by Universidad Nacional Autonoma de Mexico (UNAM, 2004), with partial contribution in development of 151 of 381 total specimens.

Data included in the tables is classified in two major groups; those directly extracted from the references and those that were calculated on the basis of the first category. To differentiate between them, the former group is shown in black throughout the database, while the calculated variables are shown in blue. To maintain consistency, units of original data were converted into KN, mm, and MPa. The accuracy of the extracted information was verified when accompanied with supporting data, or when an experimental test was addressed by more than one reference.

³ Developed at the University of British Columbia, Riahi, Z, 2006

Appendix A: Confined masonry database

The main objective of this chapter is to elaborate the basics and principles of the quasi-static database, the input of the empirical model developed in this study. The characteristics of the shake-table specimens will in some cases also be briefly discussed. Material properties and reinforcement detailing of both masonry panels and confining elements, together with loading conditions and results of each experiment will be described, and are the main classes of data represented in the table.

A.2 General information

A.2.1 Reinforcement characteristics

In developing the database, all confined masonry specimens were considered, regardless of reinforcement detailing of their panels and confining elements. However, to assist identification of specimens with different reinforcement characteristics, symbols were assigned to each category. The symbols are described in Table A-1

Table A-1: Reinforcement detailing of CM panels

Symbol	Description	Percentage
N	No Additional Reinforcement (only confining elements)	66.1
H	Wall Horizontal Reinforcement	11.1
C	Connection Rebar	2.6
I	Intermediate Bond Beam	3.5
V	Panel Vertical Reinforcement	6.1
HV	Panel Vertical and Horizontal Reinforcement	7.9
WWM	Welded Wire Mesh (external reinforcement of the panels)	2.7

As this table indicates, typical confined masonry walls (consisting only of plain panels confined with tie columns and bond beams along their borders) comprise approximately 70% of the overall data.

Appendix A: Confined masonry database

A.2.2 ID

Regardless of its original title, each data point has been provided with an ID number ranging from 1-357, in order allow uniform comparison, and to avoid confusion where specimen titles coincide.

A.2.3 Test category

To develop the quasi-static database, the results of both monotonic (*M*) and reversed cyclic (*RC*) tests were considered. Test category was utilized to distinguish between loading protocols, and to clarify which method (displacement-based, force-based) was employed to apply the load during different stages of the tests. As shown in Figure A-1, cyclic loading was predominantly used to test specimens.

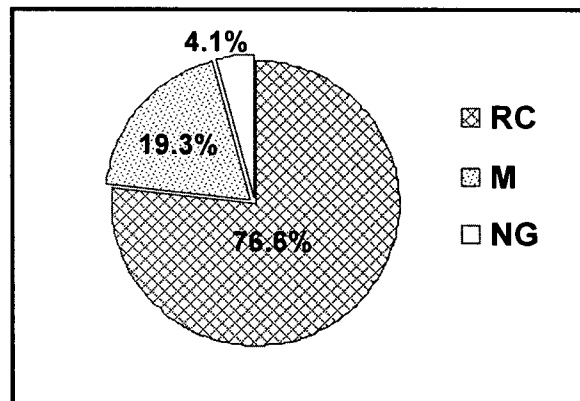


Figure A-1:⁴ Different testing methods

A.2.4 Scaling

Specimens comprised in the dataset were either tested in their natural scales, or modeled using simple or complete similitude laws. When deriving the simplified database from the original quasi-static database as the basis of the analytical work however, the four specimens that were scaled using complete similitude laws were excluded, due to the difference between the strength characteristics of the models and prototypes for the modeling method.

⁴ NG refers to not given.

A.3 Panel Characteristics

Depending on material properties, specimen geometry, and reinforcement detailing of the panel, characteristics of the masonry walls could vary between specimens. Industry-manufactured and hand-made masonry units have various configurations and constituent materials which are generally described across the table using Unit Type. However, when forming the simplified table, it is important to differentiate these properties, since they could greatly affect the characteristics of the panels and the resulting models.

Parameters describing detailed panel characteristics are Unit-type and Unit-material. Unit type identifies whether masonry units are Hollow (*H*), Solid (*S*) or Multi-perforated (*MP*). Unit material differentiates Concrete (*Co*), Clay (*Cl*), Ceramic (*Cr*), and other miscellaneous materials (*O*) frequently used for the production of masonry units. Figure A-2 illustrates the frequency of the unit types and materials throughout the database.

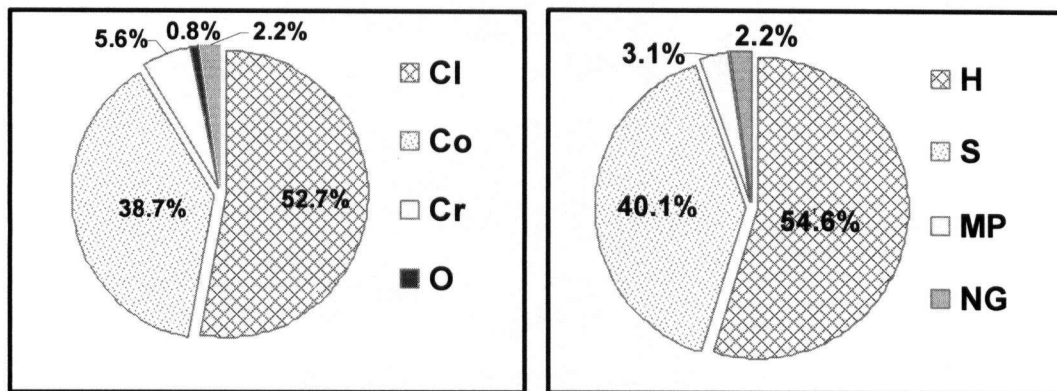


Figure A-2: Distribution of different unit types in the database

Key parameters that best describe the characteristics of the masonry panels are presented in Table A-2 in terms of notations, remarks, units, and their definitions. Wall density is shown in yellow to stress the point that this parameter is only used for dynamic and pseudo-dynamic experiments.

Table A-2 (a): Panel Geometry and reinforcement details

Notations	Description	Remarks	Units
L_w	Length	—	mm
H_w	Height	From the top of the foundation to the top of the bond beam	mm
t_w	Thickness	For panels with cover mortar the entire thickness is reported in the database.	mm
H_w/L_w	Aspect Ratio	To determine the aspect ratio overall length and height regardless of the number of panels were considered. However, for multi-story specimens where load is applied at all floor levels aspect ratio is determined for each individual story.	—
M/Qd	Shear Span Ratio	—	—
L'	$L_w - w_{tc}$	—	mm
H_w/t_w	Slenderness Ratio	Of paramount importance when investigating out-of-plane seismic behaviour	—
ρ_{hw}	Horizontal Reinforcement Ratio	—	%
S_{hw}	Vertical Space Between Horizontal Rebar	—	mm
ρ_{vw}	Vertical Reinforcement Ratio	—	%
S_{vw}	Horizontal Space Between Vertical Rebar	—	mm
$^*\rho_{CR}$	Ratio of Connection Rebar	—	%
S_{CR}	Vertical Space Between Connection Rebar	—	mm
L_{CR}	Connection Rebar Length	—	mm
d	Wall Density (A_w / A_n)	Highly variable For dynamic and pseudo-dynamic tests, depending on the specimen configuration and the code used to design and construct the CM walls.	%
A_w	Horizontal Cross Sectional Area	considering both panel and confining elements	mm ²

*Connection rebar refer to the discontinuous horizontal reinforcement utilized to connect the panels with their confining elements and avoid their disintegration at large displacements.

(b): material properties

Notations	Description	Remarks	Units
f_{yhw}	Yielding Strength of Panel Horizontal Reinforcement	—	MPa
f_{yvw}	Yielding Strength of Panel Vertical Reinforcement	—	MPa
f_{yCR}	Yielding Strength of Connection Rebar	—	MPa
f_{mr}	Mortar Compressive Strength	—	MPa
C:S:L	Mortar Composition (Cement: Lime: Sand)	Depends on the type of mortar being utilized (Cement-based, Cement-lime) and the proportioning of the constituents.	—
f_{mrc}	Cover Mortar Compressive Strength	—	MPa
f_b	Masonry Unit Compressive Strength	—	MPa
f_m	Prism Compressive Strength	—	MPa
v_m	Prism Shear Strength	Determined using the results of compression diagonal tests	MPa

Table A-3 shows the ranges of the most important panel design variables, their mean, and coefficients of variation. Characteristics of the masonry panels are shown to be highly variable between specimens, and this to some extent explains why material properties, construction details and workmanship are considered significant contributors to the overall performance of CM walls.

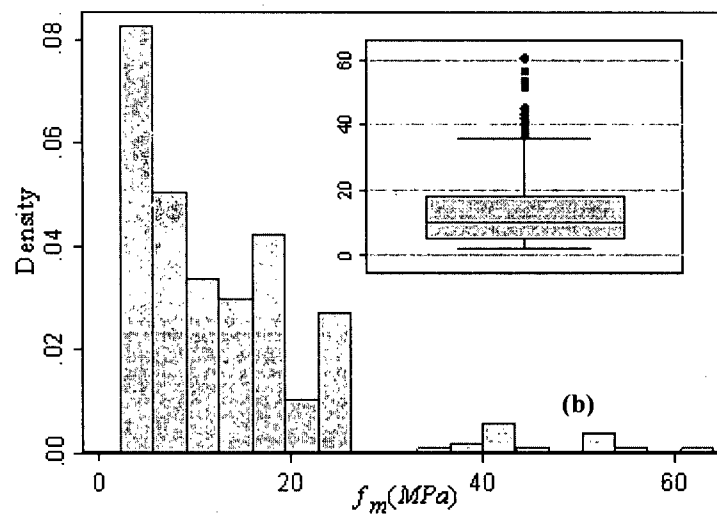
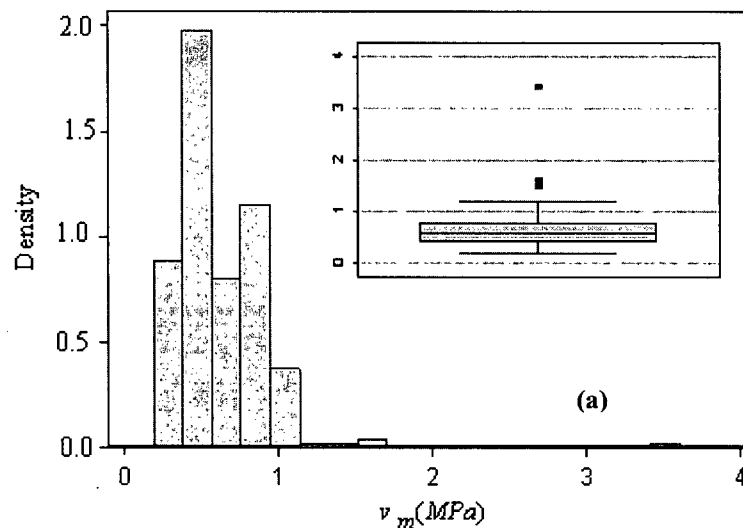
Table A-3: Panel property statistics

Notations	Range	Mean	Cov
t_w	110-240	158	36
H_w/L_w	0.50 -3.13	1.00	0.36
H_w/t_w	5.9-22.7	16.8	2.3
* ρ_{hw}	0.016- 0.241	0.114	0.064
* ρ_{vw}	0.031-0.633	0.154	0.141
f_m	2.26-60.60	13.05	10.31
v_m	0.19 -3.42	0.62	0.29
*Only for panels with horizontal/vertical reinforcement			

Appendix A: Confined masonry database

The distribution of v_m , f_m , H_w/L_w , H_w/t_w and t_w (adjusted for scale factors) as the key design variables are shown in Figures A-3-a to A-3-e. The extreme values of these parameters are also included in each figure, so as to highlight the anomalies that are potentially present in the database. These highly influential points, as described in the study report, may adversely affect the results of the analytical models, and therefore their recognition under close scrutiny of data is of high priority.

Among these parameters, panel slenderness ratio and masonry shear strength could be perfectly idealized by lognormal distributions. The remainder are usually weighted around their means in an arbitrary manner, and cannot be characterized simply by a defined distribution.



Appendix A: Confined masonry database

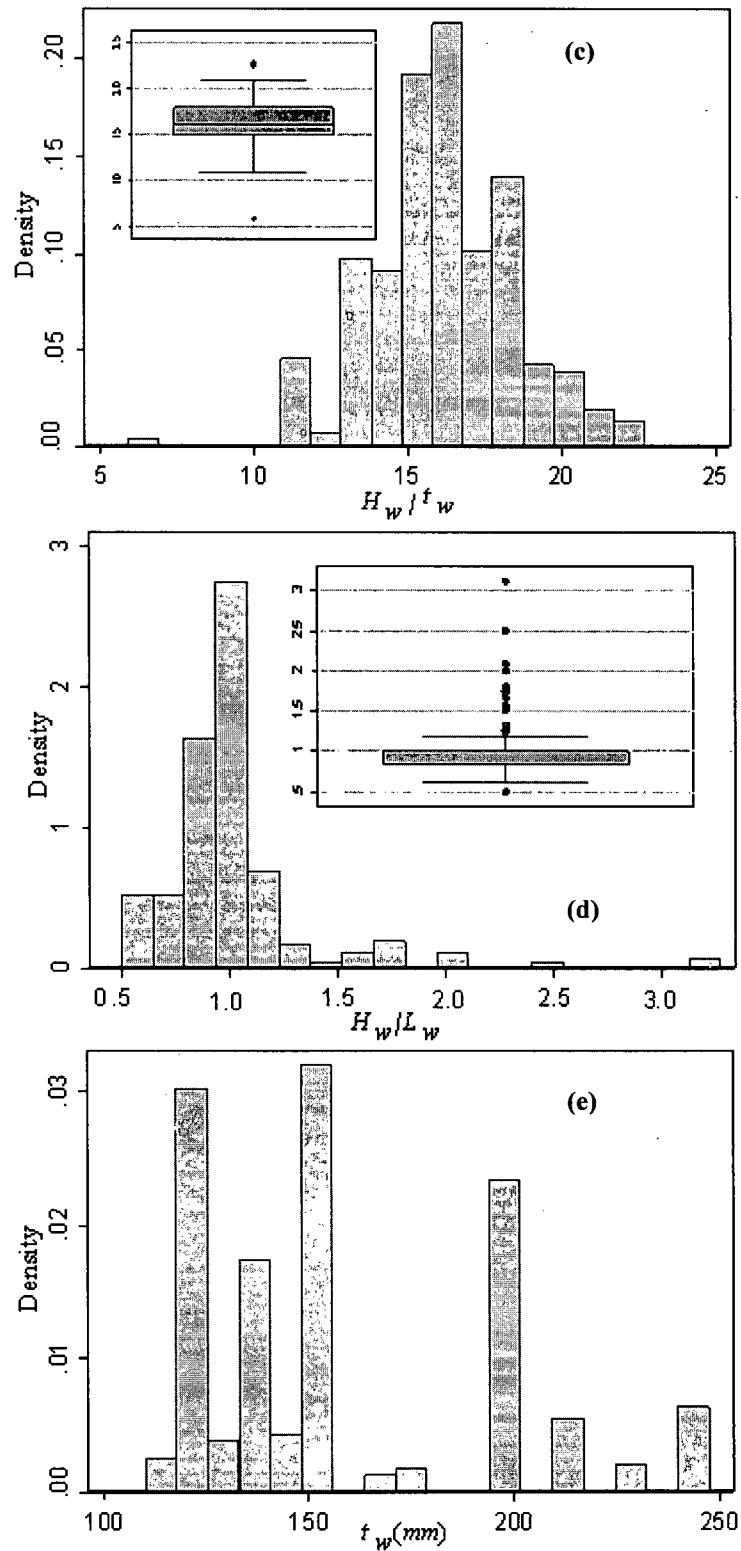


Figure A-3: Distribution of some of the most important panel design variables

A.4 Tie column properties

Reinforcement detailing of tie columns, their location, type, and the number of tie columns provided to masonry panels, together with such factors as material properties, and tie column dimensions, control the contribution of these confining elements to the overall seismic response of CM walls.

The location of tie columns, and thus, their number, is greatly influenced by the number of panels within an individual wall, and the presence of openings. Most of the specimens included in the database are provided with only two tie columns with symmetric reinforcement. However, when panels are pierced with openings, these confining elements also appear at the opening borders, so as to avoid instability in these critical zones which are highly susceptible to damage. As is evident from the database, these secondary columns usually have the same thickness as other tie columns frequently corresponding to the panel thickness. However, width is usually reduced and reinforcement detailing is somewhat simplified (2 longitudinal rebar and cross ties instead of four rebar and stirrups), so that the resultant longitudinal reinforcement ratio remains almost unchanged compared to columns at wall extremes.

The number of tie columns may also exceed the minimum number of two, when intermediate tie columns are provided in order to control the extent of damage. Figure A-4 illustrates the distribution of the number of tie columns throughout the database. Based on this distribution curve, almost 80% of specimens consist only of single solid panels, provided with two tie columns along their borders.

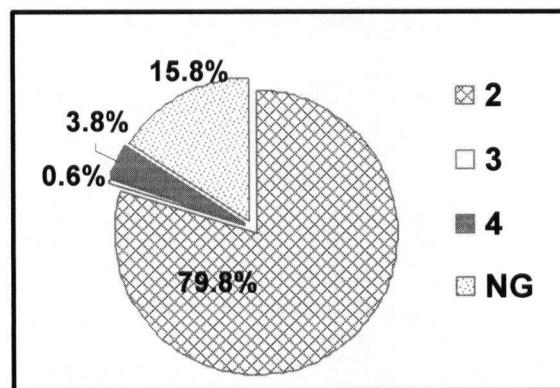


Figure A-4: Distribution of the number of tie columns

Appendix A: Confined masonry database

The dimensions of tie columns are not only influenced by panel thickness, but also by the type of tie columns. Typical reinforced concrete columns that are cast against masonry are referred to as Exterior tie columns (*E*). However, when panels are made of hollow bricks/blocks, confinement may be provided by placing the reinforcement within the holes of units and grouting them. These are called Interior tie columns (*I*) and are classified into single-hole, double-hole and double-hole integral subcategories, depending on the number of reinforced holes and whether the intermediate wall between individual holes has been removed. Figure A-5 contrasts the percentage of these two types of columns in the database.

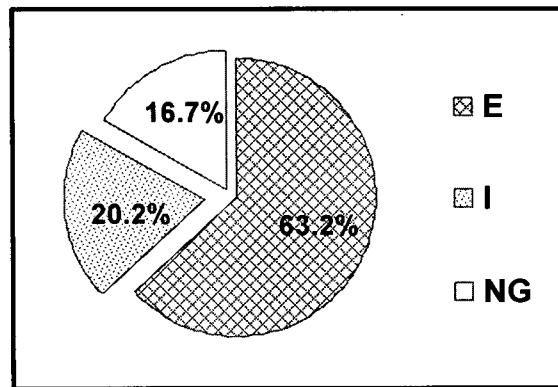
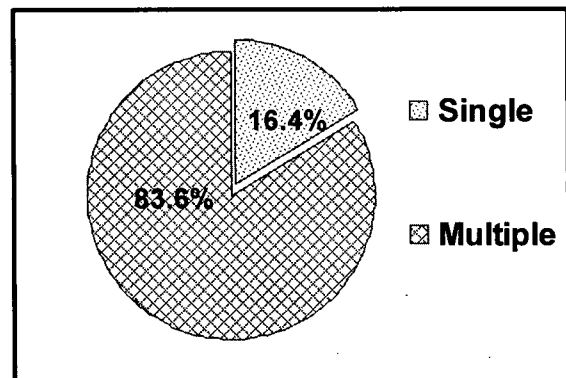


Figure A-5: Distribution of different types of tie columns

Simplicity at the cost of only a marginal decrease in the capacity of structural systems has always been favoured in practice. As a result, some specimens within the database are either provided with single rebar (rather than multiple longitudinal reinforcement) and spiral hoops, or are left horizontally unreinforced, to investigate how these factors would affect the seismic response of confined masonry walls. However, as Figure A-6 indicates, single-rebar tie columns comprise only a small portion of the database compared to tie columns with multiple rebar.

Figure A-6: Distribution of tie columns with different reinforcement detailing



Appendix A: Confined masonry database

Factors describing the tie column characteristics are presented in Table A-4, in terms of notations and definitions.

Table A-4: Tie column characteristics

Notations	Definition	Units
N_{tc}	Number of Tie Columns	—
t_{tc}	Thickness	Mm
w_{tc}	Width	Mm
A_{tc}	Area	mm ²
ρ_{vc}	Longitudinal Reinforcement Ratio	%
f_{yvc}	Yielding Strength of Longitudinal Rebar	MPa
$\rho_{hc\ end}$	Transverse Reinforcement Ratio at Critical End Zones	%
$\rho_{hc\ mid}$	Transverse Reinforcement Ratio excluding Tie Column Ends	%
f_{yhc}	Yielding Strength of Transverse Reinforcement	MPa
f_c	Concrete Compressive Strength	MPa

Table A-5 depicts the ranges of the most important tie column design variables, along with their means and coefficients of variation where these statistics are helpful.

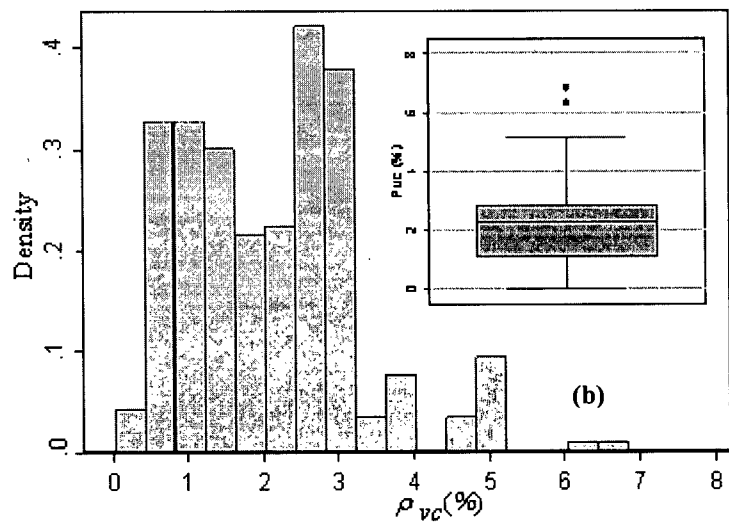
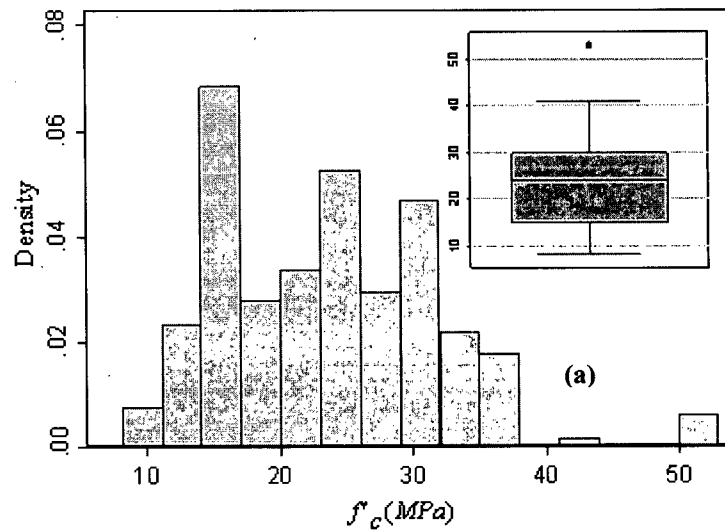
Table A-5: Statistics of Tie column design variables

Notations	Range	Mean	Cov
$t_{tc} (mm)$	70-250 (E)	—	—
	80-190 (I)		
$w_{tc} (mm)$	70-250 (E)	—	—
	150-340(I)		
$A_{tc\ min} (mm^2)$	9800(E)	—	—
	13500(I)		
$\rho_{vc} (\%)$	0.30-6.84	2.09	1.19
$\rho_{hc\ end} / \rho_{hc\ mid}$	1.00-3.46	1.73	0.69
* $\rho_{hc\ mid} (\%)$	0.00-1.05	0.26	0.24
$f_c (MPa)$	8.14-52.97	23.56	8.31
*Some columns are horizontally left unreinforced.			

Appendix A: Confined masonry database

The variance of the end to middle transverse reinforcement ratio between 1 and 3.46 indicates that for some specimens, despite the importance of column ends in the final collapse pattern of CM walls, stirrups are uniformly distributed over the entire tie column length.

The distribution of $\rho_{hc\ mid}$, $\rho_{hc\ end}/\rho_{hc\ mid}$, ρ_{vc} , and f'_c , as the key design parameters, along with the extreme values of each variable are presented in Figure A-7-a to d. Based on these graphs, only ρ_{vc} and $\rho_{hc\ mid}$ could be approximated by lognormal distributions.



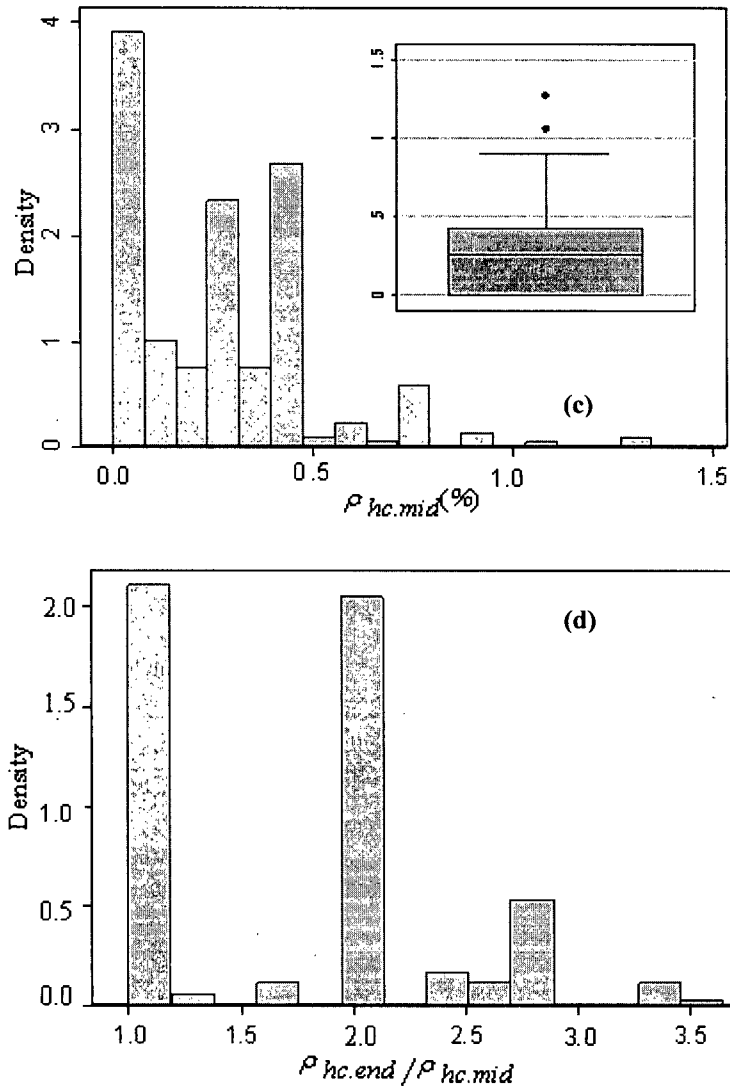


Figure A-7: Statistical distribution of tie column design variables

A.5 Bond beam characteristics

The location and number of bond beams are directly influenced by the number of vertical panels within CM walls, and the presence of openings. For multi-story CM specimens, bond beams are usually provided at each floor level. However, for some specimens, these confining elements are also provided at wall mid-height to improve the overall seismic performance of CM walls by confining the extent of damage.

When panels are pierced with openings, bond beams usually would appear at sill and/or lintel levels. Intermediate bond beams and those atop and/or below openings usually have the same width as other bond beams. However, the number of longitudinal rebar and the

Appendix A: Confined masonry database

height are usually reduced so that longitudinal reinforcement ratio stays almost constant compared to primary bond beams. In these cases, transverse reinforcement is usually provided by means of cross ties.

For typical single-panel CM walls, bond beams are either provided at the top of the structural walls or at both top and bottom of the panels. Instead of small-size bond beams, as is common in practice, some specimens are provided with large concrete beams at their tops to facilitate the distribution of vertical loads. The dimensions of these rigid beams are usually analogous to those of foundations, whereas the dimensions of typical bond beams are usually controlled by the thickness of the panels.

Bond beams are usually provided with four longitudinal rebar. However, only a handful of them are left horizontally unreinforced across the database. The reinforcement detailing and material properties of bond beams, with designating notations and general definitions are listed in Table A-6

Table A-6: Bond beam characteristics

Notations	Definition	Units
H_{bb}	Height	mm
W_{bb}	Width	mm
ρ_{vb}	Longitudinal Reinforcement Ratio	%
$\rho_{hb\ end}$	Transverse Reinforcement Ratio at Critical End Zones	%
$\rho_{hb\ mid}$	Transverse Reinforcement Ratio excluding the Critical End Zones	%
A_{bb}	Area	mm ²
Concrete compressive strength for bond beams is analogous to that of tie columns.		

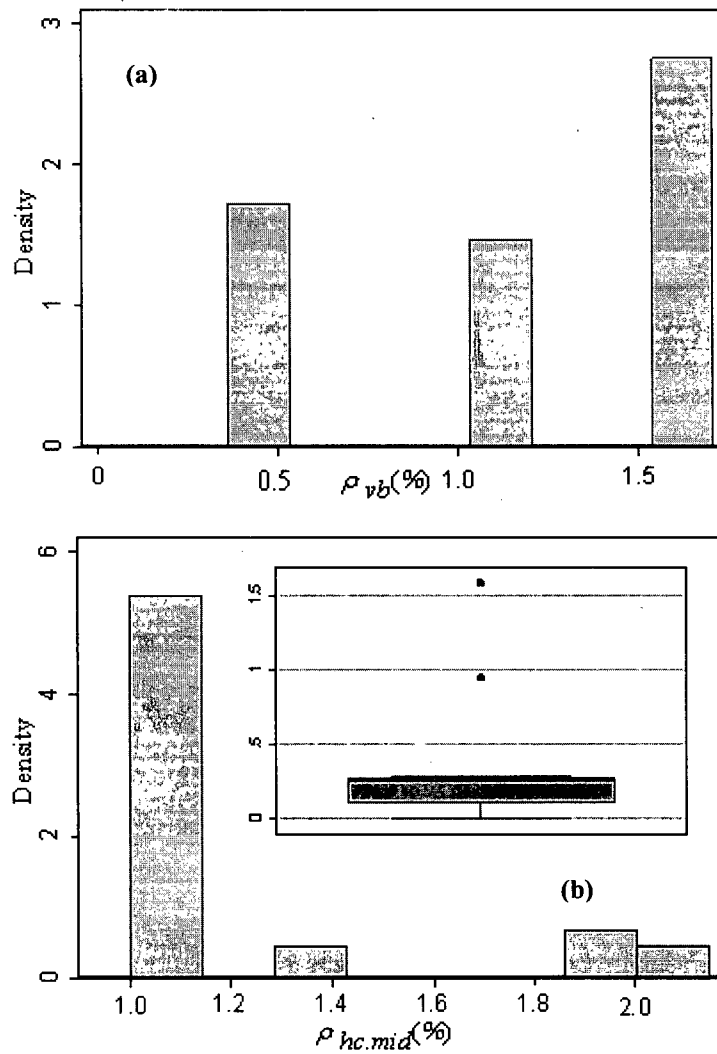
Table A-7 documents the range, mean and coefficient of variation for the chief variables that best define the characteristics of bond beams. As appears from the table, for some specimens bond beams are provided with evenly distributed stirrups over their entire spans, whereas for others, the space of transverse reinforcement is tightened at critical end zones susceptible to concrete crushing/spalling.

Table A-7: Statistics of bond beam design variables

Notations	Range	Mean	Cov
H_{bb} (mm)	200–250	—	—
W_{bb} (mm)	120–300	—	—
$A_{bb\ min}$ (mm ²)	14400	—	—
ρ_{vb} (%)	0.36–1.70	1.20	0.50
$\rho_{hb\ end} / \rho_{hb\ mid}$	1.00–2.00	1.18	0.37
* $\rho_{hb\ mid}$ (%)	0.00–1.59	0.40	0.40

*A few bond beams are left horizontally unreinforced

The statistical distribution of ρ_{vb} , $\rho_{hb\ mid}$ and $\rho_{hb\ end} / \rho_{hb\ mid}$, as the key bond beam design parameters, along with their extreme values, is presented in Figure A-8-a to c and demonstrates the peculiarities of these confining elements. As shown, none of these variables follow lognormal distribution.



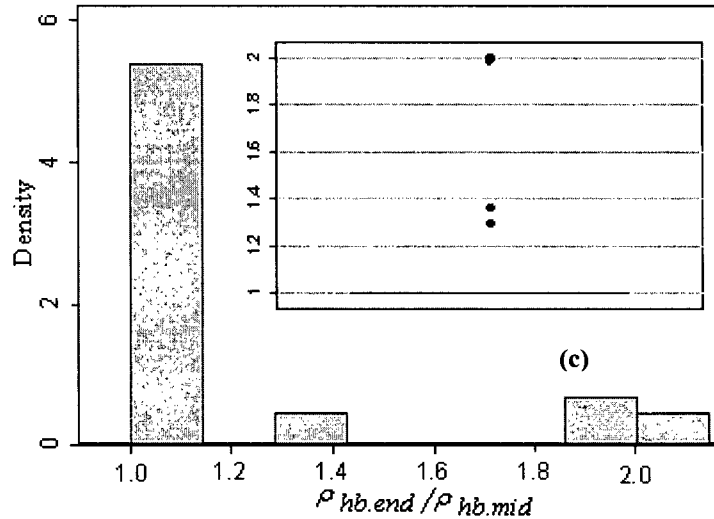


Figure A-8: Statistical distribution of bond beam design variables

A.6 Openings

Some of the specimens in the database are pierced with door/window openings, in order to investigate the effect of the openings on the seismic performance of the CM walls. Except for two experiments, specimens were provided with confining elements along the opening borders to alleviate detrimental effects and to avoid instability of the extensively damaged triangles besides the openings.

Table A-8 documents opening parameters in terms of their notations, descriptions and units.

Table A-8: Opening characteristics

Notations	Description	Units
W_o	Width	mm
H_o	Height	mm
γ_o	$\frac{(H_w - H_o)L_w + H_o(L_w - W_o)}{H_w \cdot L_w}$	—
β_o	Opening Area / Total Wall Area (0.092 -0.327, when opening exists)	—
α_o	Net Transverse Area / Total Transverse Area	—

A.7 Floors

In addition to top bond beams, some specimens were provided with reinforced concrete floors that extend from the walls at their both sides. Table A-9 documents the few parameters used to characterize these RC elements.

Table A-9: Floor characteristics

Notations	Definition	Units
t_f	Thickness	mm
A_f	Area	mm ²

A.8 Loading configuration

Specimens that are tested cyclically are always loaded as cantilever (*CR*) beams at a height less than or equal to the actual height of the panel, or atop the rigid steel/concrete beam that is installed over the wall. The height of the deflection point (the point at which lateral load is applied to the wall) at close inspection of data was found to have a great impact on the failure modes of the specimens, and for high values of this parameter, flexural deformations usually dominate the response.

For monotonically tested specimens, however, lateral loads are applied in either cantilever or compression diagonal (*CD*) configurations. In the latter case, specimens are enforced to crack in a predetermined manner, and therefore their behaviour somewhat differs from the rest of the specimens. As Figure A-9 indicates, specimens loaded as cantilever beams greatly outnumber the diagonally loaded tests.

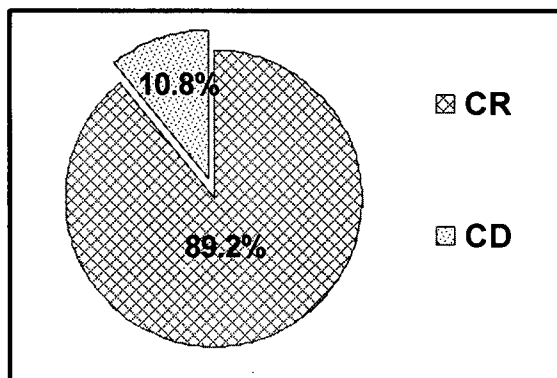


Figure A-9: Distribution of different loading configurations

Appendix A: Confined masonry database

In addition to lateral loads, specimens are frequently stressed vertically to simulate real conditions where CM walls are designed to bear both vertical stresses, induced by dead and live loads, and lateral forces. These vertical loads are applied using either rigid beams atop the panels or pre-stressed struts that pass through masonry wall at regular intervals. Axial stress, although beneficial to the seismic performance of CM walls, should be kept within a reasonable range compared to masonry compressive strength, in order to avoid premature masonry crushing. This threshold is usually in the order of $0.15f_m$. However, for some specimens in the database that are either under the effect of large axial stresses (simulating panels of the first stories in multi-story CM buildings) or suffer from low masonry compressive strength, this ratio is excessively high.

Key factors that characterize loading conditions of the quasi-static tests in terms of units, notations and general definitions are presented in Table A-10. Table A-11 documents the range, average and variability of the most important loading parameters.

Table A-10: Loading characteristics

Notations	Definition	Units
σ_v	Constant Vertical Stress	MPa
H'	Height of Applied Lateral Load	mm

Table A-11: Statistics of loading parameters

Notations	Range	Mean	Cov
σ_v	- 0.11– 1.80	0.34	0.38
σ_v/f_m	0.00 – 0.34	0.04	0.06

The distribution of both σ_v and σ_v/f_m along with the extreme values of these design variables are presented in Figure A-10-a, b, to demonstrate axial stress on its own would not control the response. Its value in proportion to masonry compressive strength is the factor that affects the performance of CM walls. As is apparent, while a few specimens have σ_v/f_m larger than 0.15, far more are characterized by high vertical loads.

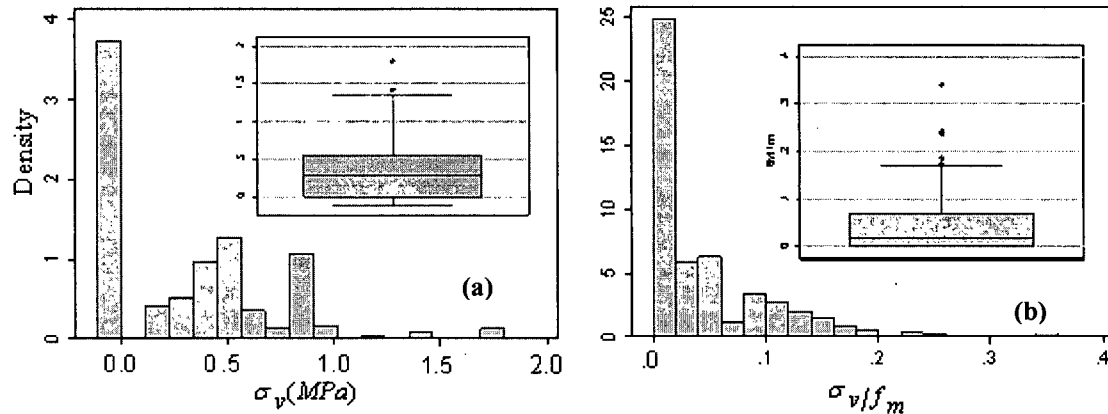


Figure A-10: Statistical distribution of loading variables

It follows from the foregoing, when high axial stresses are imposed on CM walls, panels should be designed to have higher compressive strengths. Controlling the quality and type of masonry units and mortar in addition to filling the bed joints fully with mortar would ensure higher compressive strengths.

A.9 Results

A.9.1 Damage pattern and failure modes

The sequence in which damage initiates and extends, together with the final cracking pattern of experimental tests, help identify failure modes, critical zones whose extensive damage usually lead to final collapse, and the general aspects of the seismic performance of the CM walls. Furthermore, the effect of different design variables and deficiencies present could be determined when comparing these data for specimens with varying characteristics. Visual inspection of final crack patterns (whenever presented in the database), observed failure modes, and the specific characteristics of each specimen helped identify possible failure modes, damage sequence of CM walls, and to recognize the contributing factors.

Based on this procedure, and as demonstrated repeatedly in previous seismic events, the behaviour of CM walls is predominantly controlled by shear deformations. However, under specific circumstances, these walls might fail in flexure, sliding shear, or in a combination of both flexure and shear failure.

Figure A-11 illustrates the distribution of possible failure modes for test specimens comprising the quasi-static database.

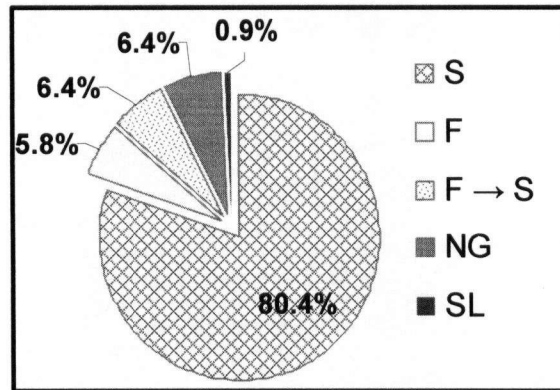


Figure A-11: Distribution of possible failure modes for CM walls

Failure modes, contributing factors, and damage sequence of the specimens up to the final collapse are described in the section below:

A.9.1.1 Shear failure

This type of failure is characterized by inclined shear cracks along principal diagonals.

Damage Pattern

- initiation of flexural cracks along the height of tie columns.
- onset of shear cracks: For solid specimens as images suggest, shear cracks usually initiate in the middle of the panels. However, when panels are weakened by the presence of openings cracks form at the corners of openings and propagate towards the middle of the piers. Based on the final damage patterns of the database specimens, these cracks could pass through both masonry units and mortar joints depending on their relative stiffness characteristics. Similar elastic modulus of the constituent materials helps propagation of cracks through both units and mortar joints, and this, in turn, somewhat compensates for the inherent heterogeneity that this composite system suffers from. Furthermore, formation of more micro-cracks would improve the energy absorption characteristics, and thus, the seismic response.

However, cracks usually pass through mortar joints in a zig-zag manner at the early stages of loading and extend into masonry units at large deformations. The inclination of shear cracks, as shown by close inspection of final damage

Appendix A: Confined masonry database

patterns for various specimens, is mainly affected by the panel aspect ratio. For nearly squat panels this angle (θ) falls between $\tan^{-1}(H/L)$ and 45° , whereas for slender walls θ happens to be between 45° and $\tan^{-1}(H/L)$.

- penetration of cracks into tie column ends: Shear cracks usually reach the end of tie columns at about the same angle at which they have traveled through the panels.
- Disintegration of panel and tie columns: relative movement of masonry units over cracks at large deformations and in the absence of adequate bond at column-wall interface would result in the partial separation of these elements (where connection rebar appears to be highly beneficial).
- Shear failure of tie columns at their ends: this failure is usually characterized by widening of cracks, concrete crushing and spalling and longitudinal rebar rupture/ buckling.
- Complete failure of the specimen

A.9.1.2 Flexural failure mode

As database results indicate, this type of failure occurs for panels with extremely large aspect ratios, insufficient tie column longitudinal reinforcement (close scrutiny of data proved all these specimens to have $\rho_{vc} < 1\%$), or when specimens are horizontally over-reinforced.

Case A

- Formation of horizontal bending cracks at lower portions of the masonry wall (zones of high negative moments) would usually bring about the partial disintegration of wall and its supporting foundation.
- Extension of these cracks towards the lower ends of tie columns would result in shear failure of these confining elements, as in the case of shear failure.

Case B: Yielding of longitudinal reinforcement at the lower ends of tie columns gives rise to uplift of the panel.

Case C: Early horizontal bending cracks at the lower portions of the panels would trigger the formation of inclined shear cracks, and therefore the response is controlled by a combination of both flexural and shear failure modes.

A.9.1.3 Sliding shear

As the results of experimental tests indicate, only a few CM walls, whose tie column longitudinal reinforcement has been replaced with a single equivalent rebar, suffer this type of failure mode.

A.9.1.4 The effect of each reinforcement method on damage pattern

Panel horizontal reinforcement / Welded wire mesh

If provided in an appropriate amount, panel horizontal reinforcement/WWM would bring about finer cracks distributed more evenly throughout the panels. On the other hand, the rupture of insufficient bed-joint reinforcement would trigger the crushing of masonry right off the rupture zone which adversely affects the seismic performance of CM walls.

Intermediate beams/columns

As final crack patterns indicate, intermediate confining elements control the extension of damage to some extent, thus improving the overall seismic performance of CM walls. However, cracks are not completely stopped at these secondary confining elements, and would pass them at large deformations.

A.9.2 Determination of result parameters

To determine the results and to verify the accuracy of the reported numbers, first, a smooth backbone was fitted to the recorded response of each individual test for both positive and negative branches. This backbone was drawn through the peak displacements of the first cycles at each deformation step. Next, positive and negative result parameters were measured for cracking, maximum load, and ultimate limit states, defined on the basis of the general aspects of the seismic behaviour of CM walls and the shape of the recorded response.

These limit states, as evident in Figure A-12 depict the point of sharp decline in the effective wall stiffness, the peak point of the observed response, and 20 % loss in the

Appendix A: Confined masonry database

maximum attained strength. Table A-12 documents the result parameters in terms of their notations, definitions, and units. Highlights in the table differentiate parameters that characterize the results of dynamic tests.

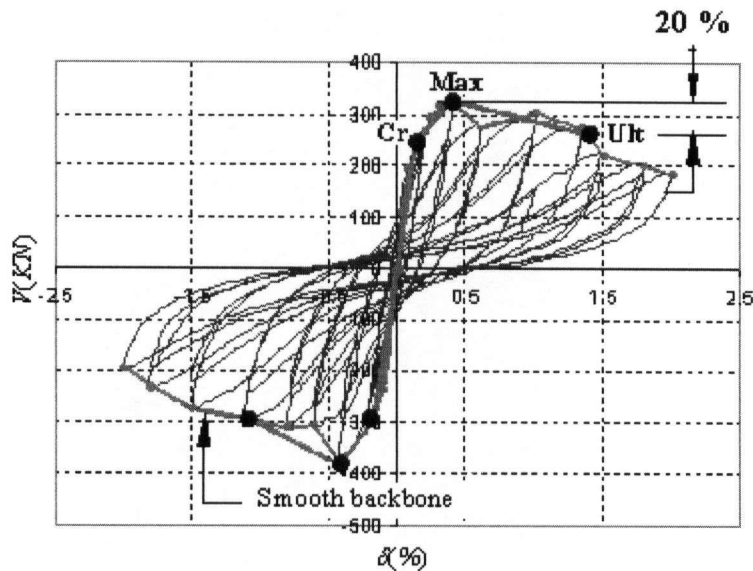


Figure A-12: Limit states and the smooth backbone

For multi-story and 3D specimens result parameters have been measured only for the critical first story and in loading direction. Result parameters have been measured for both positive and negative directions, and then the averages added as indicators of the overall seismic performance. However, for the experiments that are only supplemented with the mean recorded response, result parameters are only presented in terms of their average values.

Table A-12: Result parameters

Notations	Definition	Units
V_{cr}	Cracking Shear Load	KN
P_{cr}	Cracking Flexural Load	
V_{max}	Maximum Shear Load	
V_{ult}	Shear Load at Ultimate Limit State	
v_{cr}	Cracking Shear Stress	MPa
v_{max}	Maximum Shear Stress	
K_{int}	Initial Stiffness	KN/mm
K_{cr}	Cracking Stiffness	
K_{max}	Stiffness at Maximum Load State	
K_{ult}	Stiffness at Ultimate Limit State	
δ_{cr}	Cracking Drift ratio	%
δ_{max}	Drift Ratio at Maximum Load State	
δ_{ult}	Drift ratio at Ultimate Limit State	
C_{cr}	Elastic Seismic Coefficient Factor	—
C_{max}	Seismic Coefficient Factor at Maximum Load State	
C_{ult}	Seismic Coefficient Factor at Ultimate Limit State	
D_{cr}	Elastic Dynamic Amplification Factor	—
D_{max}	Dynamic Amplification Factor at Maximum Load State	
D_{ult}	Dynamic Amplification Factor at Ultimate Limit State	
E_{dult}	Cumulative Dissipated Energy at Ultimate Limit State	

Table A-13 documents the assumptions underlying the determination of each result parameter, and in some cases identifies anomalies which preclude determination of accurate results.

Table A-13: Basic assumptions and procedure to determine result parameters

Notations	Assumptions / Remarks
V_{cr}	Difficult to determine with sufficient accuracy when the slope of the recorded response changes steadily up to the peak point. In these cases this value has been reported <i>NG / HM</i> (Hard to measure).
P_{cr}	Mainly for specimens that failed in flexure
V_{ult}	Max (80% V_{max} , $V_{failure}$), provided that the specimen was pushed far enough to fail.
v_{cr}	Based on gross sectional area for solid panels, and effective area for specimens that were pierced with openings
v_{max}	
K_{int}	Max(secant stiffness at 1/3 V_{max} , K_{cr})
K_{cr} , K_{max} , K_{ult}	Secant stiffness
δ_{cr}	Difficult to determine with sufficient accuracy when the slope of the response curve changes steadily up to the peak point. In these cases this value has been reported <i>NG / HM</i> .
δ_{max}	When the recorded response flattens after hitting the peak point, or at the occurrence of local strength loss, its determination with sufficient accuracy is difficult. In such cases, the first point was usually considered and the model parameter was flagged for further investigation.
δ_{ult}	Not determined for specimens that were not pushed to failure, e.g. those loaded to some repairable damage, rehabilitated and then retested.
C_{cr}	For some dynamic tests instead of V_{cr} .
C_{max}	For some dynamic tests instead of V_{max}
C_{ult}	For some dynamic tests instead of V_{ult}
D_{cr}	For some dynamic tests as an indicator of deformation capacity
D_{max}	
D_{ult}	
E_{dult}	Cumulative absorbed energy at ultimate limit state

A.10 Simplified database

After the determination of all result parameters and recognition of the anomalies present in the database, some specimens whose characteristics were substantially different from the remainder, such as small-scale models that employed complete similitude laws and also those which suffered from complete lack of data, were removed from the table

Appendix A: Confined masonry database

initially developed. A simplified dataset was thus derived, providing the basis of the analytical models.

In this new database, a few of the least important panel and confining element design variables were removed. New variables, however, were derived on the basis of this initial set. Existing force-based models for cracking and maximum limit states were also incorporated in order to check how closely they followed the observed trends of the result parameters.

Where positive and negative responses were approximately the same in the original quasi-static database, the average values were selected to appear in the simplified database as presumed model parameters. However, when the responses were found to be substantially different, the most accurate value was selected, after identification of the causes of such a difference.

This simplified database includes the results of 342 of the 357 test specimens that were considered in the development of the original database. For a complete list of data points eliminated preliminary from the database, refer to Appendix B.

A.11 References

Aguilar, G., Meli, R., Diaz, R., Vazquez-del-Mercado, R., (1996). "Influence of horizontal reinforcement on the behaviour of confined masonry walls." 11th World Conference on Earthquake Engineering, Acapulco, Mexico, No 1380

Alcocer, S.M., Arias, J.G., and Vazquez, A. (2004). "Response assessment of Mexican confined masonry structures through shaking table tests." 13th world conference on earthquake engineering, Vancouver, B.C., Canada, No. 2130

Alcocer, S., Castro, D., Muria Vila, D., and Pedroza J.(1999)"Comportamiento dinamico de muros de mamposteria confinada" UNAM , Mexico

Alcocer, S.M and Meli, R. (1993) "Experimental program on the seismic behaviour of confined masonry structures." Proceedings of the sixth North American masonry conference, Philadelphia, PA ,Vol. 2

Alcocer S.M., Pineda J.A., Ruiz, J., and Zepeda, J.A. (1996) "Retrofitting of confined masonry walls with welded wire mesh," 11th World Conference on Earthquake Engineering, Acapulco, Mexico, No. 1471

Alcocer, S.M, and Zepeda, J.A (1999) "Behaviour of multi-perforated clay brick walls under earthquake-type loading." 8th North American masonry conference, Austin, Texas, USA

Alvarez, J.J (1996) "Some topics on the seismic behaviour of confined masonry structures."11th World Conference on Earthquake Engineering, Acapulco, Mexico, No 180

Astroza M.I., and Schmidt A.A. (2004) "Capacidad de deformacion de muros de Albanileria confinada para distintos niveles de desempeno (Deformation capacity of confined masonry for different performance levels)." Revista de Ingenieria Sísmica No. 70, 59-75

Bariola, J., and Delgado, C. (1996) "Design of confined masonry walls under lateral loading." 11th World Conference on Earthquake Engineering, Acapulco, Mexico, No.204

Bingzhang, Z. (1991)"Investigation of the seismic design on masonry structural buildings." Proceedings of the 1991 International Symposium on Building Technology and Earthquake Hazard Mitigation ,City of Kunming, Yunnan Province, China, 412-418

Bariola, J., Delgado, C. (1996)"Design of confined masonry walls under lateral loading." Eleventh World Conference on Earthquake Engineering , Acapulco, Mexico, No. 204

Bourzam, A (2002) "Structure behaviour of confined masonry in using solid brick" Individual Studies by Participants at the International Institute of Seismology and Earthquake Engineering. Vol. 38,179-192

Appendix A: Confined masonry database

Castilla, E., and Marinilli, A. (2000) "Recent experiments with confined concrete block masonry walls." 12th international Brick/block masonry conference, Amsterdam, Netherlands , 419-431

Chuxian, Sh., and Jianguo L., (1991)" Aseismic performance of brick masonry building with RC weak-frame and reinforced masonry wall." 9th International Brick/Block masonry conference, Berlin ,Germany, 498-503

Diez, J., Astroza, M., and Delfin, F. (1988) "Estudio experimental de modalidades de refuerzo para muros de albanileria de unidades ceramicas."Colloquia ,Madrid,Espana.

Elwood K.J., Matamoros A.B., Wallace J.W., Lehman D.E., Heintz J.A., Mitchell A.D., Moore M.A., Valley M.T., Lowes L.N., Comartin C.D., and Moehle J.P. "Update to ASCE/SEI 41 concrete provisions." Earthquake spectra, 2007

Flores, L. (2004) "UNAM Database." National disaster prevention centre, Mexico

Flores, L. E., and Alcocer, S. M. (1996) "Calculated response of confined masonry structures." 11th World Conference on Earthquake Engineering, Acapulco, Mexico, Paper No. 1830

Flores, L.E., Mendoza, J.A., and Carlos Reyes Salinas (2004) "Ensayo de muros de mamposteria con y sin refuerzo alrededor de la abertura." XIV Congreso Nacional de Ingeniería Estructural, Acapulco, Gro, Mexico

Flores, L.E., Ríos, M., and Salinas, C., (2004) "Rehabilitacion con malla y mortero de muros de memposteria con aberturas." XIV Congreso Nacional de Ingeniería Estructural, Acapulco, Gro, Mexico

Gibu, P. and Serida, C. (1993)" Confined masonry walls subjected to lateral loads (Muros Albanileria confinada sujetos a carga lateral)." National University of engineering (UNI) Lima-Peru

Gostic, S., and Zarnic, R. (1999) " Cyclic lateral response of masonry infilled RC frames and confined masonry walls." Proceedings of the eighth North American masonry conference,Austin, Texas,USA, 477-488

Grumanazescu, I.P., and Gavrilesu, I.C. (1999) "Different behaviour aspects of confined masonry piers subjected to cyclic reversal and dynamic loads." Proceedings of the Fourth European Conference on Structural Dynamics, EUROLYN 919-924

Hernandez, O., and Meli, R. (1976)"Modalidades de refuerzo para mejorar el comportamiento sismico de muros de mamposteria."Instituto de Ingenieria, UNAM, Report No.382 , Mexico

Appendix A: Confined masonry database

Ilba, M., Mizuno, H., Goto, T., and Kato, H. (1996) "Shaking table test on seismic performance of confined masonry wall." World Conference on Earthquake Engineering, Acapulco, Mexico, No 659

Irimies, M.T., (2002) "Confined Masonry Walls: the influence of the tie-column vertical reinforcement ratio on the seismic behaviour." The proceedings of the Twelfth European Conference on Earthquake Engineering , No. 7

Ishibashi, K., Meli, R., Alcocer, S.M., Leon, F., and Sanchez, T.A. (1992) "Experimental study on earthquake-resistant design of confined masonry structures." Proceedings of the Tenth World Conference on Earthquake Engineering, Madrid, Spain , 3469-3474

Kato, H.; Goto, T., Mizuno, H., and Iiba, M. (1992)."Cyclic loading tests of confined masonry wall elements for structural design development of apartment houses in the Third World." Proceedings of the Tenth World Conference on Earthquake Engineering, Madrid, Spain, 3539-3544

Liu, D., and Wang, M (2000) "Masonry structures confined with concrete beams and columns." Proceedings of the 12th World Conference on Earthquake Engineering ,Auckland , New Zealand. No. 2720

Marinilli, A., and Castilla, E. (2004). "Experimental evaluation of confined masonry walls with several confining-columns." 13th world conference on earthquake engineering, Vancouver , B.C. , Canada , Accession No. 2129

Marinilli, A., and Castilla, E. (2006) "Seismic behaviour of confined masonry walls with intermediate confining - columns." Proceedings of the 8th U.S. National Conference on Earthquake Engineering, San Francisco, California, USA, No. 607

Matsumura, 1988" Matsumura, A., "Shear Strength of Reinforced Masonry Walls," Proceedings of the 9th World Conference on Earthquake Engineering, Tokyo-Kyoto, Japan, 121-126.

Meli, R., and Salgado, G., (1969) "Seismic Behaviour of Masonry Walls Subjected to Lateral Loading (Comportamiento de Muros de Mampostería Sujetos a Carga Lateral)." Report N0. 237, Instituto de Ingenierí'a, UNAM, Mexico City.

Moroni, M. O., Astroza, M., and Tavonatti, S., (1994)."Nonlinear models for shear failure in confined masonry walls." The Masonry Society Journal. Vol. 12, No. 2, 72-78

Pineda J.A (1996)" Comportamiento ante laterales de mamposteria confinada reforzados con malla electrosoldada." Msc Thesis No 171, Mexico

Ramirez Mestas, O. (1994) " Nonlinear finite element analysis of confined masonry walls." Individual Studies by Participants at the International Institute of Seismology and Earthquake Engineering

Appendix A: Confined masonry database

Rodelio Mercado, A. (2004) "Improvement of seismic performance of confined masonry structures." Individual Studies by Participants at the International Institute of Seismology and Earthquake Engineering, vol. 40, 243-255

San Bartolome, A., Quiun, D., and Torrealva, D. (1992) "Seismic behaviour of a three-story half scale confined masonry structure." Proceedings of the 10th World Conference on Earthquake Engineering, Madrid, Spain; 3527-3531

Sanchez, T.A., Alcocer S.M., and Flores, L "Estudio experimental sobre una estructura de mamposteria confinada tridimensional, construida a escala natural y sujeta a cargas laterales." Xth National conference

Sanchez, T., Flores, L, Alcocer, S. M., and Meli, R. (1992) "Respuesta sismica muros de mamposteria confinada con diferentes tipos de refuerzo horizontal. Coordinacion de investigacion." CENAPRED, Mexico

Sánchez, T.A., Flores, L., León, F., Alcocer, S.M and Meli R. (1991) "Seismic response of confined masonry walls with different types of flexural coupling." National disaster prevention report

Sarma, B. S, Sreenath, H.G., Bhagavan, N.G., Ramachandra Murthy, A., Vimalanandam, V. (2003). "Experimental studies on in-plane ductility of confined masonry panels." ACI Structural Journal, Vol. 100, No. 3

Scaletti, H., Chariarse, V., Cuadra, C., Cuadros, G., and Tsugawa, T. (1992). "Pseudo-dynamic tests of confined masonry buildings Concrete masonry." Proceedings of the 10th World Conference on Earthquake Engineering, Balkema, Rotterdam, Vol. 6, 3493-3497

Tomazevic, M. (1997) "Seismic behaviour of confined masonry buildings, part 1, shaking-table tests of model buildings M1 and M2 : test result." Ljubljana, National Building and Civil Engineering Institute.

Tomazevic, M., Bosiljkov, V., and Weiss, P.(2004) "Structural behaviour factor for masonry structures." 13th world conference on earthquake engineering, Vancouver, B.C., Canada , No. 2642

Tomazevic, M., and Klemenc, I. (1997). "Seismic behaviour of confined masonry walls." Earthquake engineering and structural dynamics, Vol. 26, 1059-1071

Tomazevic, M., and Klemenc, I. (1997). "Verification of seismic resistance of confined masonry buildings." Earthquake engineering and structural dynamics, Vol. 26, 1073-1088

Tomazevic, M., and Klement, I.(1998) "Seismic resistance analysis of confined masonry walls and buildings." Structural Engineering World Wide, ASCE, paper T126-3

Appendix A: Confined masonry database

Yañez, F., Astroza, M., Holmberg, A., and Ogaz, O. (2004) "Behaviour of confined masonry shear walls with large openings" 13th world conference on earthquake engineering, Vancouver, B.C., Canada, No. 3438

Yamin, L., and Garcia, L.E. (1997). "Experimental development for earthquake resistance of low-cost housing systems in Colombia." *Mitigating the Impact of Impending Earthquakes: Earthquake Prognostics Strategy Transferred into Practice*, 377-39

Yoshimura, K., and Kikuchi, K. (1995). "Experimental study on seismic behaviour of masonry walls confined by RC frames." *Proceedings of the Pacific Conference on Earthquake Engineering*; Melbourne, Australia, Vol. 3, 97-106

Yoshimura, K., Kikuchi, K., Kuroki, M., Liu, L., and Ma, L. (1999). "Effect of vertical axial loads and repeated lateral forces on seismic behaviour of confined concrete masonry walls." *Eighth Canadian Conference on Earthquake Engineering*; 107-112

Yoshimura, K., Kikuchi, K., Kuroki, M., Liu, L., and Ma, L. (2000) "Effect of wall reinforcement, applied lateral forces and vertical axial loads on seismic behaviour of confined concrete masonry walls." *Proceedings of the 12th World Conference on Earthquake Engineering*, Auckland, New Zealand. No. 984

Yoshimura, K., Kikuchi, K., Kuroki, M., Nonaka, H., Croston, T., Koga, S., Kim, K. T. and Ma, L. (2000). "Experimental study for higher seismic performance of masonry walls in developing countries." *Proceedings of 25th Conference on Our World in Concrete & Structures*, 695-702

Yoshimura, K., Kikuchi, K., Kuroki, M., Nonaka, H., Kim, K.T., Matsumoto, Y., Itai, T., Reezang, W., and Ma, L. (2003). "Experimental study on reinforcing methods for confined masonry walls subjected to seismic forces." *Proceedings of the ninth North American masonry Conference*, Clemson, South Carolina, USA.

Yoshimura, K., Kikuchi, K., Kuroki, M., Nonaka, H., Tae Kim, K., Wangdi, R., and Oshikata, A. (2004). "Experimental study for developing higher seismic performance of brick masonry walls." 13th world conference on earthquake engineering, Vancouver, B.C., Canada, No. 1597

Yoshimura, K., Kikuchi, K., Kuroki, M., Nonaka, H., Tae Kim, K., Wangdi, R., and Oshikata, A. (2004). "Experimental study on effects of height of lateral forces, column reinforcement and wall reinforcement on seismic behaviour of confined masonry walls." 13th world conference on earthquake engineering, Vancouver, B.C., Canada, No. 1870

Yoshimura, K., Kikuchi, K., Okamoto, Z., and Sanchez, T. (1996). "Effect of vertical and horizontal wall reinforcement on seismic behaviour of confined masonry walls." 11th World Conference on Earthquake Engineering, Acapulco, Mexico, No 191

Appendix A: Confined masonry database

Zabala, F., Bustos, L.J., Masanet, A., and Santalucia, J. (2004)" Experimental behaviour of masonry structural walls used in Argentina." 13th world conference on earthquake engineering, Vancouver, B.C., Canada, No. 1093

Zavala, C., Cabrejos, R., and Tapia, J., (1998)" Aseismic Masonry Building Model for Urban Areas" Structural Engineering World Wide, Paper T209-1

Zavala , C., Honma, C., Gibu, P., Gallardo, P., and Huaco, G. (2004)." Full scale on line test on two story masonry building using handmade bricks" 13th world conference on earthquake engineering, Vancouver, B.C., Canada, No. 2885

Appendix B

Multiple Regression Analysis Using the Least Square Method

B.1 Getting started

Theoretical models may be developed on the basis of experimental data compiled in an extensive database, allowing investigation into how well predicted values (Y') correspond with actual response variables (Y). Although frequently utilized, regression requires more than selection of available predictor variables (X_i) whose contribution to the model is believed significant, and fitting a function to them. A number of steps are required, and several hypotheses examined, to ensure that the regression analysis results are not misleading.

Before conducting the regression analysis, the database should be closely scrutinized to identify the characteristics of the data and the conditions and constraints under which it has been developed. This straightforward first step may be significantly beneficial in identifying potential problems, errors, peculiarities, and anomalies present.

Assume a prediction of Y as a function of $x_1 \dots x_n$. First and foremost, the n predictors should be recognized. Existing models in the field may be very helpful in identifying the significant predictors and the functional form that relates them to the response.

This may be further aided by graphical tools as scatter plots of Y versus x_i and looking for trends while keeping other predictor variables almost constant. A comprehensive understanding of the fundamentals underlying the model under development, properties of materials, their mechanics, and the mechanism of the proposed system will be substantially constructive in arriving at a proper functional form of the model.

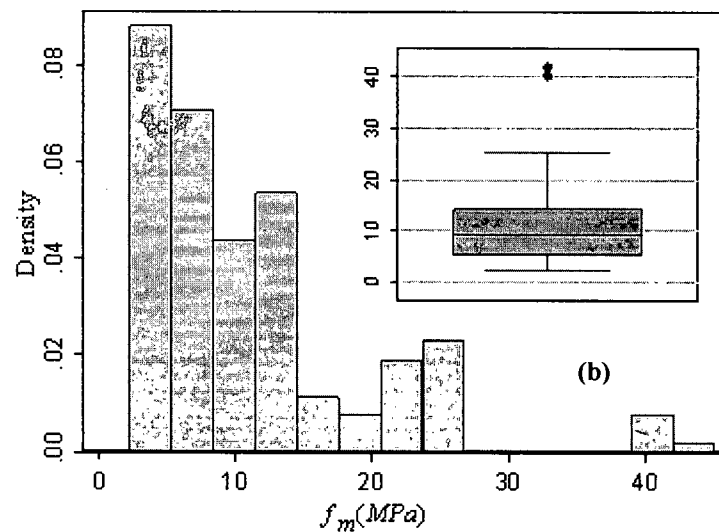
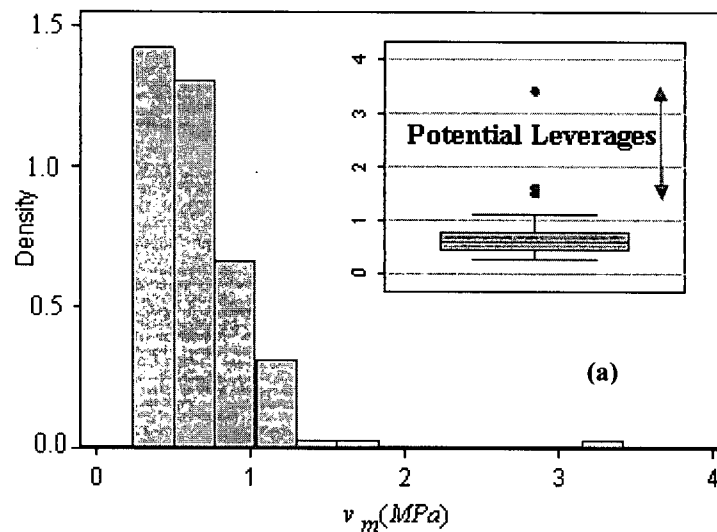
For the purpose of developing the theoretical backbone model of the present study, for instance, it would facilitate the process to know that only post-cracking contribution of tie columns is of significance to the seismic performance of CM walls.

Appendix B: Multiple regression analysis using the least square method

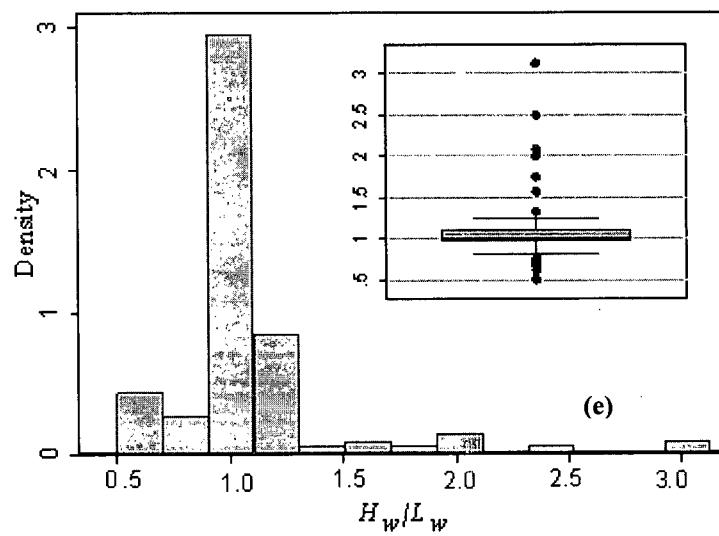
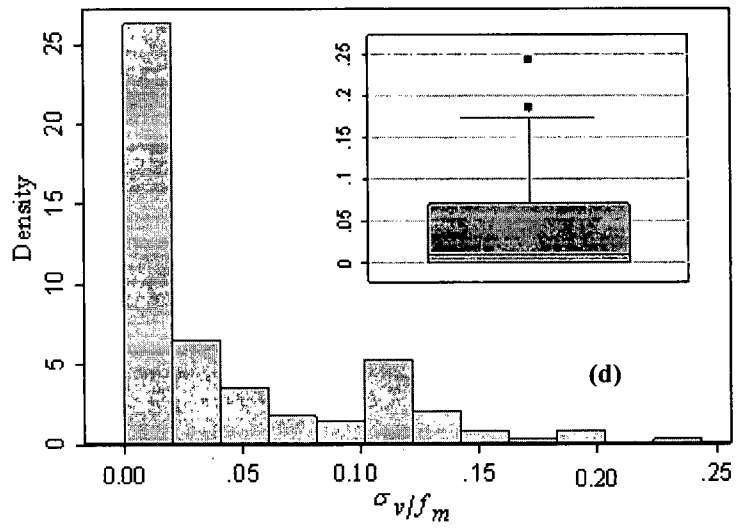
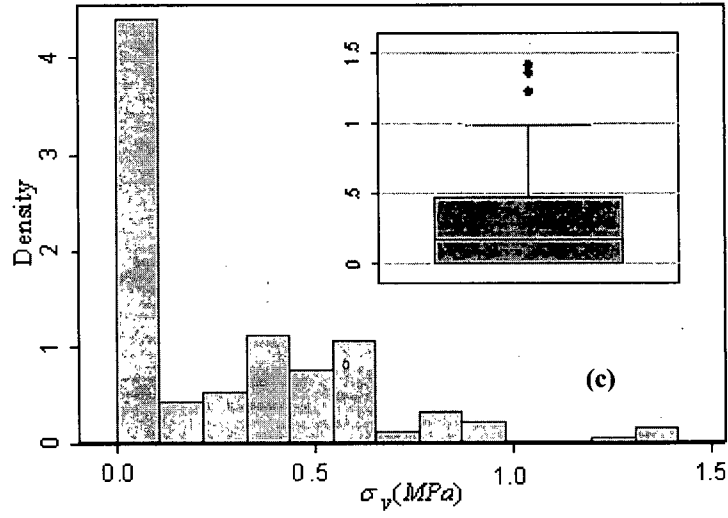
It is highly recommended those predictors which seem to affect the response be considered in the first regression. However, this does not imply including as many variables as possible. Not only would the process would be unduly time-consuming and complicated, the addition of irrelevant and trivial variables could adversely affect the final results.

All predictors should be closely examined by means of such graphical tools as histograms and scatter plots of Y versus x_i , and also through simple data inspection in order to identify the ranges covered, their extreme values, and any potential problems associated with them.

Histograms of the most important design variables for typical CM walls initially considered for the creations of the empirical equations, together with their extreme values are illustrated in Figure B-1-a to h.



Appendix B: Multiple regression analysis using the least square method



Appendix B: Multiple regression analysis using the least square method

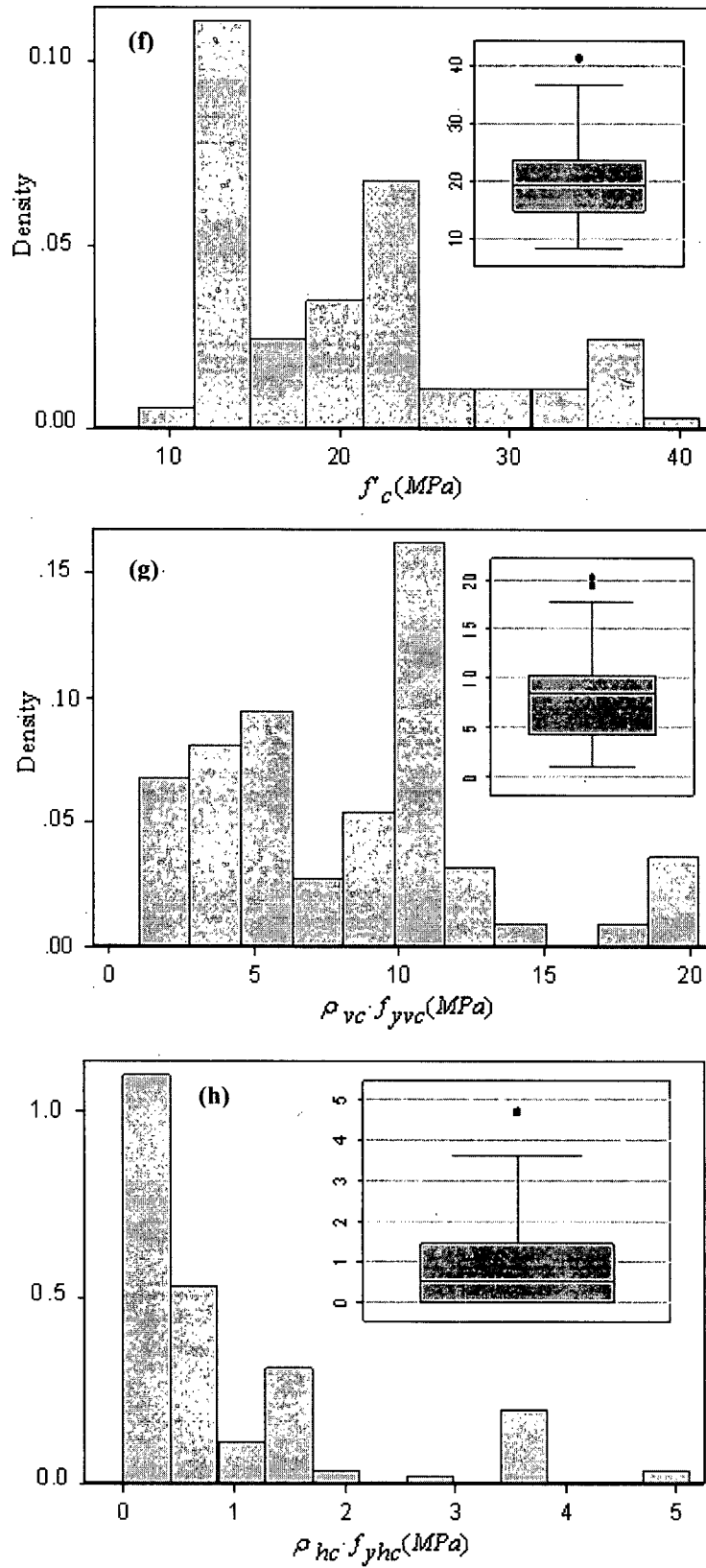


Figure B-1: Statistical distribution of CM wall design variables

Appendix B: Multiple regression analysis using the least square method

After the preliminary data inspection, and setting the functional form of the equations, the first regression analysis may be run, to see how well the independent variables predict the response. R^2 as a measure of the variance carried by the x_i 's, is usually taken as an indicator of the model fitness. This parameter, however, does not imply anything about the misspecification, i.e. if all relevant variables are included and trivial ones removed. It should therefore be used in conjunction with F -test and t -test results which are indicators of significance of the model and each individual predictor.

To be significant, the probability of the F - and t -tests should be lower than the α value (1-the confidence level). High R^2 and F -test values, although promising signs, would not imply that the regression is complete and the results can be considered for publication and future use. The assumptions underlying the linear regression should be checked for any single regression analysis, and influential points that could exert undue impact on the results should be identified.

B.2 Assumptions of Linear regression analysis

B.2.1 Linearity

Y should be linearly related to all x_i 's, otherwise the regression would try to fit a linear function to the data that are following a curve. The best diagnostic tool here would be to plot residuals $|R = Y - Y'|$ versus x_i 's and check if any trend is appearing. If yes, the corresponding variable should be properly transformed, so that the relationship between the new variable and the outcome variable becomes linear and the trends in the R - x_i plots disappear.

In the regression analysis performed in this study, the prediction of v_m by f_m instead of $\sqrt{f_m}$ (Figure B-2) resulted in a clear trend. Such a trend, however, should be eliminated by transforming f_m and repeating the analysis.

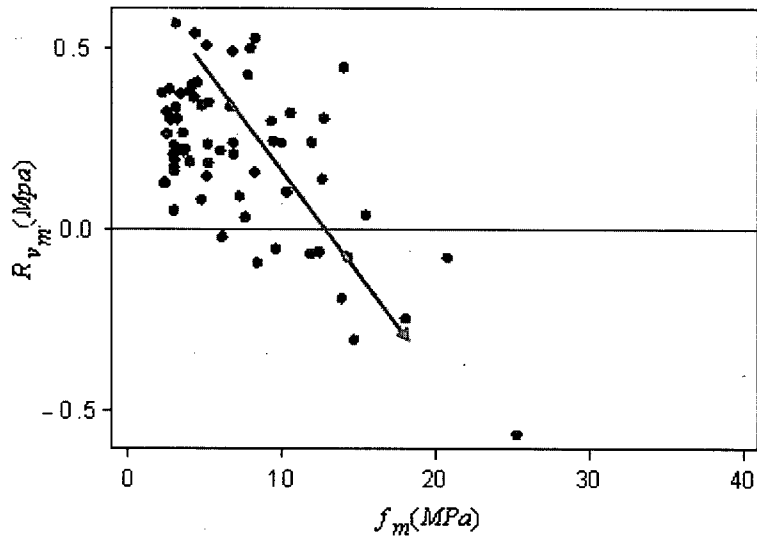


Figure B-2: Clear trend in the plot of residuals vs. the predictor variable as a measure of the model misspecification

B.2.2 Normality

Normality of the prediction errors is of paramount importance in ensuring the significance of the models, and may be evaluated by checking how the distribution of the residuals departs from normal distribution. In case of substantial deviation, independent variables should be transformed until a close match is achieved.

In this study, as it is shown in Figure B-3, this assumption was never violated and all the residuals were approximately normally distributed. However, for each empirical equation, the removal of problematic outliers and leverages often resulted in a closer match between the two distributions.

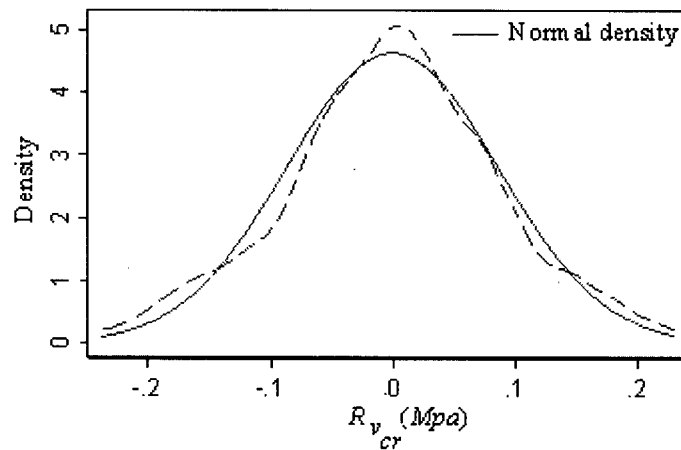


Figure B-3: Normality of the residuals

B.2.3 Homoscedasticity

If the error variance is not constant for the model, the reason should be identified by close inspection of data, and proper treatment applied. In order to check the validity of this assumption, the scatter plots of R against the predicted response(Y') may be utilized as a visual diagnostic tool. No clear trend for homogenous errors should be indicated.

This assumption, as shown in Figure B-4, was never notably violated in the regression analysis performed in developing the models, and therefore no treatment was required to redress any imbalance.

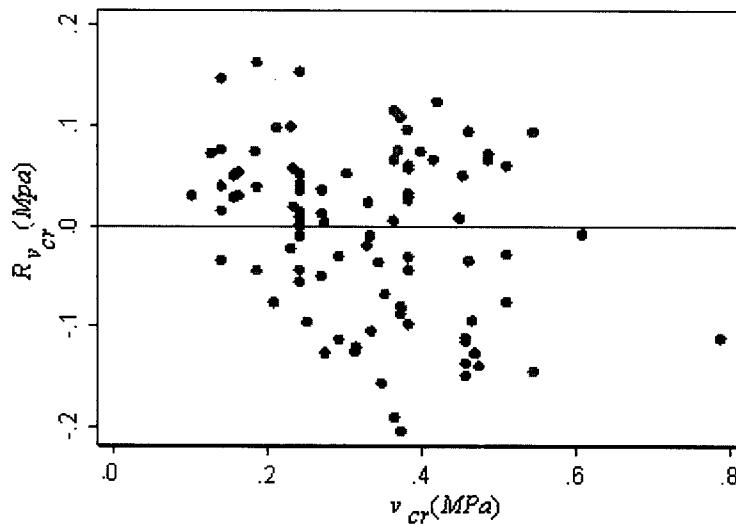


Figure B-4: Homogeneity of the residuals

B.2.4 Independence

Although in any regression analysis errors should be identically and independently distributed, this is usually of concern when sequential observations are used to develop a model. Therefore checking the validity of this assumption was not necessary in the present study.

B.2.5 Model specification

The model, as mentioned, should be properly specified by including all significant variables ($p_i \leq 0.05$)⁵, and excluding irrelevant predictors that might entirely change the format of the model. This further demonstrates the importance of proper selection of predictors; to choose as many as possible will not always lead to better results and could even alter the model accuracy. The $R-x_i$ plots help improve the functional form of the model in that they reveal any nonlinearity and suggest appropriate transformations.

Insignificant variables ($p_i > 0.05$) that could be identified after the first regression analysis would be removed from the model, provided that the prediction accuracy is not greatly affected.

In this study, all potentially important variables were considered in the first regression. Based on the results of t -tests, the least important were taken out until there was an acceptable balance between simplicity and model accuracy. For instance, the effect of different unit materials; clay, concrete and ceramic, was initially considered in the formulation of v_{cr} and v_{max} but, due to its insignificance, was eliminated from the final equations and at the cost of only a marginal change in R^2 (about 0.01).

B.2.6 Multicollinearity

Multicollinearity is not amongst the assumptions of linear regression analysis, but is of importance. If the variables are highly collinear, the model coefficients cannot be uniquely computed. As a result, estimation errors would be significantly inflated. When the statistical tests such as *collin* indicate two variables to be highly collinear, the variable less significant to the model should be eliminated. In the present analysis, none of the variables used to create the empirical equations were linearly correlated. (It may have been the case if for example, both v_m and f_m had been considered in the formulation of v_{cr} as explicit variables).

⁵ Confidence level chosen to be 0.95

B.2.7 Influential observations

Influential data points may be classified in two main categories, leverages and outliers.

The former group consists of observations with extreme values on single or multiple predictors which could substantially affect the model coefficients. A leverage is an indicator of how far an independent variable deviates from its mean. Outliers, on the other hand, are data with large residuals due to sample peculiarity, measurement/entry error and present anomalies. Influential points should be recognized, and if close scrutiny of the references identifies anomalies, their removal should be considered.

Influential points may modify results if the fitted line is adjusted to incorporate these extreme values. However, it should be kept in mind that no single data point can be arbitrarily eliminated simply because it is not consistent with the rest of the data. Any removal should be made only after investigation and identification of the cause of the problem.

To predict the model parameters in this study, a number of influential points were identified. These observations are generally referred to throughout the body of the report (section 3-3-2). Each observation is listed in this chapter, together with its type, and the cause of the problem if it was removed from the final stage of model prediction. Several statistical tests and visual aids were called for in identifying the influential points. The most important diagnostic tools utilized in creating the empirical equations, together with their general definitions and cut-off values, are listed in Table B-1

Table B-1: Diagnostic tools to identify the influential points

Tool	The type of influential points it identifies	Cut-off values
Standardized residual (rstudent)	Potential outliers	beyond 3; the observation could be removed without any need for further investigation (severe outlier), 2-3: closer scrutiny is still required (mild outliers)
Leverage	Leverages	$\frac{2k + 2}{N}$
Cooks'd	Overall measure	$\frac{4}{N}$
Dfits	Overall measure	$2 \cdot \sqrt{\frac{k}{N}}$
Dfbeta	Specific measure of influential points	—
$R-x_i$ plots	Potential outliers	—
$R-Y'$ plots	Potential outliers	—
K : the number of independent variables N: the number of observations		

B.3 Iterative regression process

As previously mentioned, regression analysis is an iterative process, to be run until removal of all deficient data points and satisfaction of every underlying assumption. In the final stage of the analysis, signs, magnitude of the coefficients, and other relevant details depending on the goals of prediction, should be checked, and the model verified for data points not originally included in the development of the analytical model. This will ensure accuracy for specimens with similar characteristics and constraints as the data being considered for the development of the model, and also determine its ability to simulate the behaviour of data points with more general properties or different characteristics.

B.4 Data removal in the present study**Table B-2: Preliminary data removal (prior to the formation of simplified database)**

ID	v_{cr}	δ_{cr}	v_{max}	δ_{max}	δ_{ult}	Supporting reasons
56				X		Anomalous backbone curve
66-68, 130			X			Scaled down based on complete similitude laws
113	X					Due to the local strength loss the distinction of cracking limit state is almost impossible.
117					X	Multiple points with 20% strength loss
137	X					Strikingly different behaviour in positive and negative response cannot be attributed to any specific reason
151-153		X		X	X	It is not clear if the hysteretic curves are given for the panel mid-height or the top, therefore the measured drift ratios cannot be reliably used for model development
154			X			3D subassembly
174						Flagged due to the local failure at the point of load application —
190		X				The shape of the recorded response makes it difficult to determine δ_{cr} with sufficient accuracy
225		X				Strikingly different δ_{max} in the positive and negative directions and no supporting hysteretic curve to identify the reason
235				X		Local strength loss makes it difficult to determine δ_{max} accurately
241-243			X			v_{cr} and v_{max} are the same but their corresponding drift ratios are different. The values of ρ_{vc} and H/L are normal, so this unusual behaviour cannot be attributed to rebar yielding. Furthermore, no supporting hysteretic curve is provided to uncover the reason.
112, 244, 246, 247, 282, 302, 303			X			Complete lack of information on model parameters
338		X				δ_{cr} is excessively large (about 0.5) , in complete contrast to the remainder of the specimens, and lack of hysteretic curve to check its accuracy

Appendix B: Multiple regression analysis using the least square method

Table B-3: Criteria for data removal during the analysis

Criteria. No	Description
1	Extremely low ρ_{vc} results in the predominance of flexural deformations
2	a: Leverages
	b: Severe outliers ($R_{stand} > 3$)
3	Overall measures of influential points substantially surpass their cut-off values
4	Specimen peculiarity
5	Cause of departure from linearity
6	Excessively large $\delta_{v/fm} (> 0.12)$
7	Compression diagonal loading
8	Data point cannot be considered in the regression analysis because its response value departs three standard deviations from its mean
9	Unreliable value due to the presence of a problem
10	Others

Table B-4: List of the specimens that were entirely removed from the analysis

Category	ID	Criteria No.
Cat-1	86, 221, 222, 300, 323, 324, 325, 353	6
Cat-2	163, 164, 193, 198, 267-290	7

Table B-5: Data points excluded from the final equation of v_m

ID	Removal Criteria for prediction of v_m
Cat-4	2a: extreme values of f_m and/or 8
	2b: rstudent > 3
Cat-4 : 13, 14, 18-22, 69-71, 82-84, 88-106, 154, 185-194, 304-307, 337	

Appendix B: Multiple regression analysis using the least square method

Table B-6: Data removal for the prediction of v_{cr}

ID	Removal Criteria
189	2a: $\sigma_v = 1.22$
	3: lev, cook's d, Dfbeta
	5
101	1: low v_{cr} due to yielding or rebar prior to cracking
	3: lev, cooks'd, Dfv _m , DF σ_v
106	2a: v_m is excessively large
	3: cook's d, lev
82	2a: very high v_m
	3: lev, DFv _m
90	9: v_{cr} cannot be determined accurately
	8
102, 103, 104	1
	2b: rstudent = - 4.2
	3 : lev, cook's d
178	1
	3: lev, cooks'd, Dfits
100	1
	3: cooks'd, DF σ_v , v_m
116, 188, 199	1
	3: cooks'd
240	4: cover mortar on both sides makes v_{cr} excessively large
298	9: very large v_{cr} , due to the lack of data on the specimen the source cannot be identified
191	1
	5
	3 : cook's d, dfits
159	1
199	8
	2b: rstudent = 4.7
299	8: v_{cr} is much larger than it should be
	2b: rstudent = 3.7
301	3: lev
	5
	2b: rstudent = 6.2

Table B-7: Data removal for the prediction of v_{max}

ID	Removal Criteria
106	2a: v_m is excessively large
90	4 : very high ρ_{nc} , very high f_m and the same v_{cr} and v_{max} ----- 9: local strength loss affects the results
175	8 ----- 2b: $r_{student} = 5.6$
194	2a :very high ρ_{vc} , f_{yvc} ; cannot be compared to the rest of the specimens ----- 3: d_{fits} , $r_{student} = 2.75$ ----- 4: very large ρ_{vc} , f_{yvc} but tie columns are not contributing to the maximum strength
*Cat-3	1: significantly large or very small tie column contribution
219, 220, 223	2a: $H/L = 3$ and flexural deformations are dominating the response, as a result tie column contribution to v_{max} is very small
186	2a :very large ρ_{vc} , f_{yvc} , very large f_c ----- 3: lev, cooks'd
*Cat- 3: 116-119, 160 -162,166, 167, 176, 177, 178, 181, 182, 183,185, 191, 122, 123, 124, 125, 126, 127	

Table B-8: Data removal for the prediction of δ_{cr}

ID	Removal Criteria
200	2b : $r_{student} = 4.2$
	8
	3: cooks'd, d_{fits}
89	2a: very large f_m ----- 3: cook's d, lev
190	8: cracking limit state can't be identified from the hysteretic curve
176,177,182	1: this effect is even more intensified by loading protocol (monotonic)
166	1
138	8
	2a : $r_{student} = 4.67$
326	9: substantially different behaviour from the other ceramic masonry walls. However, there is no supporting data to identify the reason, or to check if the cracking limit state has been determined in line with the assumptions of this study.

Appendix B: Multiple regression analysis using the least square method

Table B-8 (Cont.)

318	9: Scarcity of data makes it difficult to uncover why δ_{cr} is significantly large
131,132	4: gypsum cover
158	2b: rstudent = 3.8
219	2a: H/L = 3
160	1
161	1
173, 169, 170, 175, 183	4: concrete units, $\rho_{hc}=0$, monotonic loading ; extremely different behaviour from the rest of the specimens
	9: steady increase in the slope of the hysteretic curve up to peak point makes accurate distinction of the cracking limit state impossible
155	2b : rstudent = 3.51
	8
293	2b: rstudent = 3.1
	10: lack of information on the specimen to verify the results
263	2a: H / L = 2
264	2a: H / L = 2
114	3: rstudent = 2.34
	2a: very low f_m and large v_m

Table B-9: Data removal for prediction of δ_{ult}

ID	Removal Criteria
122-127	1: not considered in the prediction of v_{max}
131, 132	2a: very small f_m and therefore v_m
	9: strikingly different measured and predicted v_{max} due to anomalous recorded response
	4: covered by gypsum cover
160-162	1
170	2b: rstudent = 3.54
	10: γ was not calculated, because for this specimen the identification of the cracking limit state is not accurately possible due to the steady increase in the slope up to the peak point
178	1
	3: rstudent = 2.67

Appendix B: Multiple regression analysis using the least square method

Table B-9 (Cont.)

183	1
	3: dfits
194	2a: very high $\rho_{vc} \cdot f_{yvc}$ and therefore v_{max} was not predicted
240	4: mortar cover
102-104	1(H/L>1 also gives rise to the predominance of flexural deformations)
115-118	1
	3; rstudent = 2.35
167	1
	3: cooks'd
219	2a: H/L=3; predominance of flexural deformations
	3: rstudent = 2.52
263,264	2a: H/L=3; predominance of flexural deformations
	3: dfits
114	1
	2b: rstudent = 3.2
137	9: the γ value is not determined for this specimen due to anomalous recorded response
196,197	2a: very large $\rho_{vc} \cdot f_{yvc}$, and therefore, not considered in the determination of v_{max}
186	10 :very large $\rho_{vc} \cdot f_{yvc}$ and f'_c and therefore v_{max} was not determined
187	9: very large $\rho_{vc} \cdot f_{yvc}$, very small v_m compared to f_m value, v_{max} not reliable
177	1
	2a: very low v_m compared to the f_m value
100	1
	3: cooks'd
185	4: hollow clay bricks, interior tie column, $\rho_{hc}=0$, monotonic test(highly peculiar)
190	2a: very small v_m and significantly large f_m
	4: hollow clay bricks, interior tie column, $\rho_{hc}=0$, monotonic test, flexural failure mode(highly peculiar)

Appendix C

Derivation of Equations and Results

C.1 Derivation of the fundamental equations

C.1.1 Cracking drift capacity

- Considering the response to be linear-elastic and idealizing the masonry panel as shear a cantilever beam;

$$V_{cr} = k_{cr} \cdot \Delta_{cr} \quad \text{C-1}$$

$$\Delta_{cr} = \delta_{cr} \cdot H_w$$

$$K_{cr} = \beta_I \cdot K_{int} \quad \text{C-2}$$

$$K_{int} = \left(\frac{H_w^3}{3/E \cdot I} + \frac{H_w}{G \cdot A_w} \right)^{-1} \quad \text{C-3}$$

- Neglecting the first term accounting for flexural deformations for squat CM walls

$$v_{cr} \cdot A_w = \beta_I \cdot \frac{G \cdot A_w}{H_w} \cdot \delta_{cr} \cdot H_w \quad \text{C-4}$$

$$v_{cr} = \beta_I \cdot G \cdot \delta_{cr}$$

- Based on the masonry codes E is proportional to $(f_m)^c$ and G is proportional to E
- Rigidity also varies with the material type ; considering α_I as a representative of the unit materials

$$\delta_{cr} = \gamma \frac{v_{cr}}{f_m^c} \quad \text{C-5}$$

Appendix C: derivation of equations and results

For slender walls going through the same procedure;

$$\delta_{cr} = \gamma \frac{v_{cr} \left[1.6 \left(\frac{H}{L} \right)^2 + 1 \right]}{f_m^c}$$

C-6

As H/L increases the significance of the panel aspect ratio would rise and for completely slender panels $(H/L)^2$ would be controlling the response.

C.1.2 Ultimate drift ratio

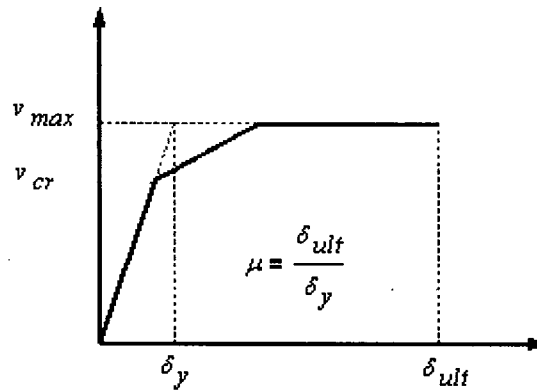


Figure C-1: The concept of ductility

- δ_y is the drift ratio of the equivalent linear system at $v_{max} \rightarrow$

$$V_{max} = \Delta_y \cdot k_{cr}$$

C-7

- considering the predominance of shear deformations for squat panels

$$V_{max} = \frac{\delta_y \cdot H_w \cdot G_{cr} \cdot A_w \cdot K}{H_w}$$

C-8

$A_w \cdot K$: shear area

- As it was noted in the derivation of δ_{cr} ; $G_{cr} = \frac{\sqrt{f_m}}{\gamma}$

$$\delta_y = \gamma \frac{v_{max}}{\sqrt{f_m}}$$

C-9

Appendix C: derivation of equations and results

$$\delta_{ult} = \mu \cdot \delta_y \quad \text{C-10}$$

$$\delta_{ult} = \mu \cdot \gamma \cdot \frac{v_{max}}{\sqrt{f_m}} \quad \text{C-11}$$

C.2 Presentation of the results

Table C-1: Masonry shear strength (v_m)

ID	$v_{m\ exp}$	f_m	$\sqrt{f_m}$	$v_{m\ cal}$	ID	$v_{m\ exp}$	f_m	$\sqrt{f_m}$	$v_{m\ cal}$
62	0.52	6.93	2.63	0.48	231	0.38	5.13	2.26	0.42
63	0.52	6.93	2.63	0.48	232	0.38	5.13	2.26	0.42
64	0.52	6.93	2.63	0.48	233	0.38	5.13	2.26	0.42
65	0.52	6.93	2.63	0.48	234	0.38	5.13	2.26	0.42
72	0.64	6.67	2.58	0.47	235	0.38	5.13	2.26	0.42
73	0.74	4.41	2.10	0.39	236	0.38	5.13	2.26	0.42
74	0.38	3.63	1.91	0.35	237	0.37	4.05	2.01	0.37
75	0.37	3.04	1.74	0.32	238	0.37	4.05	2.01	0.37
76	0.39	3.73	1.93	0.35	239	0.37	4.05	2.01	0.37
77	0.56	4.81	2.19	0.40	240	0.44	2.97	1.72	0.32
78	0.74	5.14	2.27	0.42	241	0.44	2.97	1.72	0.32
79	0.74	5.14	2.27	0.42	242	0.34	2.97	1.72	0.32
80	0.74	5.14	2.27	0.42	243	0.34	2.97	1.72	0.32
81	0.74	5.14	2.27	0.42	250	0.42	5.25	2.29	0.42
85	0.74	15.5	3.94	0.72	251	0.42	5.25	2.29	0.42
107	0.3	3.05	1.75	0.32	252	0.42	5.25	2.29	0.42
108	0.3	3.05	1.75	0.32	253	0.42	5.25	2.29	0.42
109	0.31	3.05	1.75	0.32	254	0.42	5.25	2.29	0.42
110	0.31	3.05	1.75	0.32	255	0.42	5.25	2.29	0.42
111	0.44	2.55	1.60	0.29	256	0.42	5.25	2.29	0.42
112	0.44	2.55	1.60	0.29	257	0.42	5.25	2.29	0.42
113	0.44	2.55	1.60	0.29	263	1.08	14.03	3.75	0.69
114	0.44	2.55	1.60	0.29	264	1.08	14.03	3.75	0.69
115	0.44	2.55	1.60	0.29	265	1.08	14.03	3.75	0.69
116	0.88	12.75	3.57	0.66	266	1.08	14.03	3.75	0.69
117	0.88	12.75	3.57	0.66	267	0.48	2.26	1.50	0.28
118	0.88	12.75	3.57	0.66	268	0.48	2.26	1.50	0.28
119	0.88	12.75	3.57	0.66	269	0.38	2.55	1.60	0.29
128	0.59	5.3	2.30	0.42	270	0.61	4.51	2.12	0.39
129	0.59	5.3	2.30	0.42	271	0.44	13.93	3.73	0.69
131	0.24	2.44	1.56	0.29	272	0.29	8.44	2.91	0.53
132	0.24	2.44	1.56	0.29	273	0.44	13.93	3.73	0.69
133	0.24	2.44	1.56	0.29	274	0.38	7.65	2.77	0.51
134	0.24	2.44	1.56	0.29	275	0.8	10.59	3.25	0.60

Appendix C: derivation of equations and results

135	0.55	6.89	2.62	0.48	276	0.8	10.59	3.25	0.60
136	0.55	6.89	2.62	0.48	277	0.26	6.18	2.49	0.46
137	0.49	6.04	2.46	0.45	278	0.26	6.18	2.49	0.46
138	0.49	6.04	2.46	0.45	279	0.42	7.26	2.69	0.50
139	0.55	6.89	2.62	0.48	280	0.42	7.26	2.69	0.50
140	0.55	6.89	2.62	0.48	281	0.42	7.26	2.69	0.50
141	0.49	6.04	2.46	0.45	282	0.36	14.72	3.84	0.70
142	0.49	6.04	2.46	0.45	283	0.36	14.72	3.84	0.70
143	0.55	6.89	2.62	0.48	284	0.36	14.72	3.84	0.70
144	0.55	6.89	2.62	0.48	285	0.86	20.8	4.56	0.84
145	0.49	6.04	2.46	0.45	286	0.47	11.87	3.45	0.63
146	0.49	6.04	2.46	0.45	287	0.47	11.87	3.45	0.63
147	0.55	6.89	2.62	0.48	288	0.47	11.87	3.45	0.63
148	0.55	6.89	2.62	0.48	289	0.53	8.24	2.87	0.53
149	0.49	6.04	2.46	0.45	290	0.53	8.24	2.87	0.53
150	0.49	6.04	2.46	0.45	291	0.53	8.24	2.87	0.53
155	0.57	10.33	3.21	0.59	292	0.38	9.61	3.10	0.57
156	0.57	14.28	3.78	0.69	293	0.72	9.34	3.06	0.56
157	0.57	14.28	3.78	0.69	294	0.71	12.65	3.56	0.65
158	0.57	14.28	3.78	0.69	295	0.74	15.52	3.94	0.72
159	0.57	14.28	3.78	0.69	296	0.74	15.52	3.94	0.72
160	0.57	14.28	3.78	0.69	297	0.9	8.29	2.88	0.53
161	0.57	14.28	3.78	0.69	298	0.8	6.86	2.62	0.48
162	0.57	14.28	3.78	0.69	299	0.8	6.86	2.62	0.48
163	0.57	14.28	3.78	0.69	300	0.8	6.86	2.62	0.48
164	0.57	14.28	3.78	0.69	301	0.8	6.86	2.62	0.48
165	0.57	18.07	4.25	0.78	302	0.59	4.2	2.05	0.38
166	0.57	18.07	4.25	0.78	303	0.56	3.97	1.99	0.37
167	0.57	18.07	4.25	0.78	308	0.78	7.85	2.80	0.51
168	0.57	18.07	4.25	0.78	309	0.78	7.85	2.80	0.51
169	0.57	25.3	5.03	0.92	310	0.78	7.85	2.80	0.51
170	0.57	25.3	5.03	0.92	311	0.78	7.85	2.80	0.51
171	0.57	25.3	5.03	0.92	312	0.78	7.85	2.80	0.51
172	0.57	25.3	5.03	0.92	313	0.78	7.85	2.80	0.51
173	0.57	25.3	5.03	0.92	314	0.78	7.85	2.80	0.51
174	0.57	25.3	5.03	0.92	315	0.78	7.85	2.80	0.51
175	0.57	25.3	5.03	0.92	316	0.78	7.85	2.80	0.51
176	0.57	25.3	5.03	0.92	317	0.78	11.96	3.46	0.64
177	0.57	25.3	5.03	0.92	318	0.78	11.96	3.46	0.64
178	0.57	25.3	5.03	0.92	319	0.78	11.96	3.46	0.64
179	0.57	25.3	5.03	0.92	320	0.78	11.96	3.46	0.64
180	0.57	25.3	5.03	0.92	321	0.78	11.96	3.46	0.64
181	0.57	25.3	5.03	0.92	322	0.24	2.41	1.55	0.29
182	0.57	25.3	5.03	0.92	323	0.24	2.41	1.55	0.29
183	0.57	25.3	5.03	0.92	324	0.24	2.41	1.55	0.29
184	0.57	25.3	5.03	0.92	325	0.24	2.41	1.55	0.29
195	0.69	10.01	3.16	0.58	326	0.24	2.41	1.55	0.29
196	0.69	10.01	3.16	0.58	327	0.86	7.98	2.82	0.52
197	0.69	10.01	3.16	0.58	328	0.86	7.98	2.82	0.52

Appendix C: derivation of equations and results

198	0.69	10.01	3.16	0.58	329	0.86	7.98	2.82	0.52
199	0.69	10.01	3.16	0.58	330	0.86	7.98	2.82	0.52
200	0.69	10.01	3.16	0.58	331	0.86	7.98	2.82	0.52
219	0.53	3.46	1.86	0.34	336	0.19	3.04	1.74	0.32
220	0.43	3.6	1.90	0.35	338	0.3	4.81	2.19	0.40
221	0.45	3.23	1.80	0.33	339	0.5	12.46	3.53	0.65
222	0.43	2.82	1.68	0.31	348	0.67	9.46	3.08	0.57
223	0.48	3.16	1.78	0.33	349	0.67	9.46	3.08	0.57
224	0.71	3.13	1.77	0.33	350	0.67	9.46	3.08	0.57
225	0.47	5.19	2.28	0.42	351	0.67	9.46	3.08	0.57
226	0.56	4.31	2.08	0.38	352	0.67	9.46	3.08	0.57
227	0.33	3.06	1.75	0.32	353	0.67	9.46	3.08	0.57
228	0.51	2.72	1.65	0.30	354	0.67	9.46	3.08	0.57
229	0.38	5.13	2.26	0.42	355	0.67	9.46	3.08	0.57
230	0.38	5.13	2.26	0.42	356	0.67	9.46	3.08	0.57

Table C-2: Shear cracking strength (v_{cr})

ID	H/L	v_m	σ_v	v_{cr} (exp)	v_{cr} (cal)	v_{cr} - M88	v_{cr} - CC97	v_{cr} - MAT94	v_{max} - MC04	v_{max} - CC93	v_{max} - AIJ99	v_{max} - PC98	v_{max} - MC06	v_{max} - AC83
62	0.76	0.52	0.3	0.324	0.333	0.720	0.156	0.135	0.350	0.324	0.532	0.329	0.474	0.402
74	1.00	0.38	0.49	0.308	0.345	0.523	0.133	0.131	0.337	0.318	0.348	0.303	0.546	0.375
99	0.92	1.11	0.2	0.401	0.454	0.572	0.279	0.235	0.615	0.560	0.321	0.601	0.594	0.726
111	0.70	0.44	0	0.350	0.317	0.400	0.101	0.084	0.220	0.198	0.255	0.220	0.418	0.264
114	0.70	0.44	0	0.226	0.187	0.400	0.101	0.084	0.220	0.198	0.222	0.220	0.418	0.264
115	0.70	0.44	0	0.142	0.187	0.400	0.101	0.084	0.220	0.198	0.222	0.220	0.418	0.264
117	0.70	0.88	0	0.286	0.373	0.895	0.202	0.167	0.440	0.396	0.736	0.440	0.587	0.528
131	0.81	0.24	0.34	0.208	0.230	0.464	0.084	0.087	0.223	0.211	0.261	0.199	0.439	0.247
132	0.81	0.24	0.34	0.329	0.230	0.464	0.084	0.087	0.223	0.211	0.261	0.199	0.439	0.247
135	0.61	0.55	0	0.291	0.233	0.699	0.127	0.105	0.275	0.248	0.469	0.275	0.393	0.330
136	0.61	0.55	0	0.253	0.233	0.699	0.127	0.105	0.275	0.248	0.469	0.275	0.393	0.330
138	0.62	0.49	0	0.132	0.208	0.650	0.113	0.093	0.245	0.221	0.433	0.245	0.366	0.294
155	0.96	0.57	0	0.243	0.242	0.426	0.131	0.108	0.285	0.257	0.359	0.285	0.428	0.342
156	0.96	0.57	0.23	0.310	0.329	0.537	0.159	0.136	0.355	0.326	0.461	0.339	0.486	0.412
158	0.96	0.57	0	0.233	0.242	0.501	0.131	0.108	0.285	0.257	0.422	0.285	0.428	0.342
160	0.96	0.57	0.35	0.293	0.373	0.556	0.173	0.150	0.390	0.362	0.310	0.366	0.515	0.447
161	0.96	0.57	0	0.251	0.242	0.501	0.131	0.108	0.285	0.257	0.253	0.285	0.428	0.342
162	0.96	0.57	0.35	0.482	0.373	0.556	0.173	0.150	0.390	0.362	0.310	0.366	0.515	0.447
165	1.00	0.57	0	0.257	0.242	0.534	0.131	0.108	0.285	0.257	0.497	0.285	0.492	0.342
166	1.00	0.57	0	0.198	0.242	0.534	0.131	0.108	0.285	0.257	0.297	0.285	0.492	0.342
167	1.00	0.57	0	0.242	0.242	0.534	0.131	0.108	0.285	0.257	0.353	0.285	0.492	0.342
168	1.00	0.57	0.16	0.356	0.303	0.560	0.151	0.128	0.334	0.306	0.524	0.323	0.530	0.391
169	1.00	0.57	0.33	0.430	0.364	0.683	0.170	0.148	0.383	0.355	0.641	0.360	0.568	0.440
170	1.00	0.57	0.65	0.559	0.486	0.733	0.200	0.187	0.481	0.453	0.693	0.435	0.645	0.538
171	1.00	0.57	0	0.284	0.242	0.632	0.131	0.108	0.285	0.257	0.588	0.285	0.492	0.342
173	1.00	0.57	0	0.396	0.242	0.632	0.131	0.108	0.285	0.257	0.515	0.285	0.492	0.342
175	1.00	0.57	0.98	0.602	0.609	0.783	0.200	0.226	0.579	0.551	0.745	0.511	0.722	0.636
176	1.00	0.57	0.33	0.370	0.364	0.683	0.170	0.148	0.383	0.355	0.404	0.360	0.568	0.440
177	1.00	0.57	0.65	0.553	0.486	0.733	0.200	0.187	0.481	0.453	0.457	0.435	0.645	0.538
181	1.00	0.57	0	0.186	0.242	0.632	0.131	0.108	0.285	0.257	0.352	0.285	0.492	0.342
182	1.00	0.57	0	0.294	0.242	0.632	0.131	0.108	0.285	0.257	0.418	0.285	0.492	0.342
183	1.00	0.57	0	0.278	0.242	0.632	0.131	0.108	0.285	0.257	0.588	0.285	0.492	0.342

Appendix C: derivation of equations and results

185	1.00	0.33	0	0.106	0.140	0.637	0.076	0.063	0.165	0.149	0.378	0.165	0.478	0.198
186	1.00	0.33	0	0.155	0.140	0.637	0.076	0.063	0.165	0.149	0.632	0.165	0.478	0.198
187	1.00	0.33	0	0.217	0.140	0.637	0.076	0.063	0.165	0.149	0.632	0.165	0.478	0.198
188	1.00	0.33	0.61	0.445	0.369	0.735	0.116	0.136	0.349	0.332	0.734	0.306	0.632	0.382
190	1.00	0.33	0	0.180	0.140	0.637	0.076	0.063	0.165	0.149	0.513	0.165	0.478	0.198
194	1.00	0.33	0	0.287	0.140	0.637	0.076	0.063	0.165	0.149	0.632	0.165	0.478	0.198
195	1.00	0.69	0	0.180	0.292	0.673	0.159	0.131	0.345	0.311	0.583	0.345	0.641	0.414
196	1.00	0.69	0.29	0.474	0.400	0.746	0.193	0.165	0.431	0.396	0.631	0.411	0.717	0.500
197	1.00	0.69	0	0.263	0.292	0.673	0.159	0.131	0.345	0.311	0.659	0.345	0.622	0.414
200	1.04	0.69	0.47	0.343	0.469	0.786	0.215	0.188	0.487	0.452	0.607	0.441	0.676	0.556
225	1.00	0.47	0.36	0.231	0.335		0.152	0.133	0.344	0.320		0.318	0.529	0.391
226	1.00	0.56	0.36	0.292	0.373		0.173	0.150	0.389	0.361		0.364	0.567	0.446
227	1.00	0.33	0.36	0.278	0.274		0.114	0.105	0.272	0.255		0.246	0.466	0.304
228	1.00	0.51	0.36	0.285	0.353		0.161	0.141	0.365	0.339		0.340	0.544	0.416
229	1.00	0.38	0	0.193	0.162	0.469	0.088	0.073	0.191	0.172	0.402	0.191	0.498	0.230
235	1.00	0.38	0	0.216	0.162	0.293	0.088	0.073	0.191	0.172	0.252	0.191	0.499	0.230
238	1.00	0.37	0	0.184	0.156	0.246	0.085	0.070	0.184	0.166	0.198	0.184	0.412	0.221
239	1.00	0.37	0	0.207	0.156	0.266	0.085	0.070	0.184	0.166	0.213	0.184	0.432	0.221
250	0.97	0.42	0.55	0.340	0.384		0.147	0.146	0.375	0.354		0.336	0.544	0.417
251	0.97	0.42	0.55	0.286	0.384		0.147	0.146	0.375	0.354		0.336	0.544	0.417
252	0.97	0.42	0.55	0.353	0.384		0.147	0.146	0.375	0.354		0.336	0.544	0.417
253	0.97	0.42	0.55	0.410	0.384		0.147	0.146	0.375	0.354		0.336	0.544	0.417
254	0.97	0.42	0.55	0.417	0.384		0.147	0.146	0.375	0.354		0.336	0.544	0.417
255	0.97	0.42	0.55	0.413	0.384		0.147	0.146	0.375	0.354		0.336	0.544	0.417
256	0.97	0.42	0.55	0.441	0.384		0.147	0.146	0.375	0.354		0.336	0.544	0.417
257	0.97	0.42	0.55	0.445	0.384		0.147	0.146	0.375	0.354		0.336	0.544	0.417
265	1.00	1.08	0	0.343	0.458		0.248	0.205	0.540	0.486		0.540		0.648
266	1.00	1.08	0	0.347	0.458		0.248	0.205	0.540	0.486		0.540		0.648
293	1.00	0.72	0.43	0.372	0.466		0.217	0.188	0.489	0.453		0.459		0.561
294	1.00	0.71	0.43	0.428	0.462		0.215	0.187	0.484	0.449		0.454		0.555
295	1.00	0.74	0.43	0.336	0.475		0.222	0.192	0.499	0.462		0.469		0.573
296	1.00	0.74	0	0.190	0.314		0.170	0.141	0.370	0.333		0.370		0.444
297	1.00	0.9	0	0.478	0.381		0.207	0.171	0.450	0.405		0.450		0.540
300	1.07	0.8	0.55	0.640	0.545		0.250	0.218	0.565	0.525		0.500		0.645
304	1.00	1.06	0	0.458	0.449		0.244	0.201	0.530	0.477		0.530		0.636
305	1.00	0.98	0	0.482	0.415		0.225	0.186	0.490	0.441		0.490		0.588
306	1.00	1.09	0	0.557	0.462		0.251	0.207	0.545	0.491		0.545		0.654
307	1.00	1.07	0	0.504	0.454		0.246	0.203	0.535	0.482		0.535		0.642
317	1.00	0.78	0	0.355	0.331		0.179	0.148	0.390	0.351		0.390		0.468
318	1.00	0.78	0.24	0.544	0.420		0.208	0.177	0.462	0.423		0.445		0.540
319	1.00	0.78	0.48	0.482	0.510		0.237	0.206	0.534	0.495		0.500		0.612
320	1.00	0.78	0.48	0.435	0.510		0.237	0.206	0.534	0.495		0.500		0.612
321	1.00	0.78	0.48	0.571	0.510		0.237	0.206	0.534	0.495		0.500		0.612
322	1.00	0.24	0	0.132	0.102		0.055	0.046	0.120	0.108		0.120		0.144
323	1.00	0.24	0.45	0.307	0.270		0.084	0.100	0.255	0.243		0.224		0.279
324	1.00	0.24	0.45	0.221	0.270		0.084	0.100	0.255	0.243		0.224		0.279
325	1.00	0.24	0.45	0.283	0.270		0.084	0.100	0.255	0.243		0.224		0.279
326	1.00	0.24	0.22	0.259	0.184		0.082	0.072	0.186	0.174		0.171		0.210

Appendix C: derivation of equations and results

Table C-3: Maximum shear strength (v_{max})

ID	H / L	v_m	σ_v	f'_c	$\rho_{vc} \cdot f_{yc}$	$V_{max \text{ exp}}$	$V_{max \text{ cal}}$	$V_{max-AI99}$	$V_{max-MC06}$	$V_{max-AC83}$
62	0.76	0.52	0.3	24.26	10.27	0.429	0.441	0.532	0.474	0.402
74	1.00	0.38	0.49	27.47	6.81	0.451	0.451	0.348	0.546	0.375
82	1.00	1.61	0.39	25.9	12.63	0.702	0.735	0.521	0.977	1.083
105	1.24	1.5	0.408	20	8.24	0.741	0.644	0.874	1.440	1.022
131	0.81	0.24	0.343	13.83	5.14	0.261	0.294	0.261	0.439	0.247
132	0.81	0.24	0.343	13.83	5.14	0.424	0.374	0.261	0.439	0.247
135	0.61	0.55	0	23.9	6.20	0.321	0.287	0.469	0.393	0.330
136	0.61	0.55	0	23.9	6.20	0.378	0.287	0.469	0.393	0.330
137	0.62	0.49	0	23.9	6.20	0.228	0.275	0.433	0.366	0.294
138	0.62	0.49	0	23.9	6.20	0.254	0.275	0.433	0.366	0.294
155	0.96	0.57	0	29.43	10.88	0.345	0.372	0.359	0.428	0.342
156	0.96	0.57	0.233	14.72	10.88	0.437	0.383	0.461	0.486	0.412
158	0.96	0.57	0	19.62	10.88	0.376	0.326	0.422	0.428	0.342
165	1.00	0.57	0	29.33	10.88	0.529	0.472	0.497	0.492	0.342
168	1.00	0.57	0.164	33.06	10.88	0.494	0.447	0.524	0.530	0.391
171	1.00	0.57	0	18.84	10.88	0.446	0.322	0.588	0.492	0.342
173	1.00	0.57	0	8.14	6.96	0.425	0.226	0.515	0.492	0.342
184	1.00	0.57	0	21.48	10.88	0.305	0.336	0.588	0.492	0.342
187	1.00	0.33	0	17.36	19.43	0.278	0.329	0.632	0.478	0.198
188	1.00	0.33	0.613	15.3	19.43	0.523	0.535	0.734	0.632	0.382
189	1.00	0.33	1.226	12.56	19.43	0.801	0.735	0.836	0.786	0.566
190	1.00	0.33	0	14.72	9.71	0.206	0.238	0.513	0.478	0.198
195	1.00	0.69	0	10.2	20.29	0.238	0.348	0.583	0.641	0.414
196	1.00	0.69	0.286	15.6	20.29	0.550	0.500	0.631	0.717	0.500
197	1.00	0.69	0	23.25	17.81	0.450	0.432	0.659	0.622	0.414
199	1.04	0.69	0	14.72	11.84	0.173	0.231	0.527	0.553	0.414
200	1.04	0.69	0.472	14.72	11.84	0.372	0.503	0.607	0.676	0.556
219	3.13	0.5268	0.2453	19.11	6.00	0.209	0.351	.	0.947	0.390
220	2.08	0.4316	0.2453	19.11	6.00	0.242	0.331	.	0.704	0.333
221	3.13	0.4473	0.4905	17.77	6.00	0.211	0.242	.	0.969	0.416
223	3.13	0.4846	0.1226	18.23	6.00	0.219	0.294	.	0.902	0.328
224	2.08	0.7142	0.1226	18.23	6.00	0.276	0.342	.	0.772	0.465
250	0.97	0.42	0.549	23.05	5.93	0.432	0.453	.	0.544	0.417
251	0.97	0.42	0.549	23.05	5.93	0.438	0.453	.	0.544	0.417
253	0.97	0.42	0.549	23.05	5.93	0.501	0.453	.	0.544	0.417
254	0.97	0.42	0.549	23.05	4.29	0.457	0.428	.	0.544	0.417
255	0.97	0.42	0.549	23.05	4.29	0.457	0.428	.	0.544	0.417
256	0.97	0.42	0.549	23.05	4.29	0.469	0.428	.	0.544	0.417
257	0.97	0.42	0.549	23.05	4.29	0.445	0.428	.	0.544	0.417

Table C-4: Cracking drift capacity (δ_{cr})

ID	Unit Material	H/L	$\delta_{cr\ exp}$	$v_{cr}/\sqrt{f_m}$	$\delta_{cr\ cal}$
62	Concrete	0.76	0.115	0.125	0.090
74	Clay	1.00	0.117	0.179	0.202
99	Clay	0.92	0.222	0.227	0.256
111	Clay	0.70	0.080	0.116	0.130
114	Clay	0.70	0.105	0.116	0.130
115	Clay	0.70	0.171	0.116	0.130
117	Clay	0.70	0.160	0.104	0.117
135	Clay	0.61	0.118	0.088	0.099
136	Clay	0.61	0.078	0.088	0.099
156	Concrete	0.96	0.078	0.086	0.062
161	Concrete	0.96	0.114	0.063	0.075
185	Clay	1.00	0.138	0.029	0.033
186	Clay	1.00	0.053	0.029	0.033
187	Clay	1.00	0.107	0.029	0.033
188	Clay	1.00	0.160	0.076	0.086
194	Clay	1.00	0.122	0.029	0.093
195	Clay	1.00	0.088	0.092	0.103
196	Clay	1.00	0.234	0.125	0.141
197	Clay	1.00	0.111	0.092	0.103
220	Concrete	2.08	0.105	0.143	0.103
221	Concrete	3.13	0.203	0.205	0.147
222	Concrete	2.08	0.114	0.215	0.154
223	Concrete	3.13	0.117	0.140	0.100
224	Concrete	2.08	0.107	0.195	0.140
226	Concrete	1.00	0.175	0.178	0.128
227	Concrete	1.00	0.142	0.155	0.111
228	Concrete	1.00	0.203	0.212	0.152
229	Clay	1.00	0.106	0.071	0.080
235	Clay	1.00	0.074	0.071	0.080
238	Concrete	1.00	0.063	0.077	0.055
239	Concrete	1.00	0.075	0.077	0.055
250	Concrete	0.97	0.087	0.166	0.119
251	Concrete	0.97	0.098	0.166	0.119
252	Concrete	0.97	0.068	0.166	0.119
253	Concrete	0.97	0.075	0.166	0.119
254	Concrete	0.97	0.099	0.166	0.119
255	Concrete	0.97	0.082	0.166	0.119
256	Concrete	0.97	0.070	0.166	0.119
257	Concrete	0.97	0.103	0.166	0.119
265	Ceramic	1.00	0.125	0.121	0.115
266	Ceramic	1.00	0.110	0.121	0.115
295	Concrete	1.00	0.130	0.119	0.086
296	Concrete	1.00	0.130	0.079	0.057
317	Ceramic	1.00	0.150	0.095	0.090
319	Ceramic	1.00	0.186	0.146	0.139
320	Ceramic	1.00	0.107	0.146	0.139
321	Ceramic	1.00	0.148	0.146	0.139
322	Ceramic	1.00	0.067	0.065	0.062
323	Ceramic	1.00	0.194	0.172	0.163
324	Ceramic	1.00	0.125	0.172	0.163
325	Ceramic	1.00	0.112	0.172	0.163

Appendix C: derivation of equations and results

Table C-5: Ultimate drift capacity (δ_{ult})

ID	H/L	v_{max}	δ_{max}	δ_{ult}	l/v_{max}^2	$\gamma \cdot v_{max} / \sqrt{f_m}$	μ_{exp}	μ_{cal}
62	0.76	0.43	0.271	0.371	5.524	0.101	3.44	4.02
74	1.00	0.43	0.426	0.639	5.337	0.249	2.56	3.93
82	1.00	0.63	0.234	0.392	2.522	0.180	2.17	2.53
99	0.92	0.49	0.382	0.397	4.160	0.226	1.75	3.34
101	0.92	0.51	0.342	0.392	3.807	0.237	1.66	3.17
105	1.24	0.69	0.467	0.746	2.083	0.219	3.40	2.31
135	0.61	0.30	0.535	1.132	10.837	0.127	8.92	6.66
136	0.61	0.34	0.634	1.030	8.472	0.143	7.18	5.49
165	1.00	0.43	0.401	0.616	5.405	0.211	2.92	3.96
166	1.00	0.30	0.865	0.962	11.458	0.145	6.64	6.97
168	1.00	0.47	0.284	0.372	4.441	0.233	1.60	3.48
169	1.00	0.70	0.500	0.633	2.032	0.291	2.18	2.28
171	1.00	0.45	0.317	0.795	5.027	0.185	4.30	3.77
173	1.00	0.44	0.334	0.512	5.187	0.182	2.81	3.85
175	1.00	0.79	0.524	0.524	1.622	0.326	1.61	2.08
176	1.00	0.47	0.647	0.767	4.482	0.196	3.92	3.50
184	1.00	0.33	0.543	0.844	8.916	0.139	6.08	5.71
188	1.00	0.52	0.266	0.449	3.765	0.118	3.81	3.15
189	1.00	0.76	0.345	0.400	1.719	0.175	2.29	2.13
191	1.00	0.54	0.398	0.583	3.460	0.123	4.74	2.99
195	1.00	0.32	0.295	0.582	9.823	0.111	5.27	6.16
229	1.00	0.27	0.975	0.975	13.824	0.130	7.49	8.15
235	1.00	0.22	.	1.229	20.390	0.107	11.46	11.42
250	0.97	0.45	0.383	0.445	4.968	0.123	3.62	3.74
251	0.97	0.45	0.334	0.502	4.924	0.123	4.07	3.72
252	0.97	0.48	0.336	0.502	4.275	0.132	3.79	3.40
253	0.97	0.47	0.292	0.443	4.495	0.129	3.43	3.51
254	0.97	0.45	0.252	0.494	4.942	0.123	4.01	3.73
255	0.97	0.45	0.158	0.362	4.942	0.123	2.94	3.73
256	0.97	0.45	0.208	0.473	4.857	0.124	3.81	3.69
257	0.97	0.45	0.103	0.407	5.033	0.122	3.33	3.78
265	1.00	0.42	0.292	0.655	5.776	0.108	6.08	4.15
266	1.00	0.56	0.292	0.580	3.199	0.145	4.00	2.86
297	1.00	0.64	.	0.833	2.431	0.244	3.41	2.48
300	1.07	0.83	.	0.757	1.451	0.347	2.18	1.99
301	1.07	0.83	.	0.543	1.467	0.345	1.57	2.00
308	0.74	0.37	0.190	0.310	7.500	0.082	3.79	5.00
313	0.97	0.70	0.425	0.450	2.028	0.157	2.86	2.28